DEPARTMENT OF THE NAVY
NAVAL RESEARCH LABORATORY
4555 OVERLOOK AVE SW
WASHINGTON DC 20375-5320

IN REPLY REFER TO
3905
Ser 6180/0013

07 MAR 2000

From: Commanding Officer, Naval Research Laboratory
To: Commander, Naval Air Warfare Center (Code 43520A William Leach)

Subj: BEHAVIOR OF AQUEOUS FILM FORMING FOAMS (AFFF) EXPOSED TO RADIANT HEATING

Encl: (1) Two copies of subject report

1. Enclosure (1) is forwarded for your information. This work is being performed under the Carrier Aircraft Fire Suppression Program, W1819.

2. The enclosure describes small-scale foam testing in support of the development of a fire suppression model. This model is intended as a research tool for the development of environmentally friendly firefighting foams.

3. The research indicates that model inputs for foam loss mechanisms (e.g., evaporation rate and drainage rate) and critical foam mass for fuel suppression can be determined using the test apparatus developed in this study. From tests on a single AFFF formulation (6% 3M AFFF), the evaporation rate was measured to be a function of irradiance level, and the drainage rate was dependent on foam mass per liquid content of the foam. The effective heat of vaporization, which is the irradiance necessary to vaporize 1 kg/(s m^2) of AFFF, is used in the model to determine the evaporation rate of the foam. For this AFFF formulation, the effective heat of vaporization was determined to be 4.87±0.75 kJ/kg. For a given foam expansion ratio, data from the apparatus can be used to develop a relation between drainage rate and foam mass per unit area for input into the model. Fuel layers beneath the foam did not affect the drainage or evaporation rates, and were ignited when most of the foam was depleted (average of 0.8 kg/m^2 of foam remaining at ignition). Foam height destruction rate was dependent on irradiance level and not on expansion ratio or initial foam height.

4. Future work needs to include the development of a test apparatus to provide the model with the necessary input for quantifying foam spread in a fire environment. Using the foam spread data from this apparatus the model then can be validated versus large-scale test data that exist in the literature. After validating the model performance, evaluation of other firefighting foam formulations is recommended. This would include small scale testing to determine foam loss and foam spread properties and validation with large-scale data. In future testing with the foam loss mechanism apparatus, additional instrumentation should be added to quantify the solution density distribution with foam height. Testing also needs to be performed to develop other foam properties, such as solution viscosity, at a range of temperatures.

Subj: BEHAVIOR OF AQUEOUS FILM FORMING FOAMS (AFFF) EXPOSED TO RADIANT HEATING

5. The NRL point of contact for this program is Dr. Frederick W. Williams, Code 6180, (202) 767-2476, e-mail: fwilliam@itd.nrl.navy.mil.

JAMES S. MURDAY
By direction

Copy to:
NAWC/China Lake (Code 4B3100D Bowman)
COMNAVSEASYSCOM (Code 05L4 McCrory, Williams, Hunstad, Satterfield)
AFRL/MLQC/TYNDALL AFB (Vickers)
COMNAVAIRSYSCOM (PMA 251 CWO5 McDaniel, LCDR Jackson)
HDQS/USMC (ASL-45 CWO4 Casey)
COMNAVFACENGCOM (Code CHE Gott)
COMLANTNAVFACENGCOM (Code 408 Tabet)
HQ/AFCESA/CESM (Walker)

6180/0013A:FWW
February 10, 2000

Behavior of Aqueous Film Forming Foams (AFFF) Exposed to Radiant Heating

BRIAN Y. LATTIMER
CHRISTOPHER P. HANAUSKA
JOSEPH L. SCHEFFEY
Hughes Associates, Inc.

FREDERICK W. WILLIAMS
Navy Technology Center for Safety and Survivability

WILLIAM LEACH
Naval Air Systems Command

Encl (1) to NRL Ltr
3905
Ser 6180/0013

CONTENTS

US00000518

EXECUTIVE SUMMARY

Aqueous film-forming foam (AFFF) is a very effective agent for combating two-dimensional liquid fuel fires. Current formulations of AFFF concentrates include compounds that are non-biodegradable and which have potential toxic impact on the environment. Expensive large scale testing is currently the only reliable means of assessing the performance of a new firefighting formulation. In order to stimulate and accelerate the development of environmentally improved suppression agents; a more economical approach needs to be developed to evaluate the new formulations.

There have been few studies that have been performed to understand the loss mechanism and flow of firefighting foams spreading over fuel. As a result, the physics of foam spread and a good predictive spread model have not been established and validated. Performance-based computer fire models offer perhaps the most promising and economical way for predicting the large-scale behavior of firefighting foams. These models rely on input data developed from small scale testing of a particular foam to describe the less well understood or characterized performance aspects of foam. Input data necessary for the model proposed in reference (8) require input test data on foam loss mechanisms, critical foam mass for suppression and various foam spread properties.

A test apparatus was developed and utilized in this study to quantify the foam loss mechanism and the critical foam mass for suppression with the foam exposed to a range of irradiance levels (0-50 kW/m^2). The apparatus provided data on evaporation rate, drainage rate, foam destruction rate, foam temperature, heat penetration and time to fuel ignition. Using this apparatus, the performance of a single AFFF formulation (6% 3M AFFF) was characterized.

The evaporation rate was measured to be a function of irradiance level, and the drainage rate was dependent on foam mass per unit area and liquid content of the foam. The effective heat of vaporization, which is the irradiance necessary to vaporize 1 $kg/(s\ m^2)$ of AFFF, could be used in the model to determine the evaporation rate of the foam. For this AFFF formulation, the

effective heat of vaporization was determined to be 4.87±0.75 kJ/kg. For a given foam expansion ratio, data from the apparatus were used to develop a relation between drainage rate and foam mass per unit area for input into the model. Fuel layers beneath the foam did not affect the drainage or evaporation rates, and were ignited when nearly all of the foam was depleted (average of 0.8 kg/m^2 of foam remaining at ignition). Foam height destruction rate was dependent on irradiance level and not on expansion ratio or initial foam height.

Future work needs to include the development of a test apparatus to provide the model with the necessary input for quantifying foam spread in a fire environment. Using the foam spread data from this apparatus; the model then can be validated versus large-scale test data that exists in the literature. After validating the model performance, evaluation of other firefighting foam formulations is recommended. This would include small-scale testing to determine foam loss and foam spread properties and validation with large-scale data. In future testing with the foam loss mechanism apparatus, additional instrumentation should be added to quantify the solution density distribution with foam height. Testing also needs to be performed to develop other foam properties, such as solution viscosity, at a range of temperatures.

BEHAVIOR OF AQUEOUS FILM FORMING FOAMS (AFFF) EXPOSED TO RADIANT HEATING

1.0 BACKGROUND

Aqueous film-foaming foam (AFFF) is a very effective agent for combating two-dimensional liquid fuel fires. The Naval Air Systems Command (NAVAIR) relies on AFFF Systems to protect its assets. The current formulation of AFFF concentrates includes compounds which are non-biodegradable and which have potential toxic impact on the environment. The status of the environmental impact of AFFF was previously reviewed [1]. Different approaches for developing an environmentally improved suppression agent were outlined. It was recommended that

1. The trends of regulations affecting the discharge of AFFF be monitored;
2. The development of any AFFF reformulation which reduces the amount of non-biodegradable or regulated compounds be monitored;
3. An approach be adopted to develop a long term solution which would address all aspects of the environmental issue, i.e. a next generation biodegradable fire suppression agent; and
4. A fire suppression model be developed which could be used to support the formulation of the next generation agent.

Full-scale fire testing of fire fighting foams is currently the only reliable method for evaluating foam performance [2,3]. These tests are expensive for determining the performance of new formulations of foam. NFPA 11 [2] and MIL-F-24358F [3] recommend a few different small-scale tests to evaluate the performance of foam. These include tests for measuring the drain time, foam expansion ratio and the film formation and sealibility.

Though these tests do provide insight on some aspects of the foam, passing all of the tests does not ensure that the foam will be capable of extinguishing the fire. Previous analysis of these parameters indicated no across-the-board correlation between these parameters and fire extinguishment performance [4].

Performance based computer fire models offer perhaps the most promising way for predicting the full-scale behavior of the foam. These models rely on input data developed from small-scale testing of a particular foam to describe the less well understood or characterized aspects of foam. Examples of some input data that may be necessary for the models are foam loss mechanisms, heat transfer through the foam, ignition of fuel, foam viscosity, viscosity between the foam and the fuel and foam spread. Researchers at the Swedish National Testing and Research Institute have developed test methods for determining some of these data and a model for predicting foam spread [5-7].

Reference [1] provided a work plan for the development of the fire suppression model. Reference [8] identified the theory underlying the development of a foam extinguishment model. This model characterizes extinguishment based on a summation of heat gains and losses. Heat gains, manifested in continued fuel burning, are characterized by flame radiation to the fuel surface and resultant vaporization of the fuel. Loss mechanisms are more complicated; they are characterized by cessation of fuel vaporization through establishment of vapor barrier (foam blanket) over a fuel surface and was characterized in terms of a similar physical phenomena: oil spreading over water. Using this analogy, a foam blanket flow model was developed which addresses the rheological properties of the foam.

The foam loss mechanism evaporation and drainage are dependent on a number of parameters that need to be controlled and measured experimentally. It was the objective of the experiments described in this report to begin to understand the relationships between the foam evaporation; radiant heat flux and foam drainage; fuel type and foam solution drop-through; fuel temperature and foam drainage; fuel temperature and foam solution drop-through. Foam with a range of expansion ratio and drain times was evaluated.

A new apparatus for characterizing the foam loss mechanisms, heat transfer and ignition time of fuel has been developed. Similar to one of the test designs developed in Refs. [5,6], this apparatus continuously monitors the mass of the foam and the mass of solution drained, and uses mass conservation to determine the mass evaporated. Unlike previously developed apparatuses, this apparatus is capable of electronically monitoring these masses in tests with or without fuel in the test pan. This apparatus was designed to measure the foam evaporation rate, drainage rate, thickness, temperature and heat penetration through the foam. In tests with fuel below the foam, the time to ignite the fuel after foam application was also measured.

The apparatus was used to characterize the behavior of 6% AFFF (3M formulation FC-206CF) foam when exposed to fire conditions. The tests focused on evaluating the effects of expansion ratio, initial foam height, irradiance level, fuel layers and fuel layer temperature on the foam behavior. In this series of tests, the test conditions were varied to quantify the effects of foam expansion ratio, initial foam thickness, irradiance, fuel layers and fuel layer temperature on the foam behavior.

2.0 EXPERIMENTAL DESIGN

2.1 Apparatus Design Considerations

The primary function of the test apparatus was to measure how the evaporation rate and drainage rate of foam varies with time when exposed to different irradiance levels. Also of importance was to monitor the time varying foam thickness, foam temperature and heat penetration through the foam. With some tests being performed with fuel layers, the apparatus needed to be constructed of chemically resistant hardware and be equipped with an ignition source to ignite flammable vapors.

The conceptual idea of the test apparatus was to have a test pan that contains the foam and a transparent secondary holding vessel attached to the bottom of the pan, see Figure 1. This entire assembly would be located on a load cell with the weight of all hardware tared out of the mass. Before the test begins, the secondary holding vessel would be filled with AFFF solution to a line. Foam would be added to the test pan and solution would begin to drain from the foam and down into the secondary vessel. During the test, the level of the solution in the secondary vessel would be kept constant by bleeding solution from the vessel. This solution removed from the vessel would be collected in a container located on a second load cell. The first load cell would provide the mass of the foam blanket, while the second load cell would provide the mass of solution drained from the foam. The difference between the initial mass in the test pan and the masses from the two load cells would be the mass of solution evaporated.

2.2 Apparatus Description

The small-scale test apparatus designed in this study is shown in Figure 1. The apparatus consists of a test pan, a solenoid valve, a drain collection container, two load cells, thermocouples, a total heat flux gauge, a radiant heater and a pilot flame.

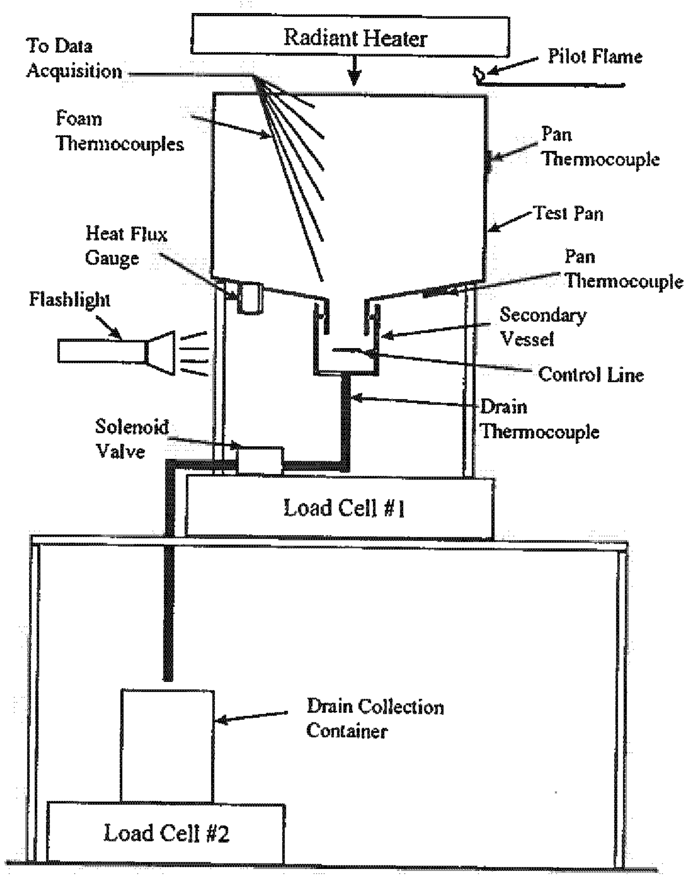

Figure 1. Small-scale test apparatus for measuring foam losses under heat. (not to scale)

US00000525

The cylindrical shaped test pan was 230 mm in diameter and 150 mm high, and was constructed of 1 mm thick stainless steel. As shown in the detailed schematic of the test pan in Figure 2, the bottom of the test pan was slightly tapered to guide the drained solution toward the center of the pan. On the bottom of the pan there were two collars. The collar whose center was approximately 50 mm from the side wall was used to mount the heat flux gauge to the pan. This collar was designed so that the heat flux gauge would be slightly elevated above the collar on the inside of the pan to minimize solution buildup on the gauge surface. The second collar located in the middle of the pan was the drain for the pan. The inside diameter of the drain collar was 53 mm. The notches on the outside of the collar were for O-rings. The secondary vessel, a 95 mm long, 60 mm inside diameter clear Nalgene cylinder, was slipped over the outside of the drain collar. Chemically resistant Viton O-rings (53 mm inside diameter, 1.5 mm gland diameter) were placed in the notches of the drain collar to seal the Nalgene cylinder to the collar. This allowed the operator to monitor the location of the interface between the drained solution and the foam or drained solution and fuel, which was critical to accurately determining drainage. Light from a flashlight was used to aid in visualizing the interface location.

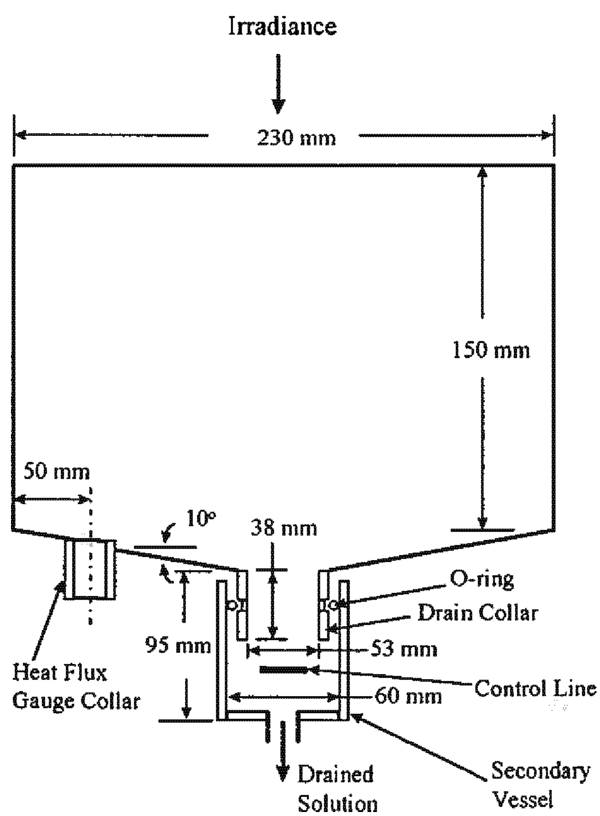

Figure 2. Detail of test pan.

The open end of the Nalgene cylinder was capped and a port was installed in the cap to allow drained solution to be removed from the test pan. The drain port was connected to an ASCO EF8210G94V-120/60 electronically actuated solenoid valve via 6.4 mm diameter copper tubing. The solenoid valve was used to control when solution was drained from the test pan. Solution was routed from the solenoid valve to the drain collection container via 6.4 mm copper tubing. The collection container used in the testing was a 1000 mL Pyrex beaker.

The foam was heated during the experiment using a 0.30 m square infrared panel heater, OMEGALUX QH-121260-T, which was capable of producing heat fluxes as high as 90 kW/m^2. The heat flux from the heater was determined by the temperature of the Quartz panels on the heater face and distance away from the heater. The heater was set at a location 0.013 m above the top of the pan. The irradiance level onto the foam was determined by the temperature setting on the heater. The Quartz panel temperature was monitored using a 3.1 mm diameter sheathed Type K thermocouple. Using the signal from this thermocouple, a controller, Omega CN77544, was used to keep the Quartz panel at a relatively constant temperature (±8°C). The heater was mounted to a track assembly that allowed it to be move horizontally over the test pan at the start of the test and removed at the end of the test. A button in the track was used to flag when the heater was over the test pan.

Two load cells were necessary in the apparatus so that the mass drained and the mass evaporated could be determined. Load Cell #1, which was an OHAUS IP15KS (0-15 kg range with 0.1 gram accuracy), was used to monitor the mass of foam remaining in the pan. To reduce vibration errors, all of the hardware and instrumentation connected to the test pan rested on the load cell. The mass of these items was tared out of the weight before the beginning of each test. Load Cell #2, which was also an OHAUS EIL210 (0-22 kg range with 0.1 gram accuracy), was used to monitor the solution drained from the foam. Both load cells were shielded from the radiant heater using calcium silicate boards. No more than 6 grams of drift was noted after any of the tests performed in this study.

The temperature of the foam was monitored using six Type K 0.5 mm diameter sheathed stainless steel shielded thermocouples. These thermocouples were mounted external of the test pan and fed into the foam through the top of the test pan. The thermocouples were located at 0.025 m increments along the height of the pan. In a test with heating, these thermocouples were found to be sensitive enough to monitor the location of the foam height with time. The temperature of the drained solution was monitored using a Type K 1.5 mm sheathed thermocouple located just downstream of the drain port. The temperature of the pan during the test was monitored using two Omega SA1-K self-adhesive Type K thermocouples mounted on the bottom of the test pan and 0.075 m up the side of the test pan.

The heat penetration through the foam was measured using a Medtherm 64-5SB-20 Schmidt-Boelter total heat flux gauge with a 0-50 kW/m^2 range. The gauge was water cooled using water at room temperature.

Data were acquired using a personal computer and Labtech Notebook. Data from all instrumentation except the load cells were sent to the computer from two external data acquisition cards. The external data acquisition cards used in the testing were Keithley Metrabyte Exp16 multiplexing cards with built in cold junction compensation. These were connected to an internal data acquisition card, Keithley Metrabyte DAS 8. Data from each of the load cells were sent to the computer via an RS232 signal. During the test, data were taken every second.

2.3 Foam Generation

All tests were performed using MIL SPEC 6% AFFF concentrate (3M, FC-206CF). As recommended for this type of concentrate, AFFF solution was made by adding 6 parts of AFFF concentrate to 94 parts of water. NFPA 11 [2] and MIL-F-24385F [3] specify the use of a two gallon per minute nozzle to generate foam. To determine expansion ratio and drain time, the foam is sprayed from the nozzle onto a backboard inclined at 45 degrees. The foam drains from the inclined bottom down to a collector container.

In this study, a repeatable but easy to perform method for generating the foam was sought. Mechanical mixing devices, such as blenders and food processors, were found to be capable of making repeatable foam. To generate foams with expansion ratios of nominally 3.3 and 6.0, three 0.12 m diameter, 1200 mL Hamilton Beach blenders, Model 56300 were operated on "high pulse" speed for a particular duration. Foams with an expansion ratio of nominally 9.7 were generated using three 0.16 m diameter, 1200 mL Hamilton Beach food processors, Model 702R operated on "high pulse" for a particular duration. In each test, the mixing duration was timed using a stopwatch.

A series of drain time and expansion ratio tests were performed to determine the most repeatable method for making the foam using the mixing devices. Through these tests, it was determined that the initial amount of solution in the mixing device needed to remain relatively constant to achieve repeatable foam for a fixed mixing duration. The drain time and expansion ratio results for several tests are provided in Table 1. From these results, the expansion ratio of the foam was repeatable to within ±7% while the 25% drain time was repeatable to within ±13% of the average.

Table 1. Expansion Ratio and Drain Time for Foams Made Using Mixing Devices

Test No.	Expansion Ratio	25% Drain Time [s]	Initial Volume of Solution [mL]	Mixing Duration [s]
1	3.2	- -	400	0.6
2	3.3	47	400	0.5
3	3.3	53	400	0.6
4	3.4	59	400	0.6
5	3.3	47	400	0.5
Average	3.3±0.1	52±7		
1	5.9	209	200	5.2
2	5.7	187	200	5.0
3	6.1	214	200	5.2
4	6.3	203	200	5.2
5	6.1	210	200	5.1
Average	6.0±0.3	205±18		
1	9.3	216	133	10
2	9.3	210	133	9.5
3	9.1	222	133	9.5
4	10.4	202	133	10
5	10.3	222	133	9.5
Average	9.7±0.7	214±12		

Drain time results from the 3.3 and 6.0 expansion ratio foams were compared with results from foam made using a non-aspirated nozzle and an aspirated nozzle, respectively. In two MIL-SPEC tests with non-aspirated nozzle, the average expansion ratio was measured to be 3.4±0.1 and the average 25% drain time was 53±5 s. These values compare well with the expansion ratio and 25% drain time of the foams generated using the mixing device. In the three MIL-SPEC tests with an aspirated nozzle, the expansion ratio was measured to average 7.0±0.1 while the 25% drain time averaged 176±4 s. Comparing the aspirated nozzle results with the 6.0 expansion ratio foam produced using the mixing devices; the foam from the aspirated nozzle had an expansion ratio 15% higher and a 25% drain time that was 17% lower. In general, the foam generated using the mixing devices compared well with the foam generated with the nozzles.

2.4 Heater Calibration

A series of tests was performed to determine the irradiance distribution inside the pan from the heater at a particular setting. Irradiance measurements were performed using a Medtherm 64-5SB-20 Schmidt-Boelter total heat flux gauge with a 0-50 kW/m^2 range. For the calibration tests, the secondary vessel was removed from the test pan and the heat flux gauge was fed up into the pan through the drain collar hole. Tests were performed with the heat flux gauge at various heights in the pan for a range of heater settings. As shown in Figure 3, the heat flux was measured to vary by approximately 30% of the level measured near the heater. Tests were performed with an initial foam thickness of 25, 50 and 75 mm. As will be shown, the addition of heat caused the foam to expand causing the thickness to briefly increase by nominally 25 mm. Therefore, during a test the irradiance at the foam surface may vary by as much as 17% from the initial setting.

A representative variation in the irradiance away from the centerline is shown in Figure 4. At positions up to 30 mm from the centerline, irradiance levels were measured to be within 5% of the centerline irradiance. Near the side of the test pan the irradiance levels were within 15% of the centerline value.

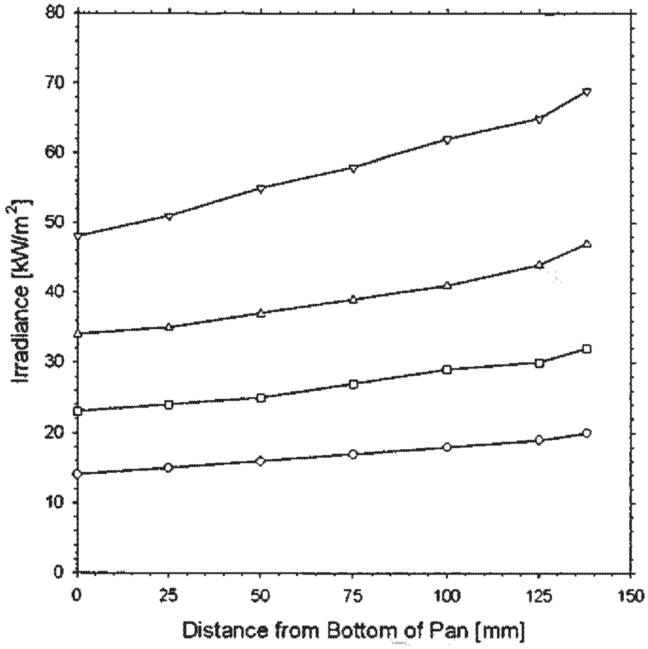

Figure 3. Centerline irradiance levels from the heater along the height of the test pan with the heater at different set points. (O)1000°F, (□)1200°F, (Δ)1400°F, (Δ)1600°F.

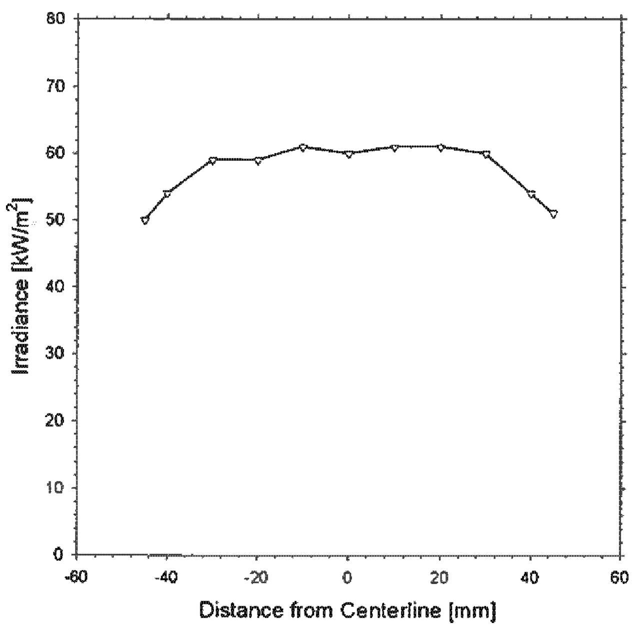

Figure 4. Variation in irradiance from heater with distance away from centerline. Heater set point = 1600°F, 125 mm from bottom of pan.

3.0 TEST PROCEDURES

A consistent test procedure was followed to minimize repeatability errors in the test results. Initially, the heater was set to the desired heat flux level using the controller, and allowed to reach a steady state (approximately 10 minutes). Before starting the data acquisition system, proper amount of solution was added to the mixing devices. AFFF solution was added to the secondary vessel until the solution was at the control line. Both load cells were tared and the data acquisition was started. If fuel was used in the test, approximately 0.77 L of JP-5 fuel was added to the test pan. This amount of fuel was used to provide sufficient separation between the fuel layer and the bottom of the test pan (approximately 12 mm). The weight of the fuel was recorded and then Load Cell #1 was tared again. If necessary, the pilot flame was lit and put into position. After a 30 second baseline, the foam was generated and added to the test pan. In cases where the foam was to be heated, the heater was moved over top of the test pan. The operator then bled solution from the secondary vessel as required to keep the solution level in the vessel at the control line. In tests with no fuel, the test was ended when less than 10% of the original mass remained in the test pan. In tests with fuel, the test was ended when the fuel ignited. Fires were extinguished by placing a noncombustible board over the pan.

A parametric study was performed using a single formulation of AFFF to determine what the impact of different variables was on the foam behavior when exposed to heat. The experimental variables considered in this study were

- Expansion Ratio
- Initial foam thickness
- Irradiance level
- Fuel beneath the foam
- Initial fuel temperature

Analysis of the results focused on the effects of the above variables on evaporation rate, drainage rate, foam thickness, thermal penetration through the foam,and time to fuel ignition. The error associated with such measurement was estimated through an error analysis (Appendix A). A summary of all the data is provided in Appendices B - D.

4.0 TEST RESULTS

A sample set of mass and temperature data from the apparatus is shown in Figs. 5 and 6. The mass data are shown normalized versus the initial foam mass per unit area, m_o''. This test was performed with foam at an expansion ratio of 6.0, initial foam thickness of 50 mm, irradiance level of 35 kW/m^2 and no fuel layer. At time equal to zero, the heater was placed over the test pan and foam was measured to evaporate from the pan. Evaporated mass is shown in Figure 5 to increase linearly with time, indicating a constant evaporation rate. Draining of solution from the pan was not started until the interface between the foam and drained solution was visually apparent, which was about 30 seconds into the test. In tests with a fuel layer, the draining process could be started immediately since the interface between drained solution and fuel was always visually apparent. The drain and evaporation mass curves were used to calculate drainage rate and evaporation rate, respectively, during the test.

The temperature data shown in Figure 6 provided both an indication of foam temperature distribution and information on the foam height. When the heater was placed over the foam, all thermocouples above the foam blanket (greater than 50 mm) measured temperatures of greater than 100°C. All temperatures less than 100°C were measured by thermocouples immersed in the foam blanket, which were initially all thermocouples at heights less than or equal to 50 mm. After 20 seconds of heating, the thermocouple at 75 mm begins to decrease from 175°C to a temperature of approximately 95°C. This was due to the foam blanket expanding from its initial height of 50 mm to 75 mm. As the heating continued, foam was evaporated and the foam height began to decrease. This is evident in Figure 6 by thermocouples in the lower part of the pan rising above 100°C. Foam height depletion rates were accurately determined using the thermocouples; however, a more refined array of thermocouples is necessary to accurately describe the expansion process. For this reason, results reported in this paper focus on the depletion of the foam after the initial expansion.

The data in Figs. 5 and 6 show that the foam behavior is quite complex since its mass, height and temperature are changing with time. The apparatus designed in this study was able to quantify the time variations in these variables. Using this apparatus, a series of tests were performed on one type of AFFF to determine the impact of initial conditions on the foam behavior.

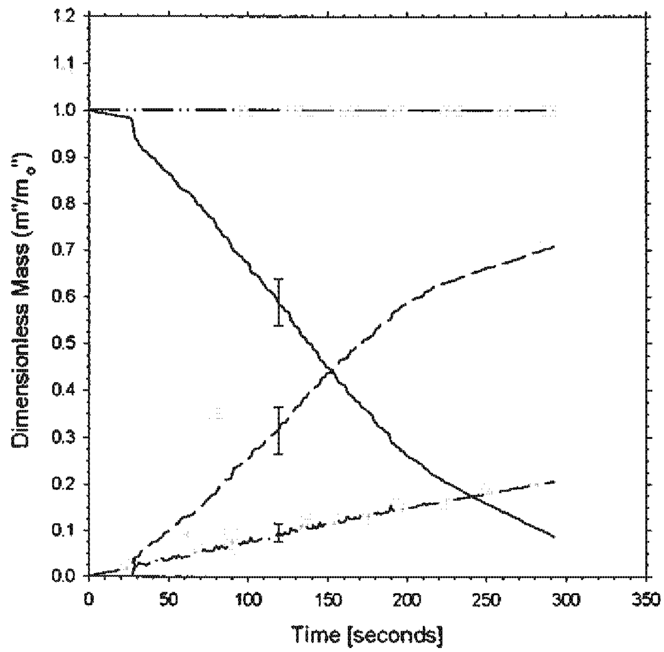

Figure 5. Sample data from the test apparatus showing the temporal variation in the mass in the pan (Foam) ( ), mass drained ( ), mass evaporated ( ) and mass balance ( ).

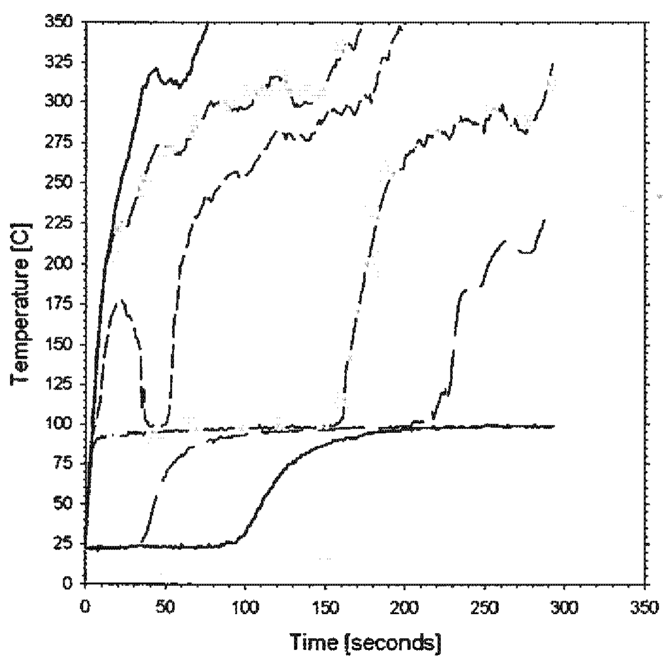

Figure 6. Sample data from the test apparatus showing the temporal variation in temperature within test pan containing foam. Distance from base of pan: 0 mm (—), 25 mm (— —), 50 mm (- · -), 75 mm (- -), 100 mm(- · · -), 125 mm (-).

4.1 Effect of Irradiance Level

The irradiance level incident on foam may affect the foam evaporation rate, drainage rate and height. To quantify the effect of irradiance, tests were performed exposing foams of different expansion ratios and foam heights to a range of irradiance levels. Analysis of the data showed the effect of irradiance on foams was similar for the different expansion ratios and foam heights evaluated. Effects of irradiance on evaporation rate, drainage rate and foam height are shown in Figs. 7-9, respectively. These data are from four different tests performed using a foam with an expansion ratio of 5.7±0.3, thickness of 75 mm, and initial mass of 14.4± 0.95 kg/m^2. In each test, the foam was exposed to a different irradiance level, 0, 20, 35, or 50 kW/m^2, for the entire test.

The evaporation rate of the foam during tests at these four irradiance levels is shown in Figure 7. As the irradiance level increases, the evaporation rate of the foam increases. This evaporation rate remains relatively constant during the test, but decreases slightly toward the end of the test. This was attributed to the gradual decrease in irradiance incident on the foam surface as the foam blanket surface depletes and subsequently gets further from the heater (see Figure 3).

The effect of irradiance level on the foam drainage rate is shown in Figure 8 plotted against the mass of foam per unit area. At time equal to zero, the foam mass per unit area is at a maximum and is equal to the initial foam load. As the test progresses, the foam mass per unit area decreases to zero due to evaporative and drainage losses. In the test at 20 kW/m^2, the peak in the data from 12.5-14.5 kg/m^2 was due to waiting too long to start bleeding off the drained solution and should be ignored. All of the tests with an irradiance incident on the foam were measured to have the same drainage rate. In fact, the drainage rate remains constant until a foam mass of approximately 3.0 kg/m^2. Below this, the drainage rate decreases linearly to an almost zero drainage rate at a foam mass of 1.5 kg/m^2. In the test with no irradiance, the drainage rate was equal to that measured in tests with irradiance down to a foam mass per unit area of 7.0 kg/m^2. As the test with no irradiance progressed, the drainage rate begins to decrease linearly to almost zero drainage at 1.5 kg/m^2.

The difference in the no irradiance data and irradiance data between foam mass levels of 7.0 and 1.5 kg/m^2 was partly attributed to the heating decreasing the foam solution viscosity and causing bubbles to coalesce or to expand and break [9]. The expansion and breaking of bubbles increases the amount of solution surrounding the remaining bubbles, decreasing the drainage resistance. Increasing the irradiance from 20 to 50 kW/m^2 was measured to have no effect on the drainage. This may be partly due to the foam temperature increasing to approximately 95°C and remaining at that temperature until the foam is depleted and the heating was sufficient to induce similar bubble breakage.

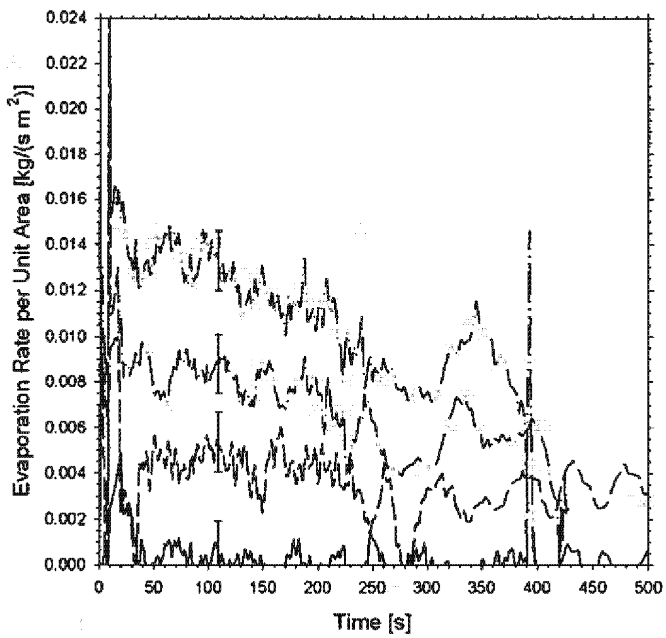

Figure 7. Foam evaporation rate per unit area at irradiance levels of (—) 0 kW/m^2, (– –) 20 kW/m^2, (– · –) 35 kW/m^2, and (– · · –) 50 kW/m^2. Foam: m_o''=14.4± 0.95 kg/m^2, h_o=75 mm, E=5.7 ±0.3. Fuel: JP-5 at T_i=20°C.

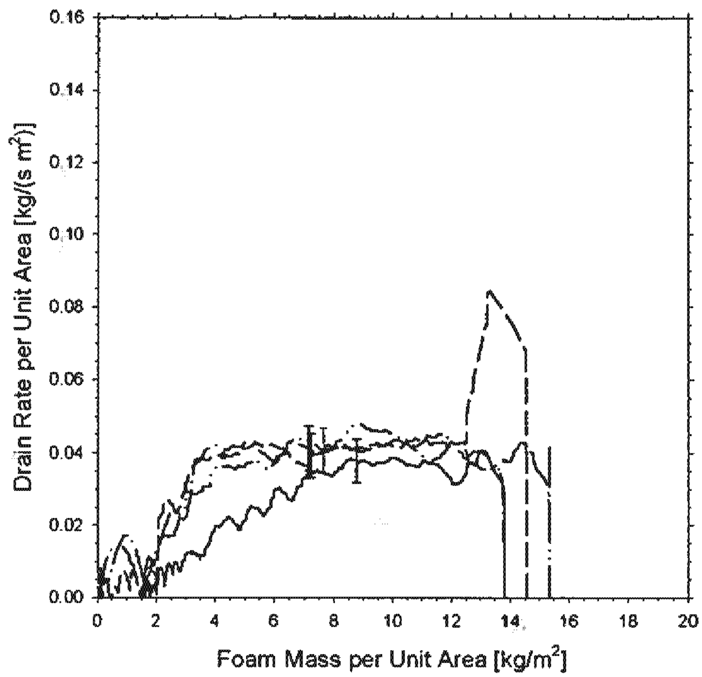

Figure 8. Foam drainage rate per unit area at irradiance levels of (—) 0 kW/m^2, (– –) 20 kW/m^2, (– · –) 35 kW/m^2, and (– · · –) 50 kW/m^2. Foam: m_o''=14.4±0.95 kg/m^2, h_o=75 mm, E=5.7 ±0.3. Fuel: JP-5 at T_i=20°C.

The change in foam height is shown in Figure 9 for tests with different irradiance levels incident on the foam. In tests with heating, the foam height was determined using temperature measurements in the pan as described previously. The foam height in the test with no irradiance was observed to be relatively constant throughout the test. Heating the foam caused dramatic changes in the foam height during the test. In the test with an irradiance of 50 kW/m^2, heating caused the foam to increase in thickness by 25 mm before decreasing in thickness. This phenomenon has been observed elsewhere [5,6,9] and is attributed to the rapid expansion of air inside the foam bubbles. The test average foam height depletion rate was measured to increase with an increase in irradiance.

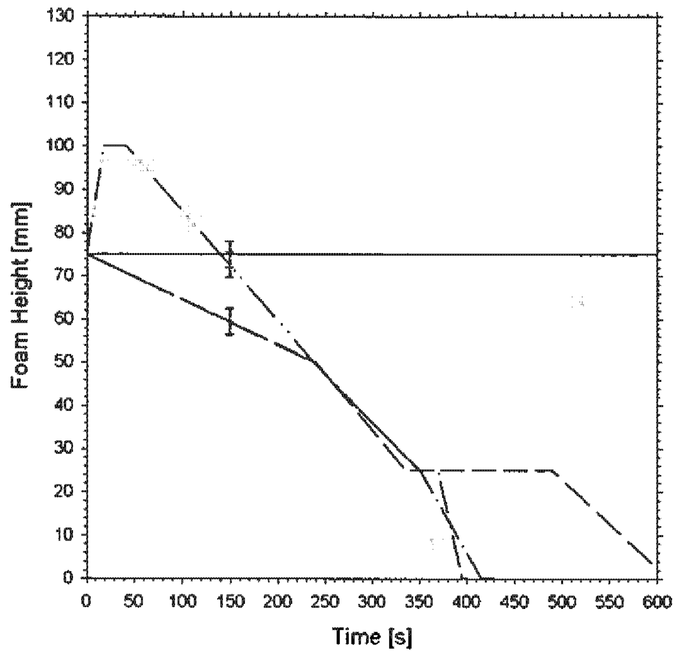

Figure 9. Foam height during tests at irradiance levels of (—) 0 kW/m^2, (- -) 20 kW/m^2, (- · -) 35 kW/m^2, and (- · · -) 50 kW/m^2. Foam: m_o''=14.4±0.95 kg/m^2, h_o=75 mm, E=5.7 ±0.3. Fuel: JP-5 at T_i=20°C.

4.2 Effect of Foam Mass

Drainage of solution from the AFFF foam evaluated in this study was initially driven by globally changed hydrodynamics to hydrostatics. Because of this, the mass and height of the foam contribute to the rate of drainage of the foam. Tests were performed with various foam expansion ratios and foam heights to study the impact of initial foam height on foam behavior.

Test results using foams having nominal expansion ratios of 6.0 and 9.7 were similar in trend but quantitatively different. Data on evaporation rate, drainage rate and foam height from a series of tests on foam with an expansion rate of 6.0 are shown in Figs. 10-12, respectively. These data were from three different tests with initial foam heights of 25, 50 and 75 mm. Tests were performed using foam at an expansion ratio of 5.9±0.3, an irradiance of 35 kW/m^2 and JP-5 fuel layer at an initial temperature of 20°C. The initial mass of foam was measured to range from 3.9 to 13.8 kg/m^2.

The initial foam mass did not affect the evaporation rate of the foam blanket, see Figure 10. With the irradiance level constant in these three tests, this result was expected.

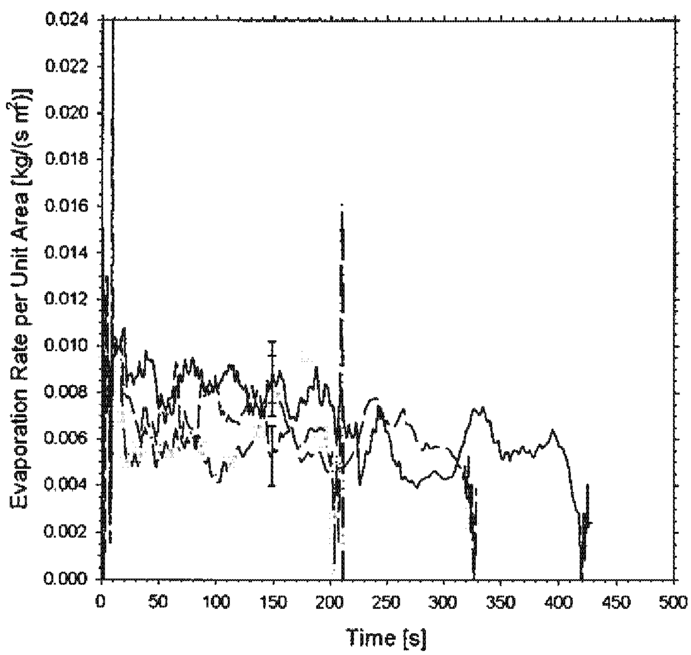

Figure 10. Evaporation rate per unit area during tests with (– · · –) h_o=25 mm and m''_o=3.9 kg/m^2, (– –) h_o=50 mm and m''_o=8.4 kg/m^2, and (—)h_o=75 mm and m''_o=13.8 kg/m^2. Foam: ER=5.9±0.3, q"=35 kW/m^2. Fuel: JP-5 at T_i=20°C.

The drain rate per unit area is shown plotted versus foam mass per unit area in Figure 11. The drain rate in all three tests was determined to follow a single curve, indicating that foam mass per unit area correlates with the drainage rate. Based on the data in the previous section, this curve is expected to be valid for this expansion ratio of foam for irradiance levels between 20 and 50 kW/m^2.

A similar result was measured for foam with an expansion ratio of 9.7 except the steady-state drainage level was 0.028 kg/(s m^2). For both expansion ratios, drainage rate was measured to begin decaying at a foam mass of approximately 3 kg/m^2.

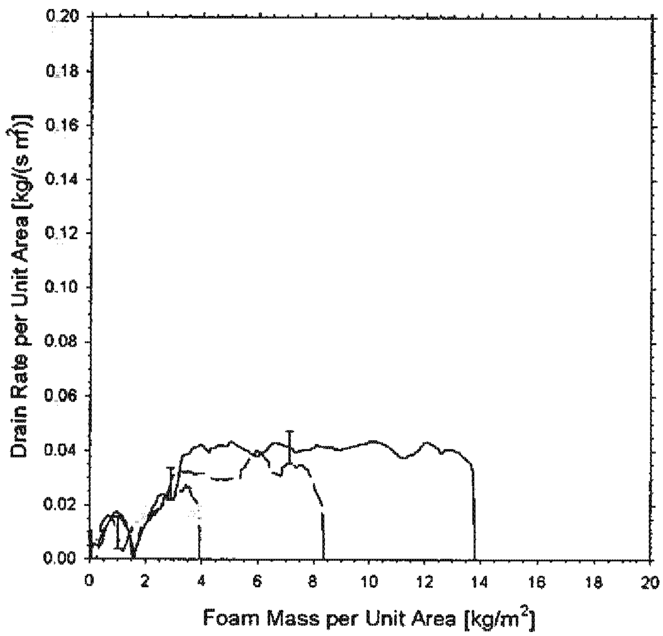

Figure 11. Drain rate per unit area during tests with (– ·· –) h_o=25 mm and m''_o=3.9 kg/m^2, (– –) h_o=50 mm and m''_o=8.4 kg/m^2, and (—) h_o=75 mm and m''_o=13.8 kg/m^2. Foam: ER=5.9±0.3, q"=35 kW/m^2. Fuel: JP-5 at T_i=20°C.

The foam thickness measured during these tests is shown in Figure 12. After the initial expansion period during the first 150 seconds of the test, the foam depletion rate was measured to be 0.37 ± 0.04 mm/s for all tests.

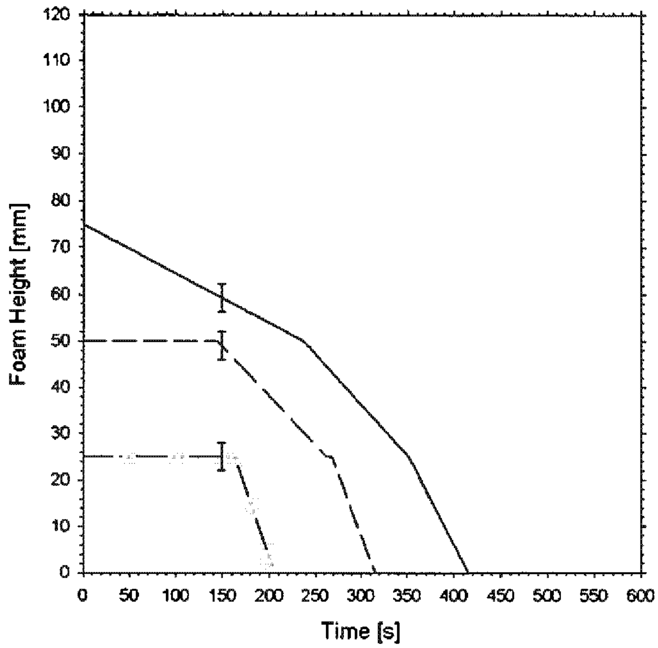

Figure 12. Foam height during tests with (– · · –) h_o=25 mm and m''_o=3.9 kg/m^2, (– –) h_o= 50 mm and m''_o=8.4 kg/m^2, and (—)h_o=75 mm and m''_o=13.8 kg/m^2. Foam: ER=5.9± 0.3, q"=35 kW/m^2. Fuel: JP-5 at T_i=20°C.

In tests with an expansion ratio of nominally 3.3, the evaporation rate and foam height behaved similar to tests with higher expansion ratios, but the drainage rate was different. Figure 13 is a plot of the drainage rate per unit area versus the foam mass per unit area for tests using a foam at an expansion ratio of 3.0±0.2, an irradiance of 35 kW/m^2 and JP-5 initially at 20°C. The initial mass of the foam was measured to be 6.0, 12.0, and 28.0 kg/m^2 for foam heights of 25, 50 and 75 mm, respectively. Unlike tests with higher expansion ratio foams, the data were not measured to collapse to a single curve. This was attributed initially to having a large amount of solution in the foam (i.e., high foam liquid content) that can readily drain from the foam.

The effects of foam liquid content can be seen by comparing the 25 mm thick foam drainage rate data in Figure 13 with the other foam data shown in the plot. With a foam mass per unit area of 4-6 kg/m^2, the 25 mm thick foam drainage rate was measured to be 0.12-0.18 kg/(s m^2). This is 3-5 times greater than the drainage rate measured for the other two tests with foams 50 mm and 75 mm thick. The 50 and 75 mm thick foams had been losing mass through drainage and evaporation for 50 seconds and 120 seconds, respectively, before reaching a foam mass per unit area of 4-6 kg/m^2. As a result, these foams had less solution per unit volume compared with the foam just added in the 25 mm thick foam test. All data do collapse to a single line at a foam mass per unit area of approximately 3 kg/m^2.

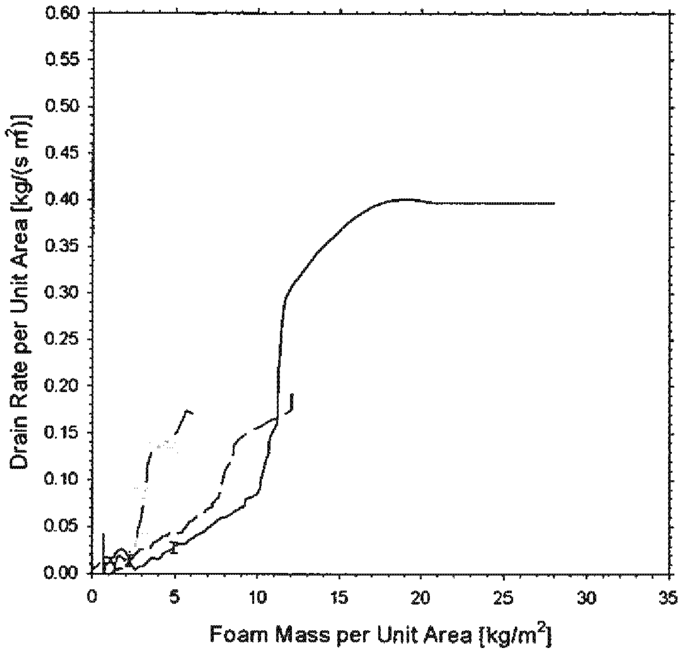

Figure 13. Drain rate per unit area during tests with (– · · –) h_o=25 mm and m''_o=6.0 kg/m^2, (– –) h_o=50 mm and m''_o=12.0 kg/m^2, and (—) h_o=75 mm and m''_o=28.0 kg/m^2. Foam: ER=3.0±0.2, q"=35 kW/m^2. Fuel: JP-5 at T_i=20°C.

4.3 Effects of Foam Liquid Content

The results in the previous section indicate that foam behavior, in particular the foam mass drainage, is affected by the foam liquid content. The effect of foam liquid content on drainage rate was evaluated by comparing test results with foams having expansion ratios of 3.3, 6.0 and 9.7. All tests had a foam height of 75 mm, an irradiance of 35 kW/m^2 and JP-5 at an initial temperature of 20°C.

The plot of drain rate shown in Figure 14 clearly demonstrates the variation in the drainage rate for foams of different expansion ratios. The low expansion ratio foam (ER=3.3) initially has a drain rate an order of magnitude higher than that measured for the higher expansion ratio foams. As the foam mass decreases from 20 kg/(s m^2) to 10 kg/(s m^2), the foam appears to go through a transition from draining like a liquid to draining at a rate similar to a foam. Below a foam mass of 10 kg/m^2, the foam drains at a rate similar to the other foams. There was a 40% difference between the steady-state drainage rate of the foams at expansion ratios of 6.0 and 9.7.

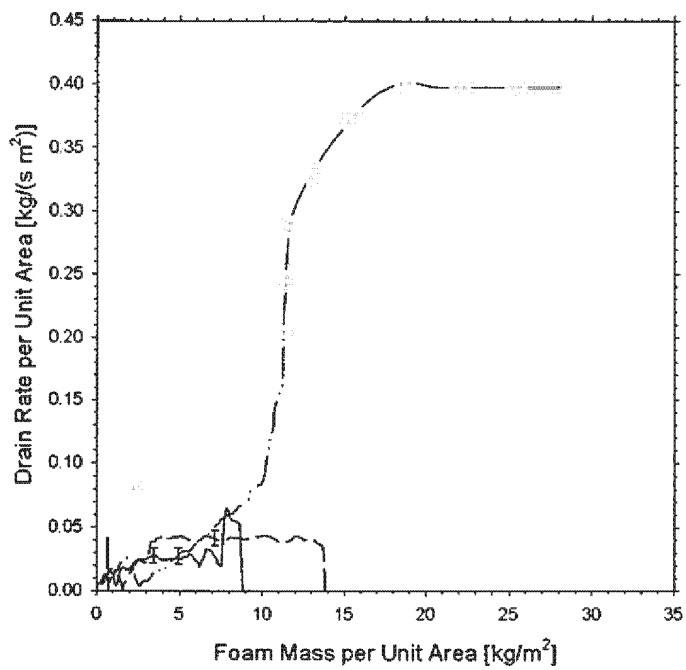

Figure 14. Drain rate per unit area during tests with (– · · –) ER=3.3 and m''_o=28 kg/m^2, (– –) ER=6.0 and m''_o=13.9 kg/m^2, and (—)ER=9.7 and m''_o=8.9 kg/m^2. Foam: h_o=75 mm, q"=35 kW/m^2. Fuel: JP-5 at T_i=20°C.

4.4 Effect of Fuel Layers

Interfacial surface tension measurements between fuel and AFFF foam indicate that there is some resistance to drained solution falling through the fuel surface. A series of tests was performed to determine whether this resistance is significant enough to change the mass drain rate of the foam. Tests were performed using JP-5 fuel for two reasons. First is that JP-5 is less flammable than other fuels typically used in evaluating AFFF (e.g., *n*-heptane). The second reason was that the interfacial surface tension between JP-5 and 6% AFFF solution (4.4 dynes/cm) was higher than that of *n*-hexane and 6% AFFF solution (3.0 dynes/cm) and most other fuels [10]. Thus, JP-5 would provide a bounding estimate on the effect of the fuel layer on the foam drainage. Tests were performed with JP-5 at initial temperatures of 20°C and 100°C.

A comparison of the drain rate from tests with foam only, foam over JP-5 at 20°C, and foam over JP-5 at 100°C is shown in Figure 15. Tests were performed with an initial foam height of 50 mm, foam expansion ration of 5.7±0.4, initial mass of 9.3±1.8 kg/m^2, and irradiance level of 20 kW/m^2. The spike in the drain rate during the foam only test was due to bleeding off the drained solution that had accumulated before the interface between the foam and the solution was visually evident. In tests with the fuel layer, the interface between the fuel and drain solution was always apparent. This allowed the operator to immediately begin bleeding off drained solution. Disregarding the spike in the foam only data, the drain rate was the same in all three tests. The drain rate remained constant until the foam mass had been reduced to 3 kg/m^2, at which point it decayed linearly to zero at a mass of 1.5 kg/m^2.

From this data, the presence of fuel does not have an impact on the drain rate. This was due to the amount of solution draining from the foam being greater than the minimum amount of solution necessary to drop through the fuel surface.

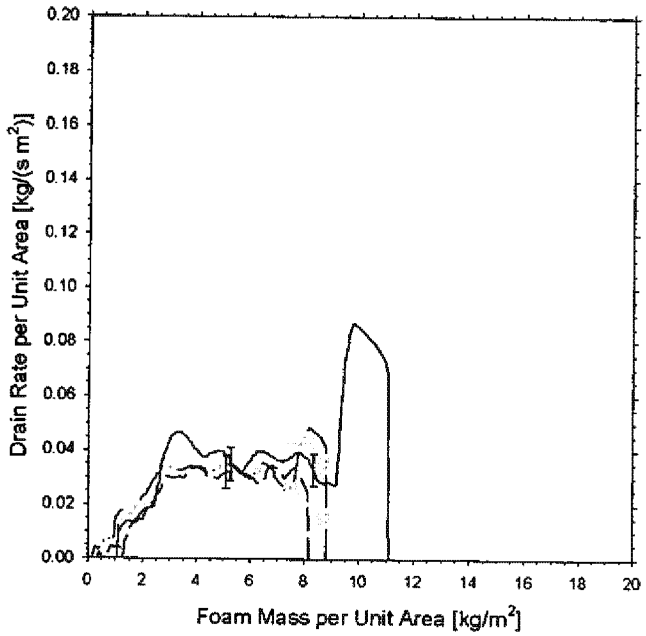

Figure 15. Comparison of drainage rate per unit area in tests with (—) foam only, (- - -) foam on JP-5 at T_i=20°C, and (- · · -) foam on JP-5 at T_i=100°C. m_o"=9.3±1.8 kg/m^2, ER= 5.7±0.4, h_o=50 mm, and q"=20 kW/m^2.

An estimate of the minimum amount of solution necessary for drop through was measured in a drop through test described in Appendix E. In this test, the bottom 25 mm of the container was filled with fuel, and solution was added directly to the fuel surface using a syringe. The syringe was also used to monitor the level of solution added to the fuel. Tests were performed adding the solution at a single location and at various random locations on the surface. A summary of some of the test results is provided in Table 2 for tests performed with the fuel at 20°C. Of the fuel tested, JP-5 required the most solution to cause the first drop to fall through the surface while n-heptane required the least. These results correlate well with the interfacial surface tension between the fuel and AFFF, see Table 3 and Appendix F. Less solution had to be added to the surface to cause subsequent drops to fall through. The amount to cause subsequent drops to fall through the surface ranged from 0.0056-0.0076 and was independent of fuel type. Comparing these results to drain rate data taken in the foam loss tests, fuel may cause a 1-2 second delay in the initial draining of the slowest draining foam tested (9.7 expansion ratio foam). However, after this initial drop falls through the surface, fuel is not expected to have an impact on the drain rate until it falls well below 0.0056 kg/(s m^2). This drain rate was not measured until nearly all of the foam had drained from the test pan. These results support the data shown in Fig. 15, which indicate the fuel has no impact on the foam drain rate.

Table 2. Minimum AFFF Solution Necessary for Drop Through with Fuel at 20°C.

Fuel Type	Addition Method	1st Drop		Subsequent Drops	
		Critical Volume [μL]	Critical Mass per Unit Area [kg/m^2]	Critical Volume [μL]	Critical Mass per Unit Area [kg/m^2]
n-Heptane	Single	45	0.0045	31	0.0031
n-Heptane	Random	65	0.0065	76	0.0076
Cyclohexane	Single	163	0.0163	27	0.0027
Cyclohexane	Random	395	0.0395	39	0.0039
JP-5	Single	192	0.0192	56	0.0056
JP-5	Random	646	0.0646	32	0.0032

Table 3. Surface Tension Data

Fuel	Fuel Temp. [C]	AFFF Temp. [C]	Interfacial Surface Tension [dynes/cm][1]	Spreading Coefficient [dynes/cm][1]
n-Heptane	25	25	3.40	0.76
n-Heptane	25	25	3.40	0.76
JP-5	25	25	4.43	5.20
JP-5	25	25	4.43	5.20
Cyclohexane	25	25	3.48	5.21
Cyclohexane	25	25	3.48	5.21

[1]From Ref. [10] with data taken at 25°C

Drop through tests were also performed with *n*-heptane and JP-5 at elevated temperatures (50°C). In these tests, solution at ambient temperature (20°C) and at elevated temperature (~50°C) was observed to drop directly through the fuel surface upon addition. This result is different than what would be expected from the spreading coefficient data. Leonard *et al.* [10] reported that increasing the temperature does not have a significant effect on the spreading coefficient, unless the spreading coefficient is close to zero. The spreading coefficient for *n*-heptane is close to zero, but the JP-5 value is not. However, in both cases the solution drops directly through the surface, which would be consistent with a system having a negative spreading coefficient.

4.5 Foam Depletion

Foam exposed to heat has been shown to initially increase in height due to expansion and then be depleted in height as the heating continues. Using the foam height data determined from thermocouple measurements, foam height depletion rate was calculated for each test. Average depletion rates were determined by averaging over the entire period when the foam height was being depleted. Average values were determined to be within 40% of instantaneous values. These average values also made it convenient to determine which variables have an impact on the foam height depletion rate. Since there were more thermocouples in the foam during tests with foam only, tests with foam only was used in this analysis. Results from tests with a JP-5 layer were found to have trends similar to those measured in the foam only tests.

The average foam height depletion rate data were from tests using foams with three different expansion ratios, three different foam height and three irradiance levels. Foam height depletion rate was found to be sensitive to irradiance but not to initial foam height. For this reason, data from tests with different foam heights but fixed expansion ratio and irradiance were averaged. Figure 16 shows the average foam height depletion rates from tests at different expansion ratios and at different irradiance levels. This graph shows that the foam height depletion rate increases with an increase in irradiance. Foam expansion ratio does not have a significant impact on the foam height depletion rate.

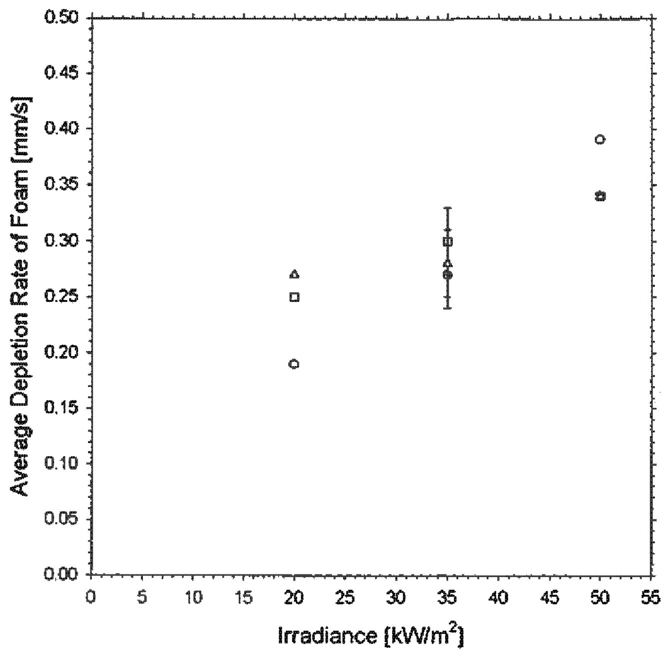

Figure 16. Effect of irradiance level on the average foam height depletion rate using foams with an expansion ratio of (O) 3.3, (☐) 6.0, and (△) 9.7.

4.6 Heat Penetration

Heat penetration through the foam was measured in tests with no fuel layer in the pan. The heat flux measured in this test is the total heat flux, which was a combination of radiation being transmitted through the foam and heat flux from heated foam. This heat flux provides an indication of the heat flux levels transmitted through the foam to the fuel during a fire.

A conservative estimate of how well the foam is protecting the fuel from heat is the time necessary for initial heat penetration. Here time for initial heat penetration was taken as the time at which the heat flux had reached 1 kW/m^2. Table 4 contains the results from tests where heat flux measurements were made. Under the initial heat penetration data column, the time for initial heat penetration is provided along with the foam height and foam mass per unit area at this time. These data indicate that the foam height and foam mass per unit area at initial heat penetration were at nominally the same level in all tests. Foam height was 50±7 mm and the foam mass per unit area was approximately 4.2±1.2 kg/m^2.

Heat penetration times increased with an increase in foam thickness for all foam expansion ratios tested. For foams with an expansion ratio of 9.7, the heat penetration time increased with an increase in irradiance level. This was attributed to the expansion of the foam in the initial part of the test.

Table 4. Initial Heat Penetration through Foam

Expansion Ratio	Irradiance [kW/m^2]	Initial Foam Height [mm]	Initial Foam Mass per Unit Area [kg/m^2]	Initial Heat Penetration Data		
				Time [s]	Foam Height [mm]	Foam Mass per Unit Area [kg/m^2]
3.3	20	25	11.5	40	25	3.2
3.3	20	50	19.8	84	52	5.2
3.3	20	75	28.4	101	43	5.9
3.3	35	25	10.8	35	25	2.8
3.3	35	50	18.2	85	51	6.0
3.3	35	75	29.2	109	51	7.0
3.3	50	25	8.9	32	45	3.0
3.3	50	50	17.6	78	49	4.4
3.3	50	75	28.8	103	49	5.5
6	20	25	5.7	76	50	4.4
6	20	50	11.1	163	44	5.5
6	20	75	15.5	218	60	6.7
6	35	25	6.1	64	47	4.5
6	35	50	11.0	135	56	5.7
6	35	75	16.0	184	57	6.3
6	50	25	6.4	54	49	4.9
6	50	50	10.8	129	58	5.4
6	50	75	15.8	196	58	5.4
9.7	20	25	3.5	40	70	2.8
9.7	20	50	6.7	94	48	3.9
9.7	20	75	9.4	129	53	4.2
9.7	35	25	4.1	48	25	3.3
9.7	35	50	6.7	99	50	3.6
9.7	35	75	9.7	157	58	3.8
9.7	50	25	3.9	50	50	2.9
9.7	50	50	7.3	104	55	3.7
9.7	50	75	10.0	161	54	3.2

4.7 Ignition Time of Fuel

The time to ignite the JP-5 layer was recorded in all of the tests performed with a fuel layer in the test pan. These tests included foams at different expansion ratios, initial heights, different irradiance levels and different initial fuel temperatures. In tests with no irradiance, no sustained ignition was observed, but flashes were observed in tests with JP-5 initially at 100°C. In tests with irradiance, flashes were observed prior to sustained ignition. At sustained ignition, nearly all of the foam (less than 0.86 kg/m^2 or 0.035 kg) had evaporated or drained from the fuel surface.

Sustained ignition time results for these tests are shown in Figure 17 plotted versus initial foam height. Open symbols correspond to tests at an irradiance of 20 kW/m^2 while closed symbols are tests at 50 kW/m^2. This plot shows that increasing the foam height increases the time to ignition. At a particular foam height, the time to ignition appears to be relatively insensitive to foam expansion ratio and fuel temperature.

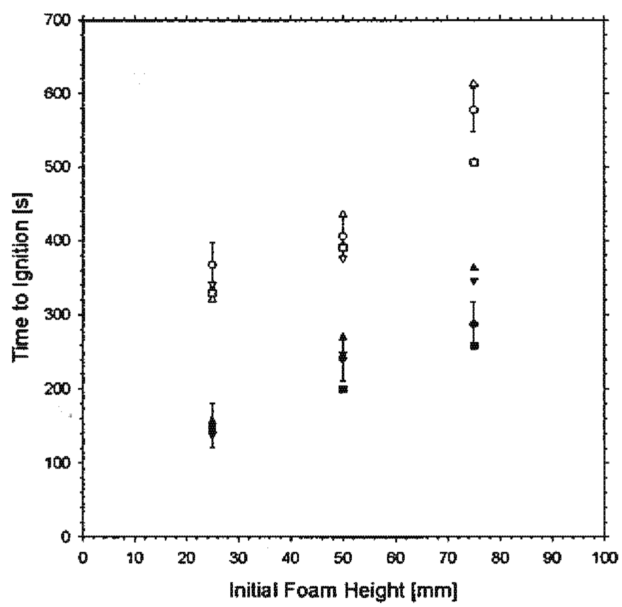

Figure 17. Time to ignite JP-5. Open symbols were tests at 20 kW/m^2 while closed symbols were tests at 50 kW/m^2. (O) ER=3.3 with JP-5 at 20°C, (□) ER=9.7 with JP-5 at 20°C, (Δ) ER=6.0 with JP-5 at 20°C, (Δ) ER=6.0 with JP-5 at 100°C.

5.0 DISCUSSION

The focus of this work was to design a test apparatus that was capable of developing input data for a predictive foam performance model. Using the trends in the data presented in the previous section, some additional analysis was performed to cast the data in terms that may be easier to input into models.

5.1 Evaporation

Evaporation rate of the foam was shown in Figs. 7 and 10 to be a function of the irradiance level on the foam. During fire fighting activities, foam sprayed onto pool fires may experience a range of heat fluxes depending on the location of the foam relative to the fire and surroundings. The heat of vaporization of the foam is defined as

$$\Delta h_v = \frac{q''_{net}}{\dot{m}''_{evap}} \qquad (1)$$

where q''_{net} is the net heat flux into the foam and $\dot{m}''_{evap}$ is the foam evaporation rate per unit area. This relates the net heat flux into the foam necessary to vaporize 1 kg/(s m^2) of solution. The difficulty in using actual heat of vaporization for predicting evaporation mass loss rate is that the heat flux absorbed by the foam needs to be known. Assuming that the heat transfer is dominated by radiation, the absorbed heat flux can be determined if both the reflectance and transmittance of the foam are known. To avoid having to determine the radiation properties, it is convenient to define an effective heat of vaporization that uses the irradiance, q''_{IRR} as the heat flux in the numerator,

$$\Delta h_{v,eff} = \frac{q''_{irr}}{\dot{m}''_{evap}}. \qquad (2)$$

Effective heat of vaporization values will be greater than the actual heat of vaporization because the irradiance is greater than the heat flux absorbed by the foam, but the effective heat of vaporization can be used directly in calculations without knowledge of foam radiation properties.

For all of the tests performed in this study, the effective heat of vaporization for this particular formulation of AFFF was determined to be 4.87±0.75 MJ/kg. This value is slightly higher than the value of 4.0 MJ/kg determined in Refs. [5,6] for AFFF. The reason for the discrepancy is unknown, but may be partly due to differences in the types of AFFF used in these studies. With AFFF being mostly water, the heat of vaporization for water should be nearly the same as that of the AFFF. The value for water is 2.26 MJ/kg, which is approximately 46% of the value for AFFF. This difference was attributed to the calculation of the effective heat of vaporization being performed with the irradiance, q''_{IRR} incident on the foam and not the net heat flux absorbed into the foam. Assuming no convection, the data imply a foam absorbance of α=0.46±0.06. Interestingly, this value is relatively close to that of snow α=0.35 [11].

5.2 Drainage

The drainage rate of solution from the foam is far more difficult to predict than the evaporation rate. Drainage rate may be affected by the fluidity of the foam and the hydrostatics of the foam layer. Foam fluidity was altered in these test in two ways: 1) raising the temperature of the foam and 2) reducing the foam expansion ratio. The hydrostatics of the foam were varied in this study by changing the pressure force causing the drainage, which was experimentally varied through the foam height and expansion ratio. Foam drainage is a dynamic phenomena so neither liquid content or the hydrostatics remain constant during the life of the foam. However, the test data show some trends that may make modeling of some of these foams significantly easier.

Exposing foams to heat was shown in Figure 8 to increase the foam drainage rate. Initially heated and unheated foams drain at nominally the same rate, but the unheated foam drains slower than the heated foam at lower foam mass levels. The higher drainage rate in tests with foam exposed to heat was attributed to both the solution viscosity decreasing due to an increase in temperature and bubbles expanding and bursting. Bursting of bubbles causes the solution from the burst bubble to drain down into the remaining foam. This increases the amount of solution between the bubbles allowing drainage to occur more readily. The impact of burst bubbles is more apparent in Figure 8 at lower foam mass levels because the unheated foam becomes "dry," causing the drainage rate to become slower than the heated cases where bubbles are bursting. The drainage rate was measured to be similar in tests where the foam was heated at different irradiances. However, tests with no heating were measured to drain at a different rate compared to tests with heating. These results are similar to those measured in Ref. [5,6] for AFFF.

Decreasing the expansion ratio of the foam both decreases the foam liquid content and increases the hydrostatic forces driving the drainage process. From hydrostatics, the pressure difference

$$\Delta P \propto \rho g h, \tag{3}$$

that is driving the drainage of foam is proportional to the foam density, ρ, the gravitational constant, g and a height, h. This can be redefined as being proportional to the foam mass per unit area, m'',

$$\Delta P \propto g m''. \tag{4}$$

The relation in Eqn. (4) indicates that the velocity of the foam drainage is proportional to the foam mass per unit area. As a result, foams at lower expansion ratios (i.e., more mass per unit area and higher foam liquid content) were anticipated to have higher drainage rates. This effect is clearly shown in Figure 14.

For foams with expansion ratios between 6 and 10 and this formulation of AFFF, the effect of expansion ratio on drainage rate was measured to be small. The drain rate was measured to be constant down to a foam mass per unit area of $\dot{m}'' \sim 3.0$ kg/m^2. Below a foam mass per unit area of 3.0 kg/m^2, the drain rate was measured to decrease linearly to near zero at $\dot{m}'' \sim 1.5$ kg/m^2. The magnitude of the constant level of drain rate was measured to vary slightly with expansion ratio, (a value of 0.04 kg/(s m^2) at an expansion ratio of 6.0 and 0.028 kg/(s m^2) at an expansion ratio of 9.7). The drainage rate per unit area versus foam mass per unit area curve developed using a foam height of 75 mm was shown in Figure 11 to be valid for foam heights equal to or less than 75 mm. From these data, it appears that the drainage rate of foam at a particular expansion ratio can be characterized using a single curve measured using the apparatus with a 75 mm thick foam. Additional testing needs to be performed to verify this for other concentrates.

The drainage rate of foams with a low expansion ratio (3.3) was not as well behaved as those at higher expansion ratios. For foam at an expansion ratio of 3.3, the drainage rates measured in tests with different initial foam heights were shown in Figure 13 to not collapse to a single curve. Instead, these low expansion ratio foams always initially drain at a rate that was 4-10 times higher than foams at higher expansion ratios. The low expansion ratio foams then appear to transition to a lower drainage rate, which may be due to the foam liquid content being low enough for bubbles to retard the drainage of solution. These initial and transition periods occur over a relatively short period of the foam life, within the first 20-60 seconds of the test depending on the initial foam mass per unit area. After this transition, the foam becomes "dry" and begins draining at rates similar to higher expansion ratio foams. The drainage rate of the lower expansion ratio foams is clearly more difficult to predict, and drainage rate curves at various heights appear to be required to characterize the drainage performance.

Tests were performed with and without a JP-5 fuel below the foam layer. In tests with fuel, the initial fuel temperature was tested at both 20°C and 100°C. From these tests, the fuel was not measured to have an impact on the drainage rate. These results are considered to be somewhat bounding since the interfacial surface tension between JP-5 and AFFF was higher than most other fuels.

5.3 Foam Height Depletion, Heat Penetration and Fuel Ignition

Foam height depletion rate was measured to be primarily a function of the irradiance level incident on the foam. As irradiance increased, the foam height depletion rate increased from 0.23 mm/s at 20 kW/m^2 to 0.35 mm/s at 50 kW/m^2. Foam height depletion rate was not measured to be dependent on initial foam height or expansion ratio. These results indicate that the depletion rate of foam height in a fire can be estimated knowing the irradiance from the fire. This estimate is conservative since it does not account for the initial foam expansion that occurs during the initial 30-60 seconds of the test.

Heat penetration through the foam was measured to be a function of foam height and foam mass. For all of the different tests where heat penetration was measured, the data indicate that heat begins penetrating through the foam when the foam becomes approximately 50±7 mm thick and has a foam mass of 4.2±1.2 kg/m^2.

Ignition time of JP-5 fuel layers was measured to be a function of both irradiance and initial foam height. Increases in irradiance and decreases in initial foam height were determined to decrease the time to ignition. This result was found to be independent of expansion ratio and initial fuel temperature. At ignition nearly all of the AFFF (less than 0.8 kg/m^2) had been lost from the fuel surface. This result indicates that the prediction of fuel ignition may be possible using a mass balance of the foam layer on the fuel.

Large-scale fire testing [12-15] has shown that, at a given foam flow rate, low expansion ratio (ER=3) AFFF foam produced using non-aspirated nozzles are able to control fires in a shorter amount of time than higher expansion ratio AFFF foams (ER>6.0) produced by aspirated nozzles. Small-scale foam loss test results indicate the opposite trend.

Small-scale test results in this report indicate nearly all AFFF must be lost from the surface before fuel ignition will occur. If it is assumed that fire control is achieved when some solution is present on the fuel surface, the control time should be related to the loss mechanisms of the foam. Foam losses were measured to be higher in tests with lower expansion ratios, indicating that more of the lower expansion ratio foam would be required to prevent ignition (i.e., control the fire). The small-scale ignition data also supports this result. In tests with the same foam height but different foam expansion ratios, the ignition time was approximately the same. These results indicate that the fire control time is also dependent on the dynamics of the system and not just the static behavior of the foam. For an overall foam performance based model, both the foam loss and foam spread behavior must be considered to provide accurate predictions of foam behavior in fire environments.

6.0 SUMMARY /CONCLUSION

A test apparatus was designed and used to measure the behavior of foam when exposed to different irradiance levels. The apparatus provided data on evaporation rate, drainage rate, foam destruction rate, foam temperature, heat penetration and time to fuel ignition. Using this apparatus, the performance of a single AFFF formulation (6% 3M AFFF) was characterized. These results may be specific to this particular type of concentrate, and tests need to be performed to characterize the performance of other concentrates.

Evaporation rates were measured to be primarily a function of irradiance, making it possible to predict evaporation using the irradiance from the fire and an effective heat of vaporization. The AFFF foam evaluated in this study was determined to have an effective heat of vaporization of 4.87±0.75 MJ/kg.

Foam drainage rate was measured to be insensitive to the irradiance level or the presence of a fuel layer below the foam. For foams with expansion ratios ranging from 6-9.7, drain rate was determined to be a function of foam mass per unit area. A single curve developed with a foam thickness of 75 mm characterized the drain rate for all foams equal to or less than 75 mm. The drainage rate was measured to be constant down to a foam mass per unit area of 3.0 kg/m^2 and decreased linearly to zero by 1.5 kg/m^2. The steady state drain rate level decreased from 0.04 $kg/(s\ m^2)$ to 0.028 $kg/(s\ m^2)$ by increasing the expansion ratios from 6.0 to 9.7, respectively.

The drainage rate of low expansion ratio foams (3.3) was as much as 4-10 times higher than levels measured at higher expansion ratios. The drainage of low expansion ratio forms (3.3) was as much as 4-10 times higher than the levels measured at higher expansion rates were attributed to the foam liquid content. Drainage measurements of foams at different expansion ratios and temperatures are necessary to further understand these trends in the data at low expansion ratios.

Foam height depletion rate was measured to be primarily a function of the irradiance level incident on the foam. As irradiance increased, the foam height depletion rate increased. Foam height depletion rate measurements were not dependent on initial foam height or expansion ratio. Initial foam height and expansion ratio were not measured to influence the foam height depletion rate.

Heat penetration through the foam was measured to be a function of foam height and foam mass. For all of the different tests where heat penetration was measured, the data indicate that heat begins penetrating through the foam when the foam becomes approximately 50±7 mm thick and has a foam mass of 4.2±1.2 kg/(s m^2).

Ignition time in tests with JP-5 fuel layers was measured to be a function of both irradiance and initial foam height. Increases in irradiance and decreases in initial foam height were determined to decrease the time to ignition. This result was found to be independent of expansion ratio and initial fuel temperature. At ignition nearly all of the AFFF (less than 0.8 kg/m^2) had been lost from the fuel surface. This result indicates that the fire containment may be possible using a mass balance of the foam layer on the fuel.

Small-scale evaluation of loss mechanisms in foams exposed to heat alone was determined to be inadequate to predict control times of foams in large-scale fires. Test data on foam spread on fuel surfaces need to be developed to adequately predict foam performance in full scale testing.

7.0 RECOMMENDATIONS

A small-scale test apparatus for measuring foam spread characteristics needs to be developed. The apparatus needs to be designed so that it not only provides spreading data for various foams but also provides the input necessary for modeling foam fire extinguishment. Initial tests should be performed on the AFFF concentrate evaluated in the small-scale foam loss test apparatus.

The foam extinguishment model needs to be further evaluated using the small-scale test data developed from the foam loss apparatus and the foam spread apparatus. In this evaluation, the model will be refined to ensure that the foam spread physics observed in the testing are being represented in the model. Initial validation of the model will be performed with intermediate scale fire tests that have been conducted using the single formulation AFFF considered in the small-scale testing.

Additional small-scale testing needs to be performed to quantify the foam losses and foam spread characteristics of other concentrates and to determine the impact of different experimental variables on the test results. Foam loss and spread data are expected to be concentrate dependent, and these data are necessary to further validate the performance of the foam extinguishment model. In order to develop a standard procedure for evaluating foam, additional tests need to be performed to determine the impact of foam generation techniques and fuel types used in the testing. The results will serve as guidance in the final development of the test procedures.

After validating the foam extinguishment model performance for a wide range of foam formulations, the model should be validated with larger scale test results. This effort may require performing large-scale fire tests that have been designed and instrumented to provide data for model validation. This would include measuring foam application rates, established foam blanket area, heat flux and temperature near the fuel and local velocities. With the validated model, researchers could estimate the extinguishing performance of new foam formulations during large-scale fires.

If necessary, additional research may be required to develop a more microscopic understanding of foam structure during the heating process. This would include investigating the effects of foam liquid content on the drainage and spreading processes, and the impact of bubble behavior (coalescing, expanding and bursting) on drainage and foam spread.

Acknowledgements

The authors are very appreciative to Mr. Dave Waller and Mr. Brian Cade for performing many of the experiments.

8.0 REFERENCES

1. Scheffey, J.L., Hanauska, C.P., Burns, R.B. and Williams F.W., "Status Report on the Development of an Environmentally Improved AFFF," NRL Ltr Rpt Ser 6180/0060, 11 March 1997.

2. NFPA 11, "Standard for Low Expansion Foam," National Fire Protection Association, Quincy, Massachusetts, (1998).

3. MIL-F-24385F, "Fire Extinguishing Agent, Aqueous Film-Forming Foam (AFFF) Liquid Concentrate for Fresh and Sea Water," Military Specification, January, 7, (1992).

4. Scheffey, J.L. and Wright, J.A., "Analysis of Test Criteria for Specifying Foam FireFighting Agents for Aircraft Rescue and Firefighting," FAA technical Report, DOT/FAA/CT-94/04, Atlantic City, NJ, August 1994.

5. Ikasson, S. and Persson, H., "Fire Extinguishing Foam – Test Method for Heat Exposure Characterisation," SP Report 1997:09, Swedish National Testing and Research Institute, Boras, Sweden, (1997).

6. Persson, H., "Fire Extinguishing Foams-Resistance Against Heat Radiation," SP Report 1992:54, Swedish National Testing and Research Institute, Boras, Sweden, (1992).

7. Persson, B. and Dahlberg, M., " A Simple Model of Foam Spreading on Liquid Surfaces," SP Report 1994:27, Swedish National Testing and Research Institute, Boras, Sweden, (1994).

8. Hanauska, C.P., Scheffey, J.L., Roby, R.J. and Gottuk, D.T., "Improved Formulations of Firefighting Agents for Hydrocarbon Fuel Fires," SBIR Phase I Final Report for U.S. Air Force, January, (1994).

9. Tafreshi, A.M., di Marzo, M., Floyd, R. and Wang, S., "Fire Protection Foam Thermal Physical Properties," NIST-GCR-98-742, U.S. Department of Commerce, NIST / BFRL, 101 p., (1998).

10. Leonard, J.T. and Burnett, J.C., "Suppression of Evaporation of Hydrocarbon Liquids and Fuels by Containing Aqueous Film Forming Foam (AFFF) Concentrate FC-196," NRL Report 7842, Naval Research Laboratory, Washington, D.C., (1974).

11. Siegel, R. and Howell, J.R., *Thermal Radiation Heat Transfer*, Third Edition, Hemisphere Publishing Corporation, Washington, (1992).

12. Jablonski, E.J., "Comparative Nozzle Study for Applying Aqueous Filmforming Foam on Large Scale Fires," U.S. Air Force Report CEEDO-TR-78-22, April, (1978).

13. Geyer, G.B., "Evaluation of Aircraft Ground Firefighting Agents and Techniques," Technical Report AFGSRS 71-1, Tri-Service System Program Office for Aircraft Ground Fire Suppression and Rescue, Wright Patterson AFB, Ohio, February, (1972).

14. Geyer, G.B., Neri, L.M., and Urban, C.H., "Comparative Evaluation of Firefighting Foam Agents," Federal Aviation Administration Report FAA-RD-79-61, Washington, D.C., August, (1979).

15. Scheffey, J.L, Darwin, R.L., and Leonard, J.T., "Evaluating Firefighting Foams for Aviation Fire Protection," *Fire Technology*, Third Quarter, pp. 224-243, (1995).

APPENDIX A

ERROR ANALYSIS

An error analysis was performed on the data developed using the test apparatus to determine the uncertainty in the measurements. With much of the data analysis relying on comparison of different tests, an thorough error analysis needed to be performed to ensure that measured difference were due to natural phenomena. For variables that are measured directly, error associated with each measurement could be due to repeatability and accuracy of the measuring device. Error associated to the measuring device was significantly smaller than the error due to test repeatability. Therefore, error due to test repeatability was used to determine error bars for the data. For variables that are calculated, the error in each value used to calculate the variable was considered in the analysis.

Except for heat penetration through the foam, the repeatability data were based on results from five tests performed using a foam expansion ratio of 6.0, a foam height of 50 mm, and an irradiance of 35 kW/m^2. Repeatability of heat penetration through the foam was determined from tests with an expansion ratio of 6.0, a foam height of 50 mm, and an irradiance 50 kW/m^2. Results of this error analysis are shown in Table A-1.

Table A-1. Error Associated With Measured and Calculated Values.

Variable	**Standard Deviation [units]**	**Standard Deviation [%]**
Drain Rate [kg/(s m^2)]	0.006	- -
Evaporation Rate [kg/(s m^2)]	0.0013	- -
Initial Foam Mass per Unit Area [kg/m^2]	0.46	- -
Initial Foam Height [mm]	0.5	- -
Expansion Ratio	- -	10
Foam Mass per Unit Area [kg/m^2]	0.5	- -
Effective Heat of Vaporization [MJ/kg]	1.03	20
Irradiance [kW/m^2]	- -	17
Ignition Time [s]	- -	11
Foam Height Depletion Rate [mm/s]	3	- -

APPENDIX B

TEST DATA – FOAM ONLY

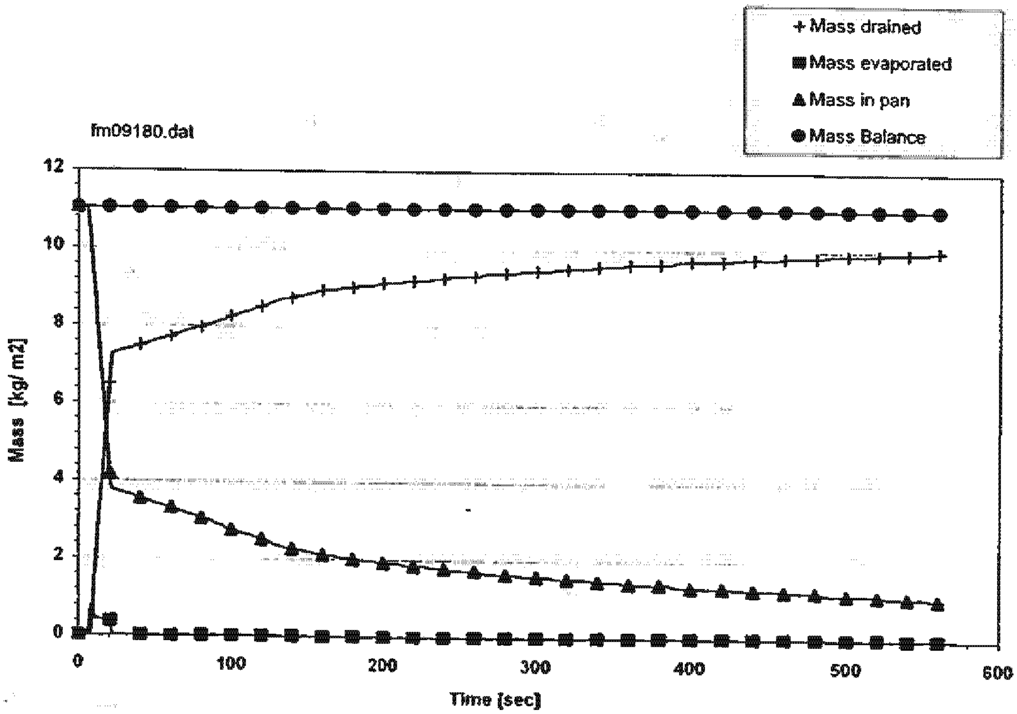

Fig. B1- Mass data in tests with foam only. Test conditions: expansion ratio= 2.96, irradiance= 0kW/m2, initial foam height= 25mm.

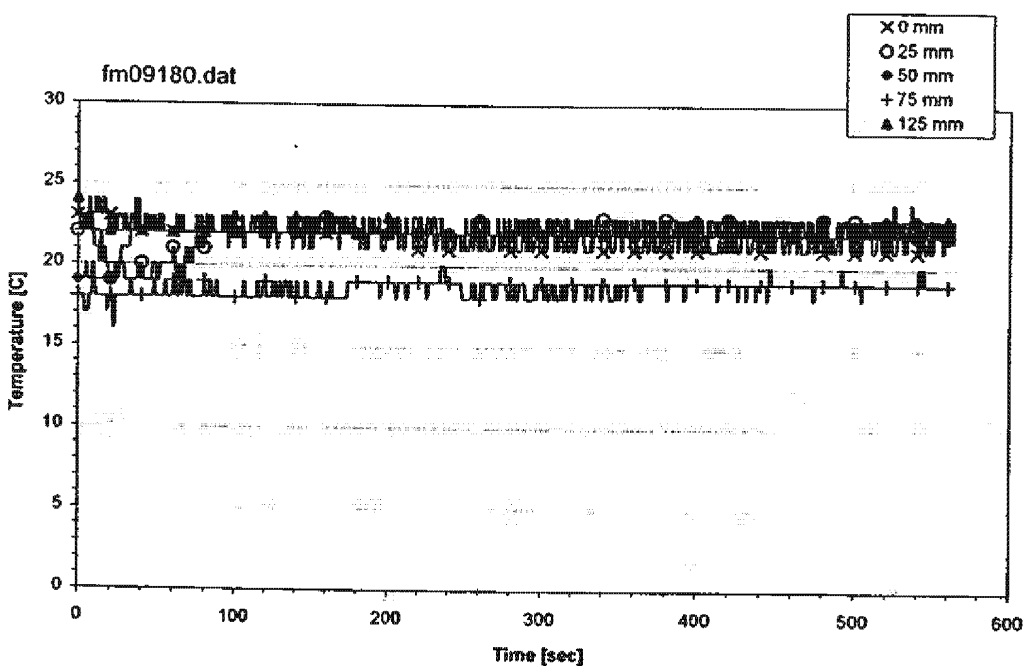

Fig. B2- Foam temperature in tests with foam only. Test conditions: expansion ratio= 2.96, irradiance= 0kW/m2, initial foam height= 25mm.

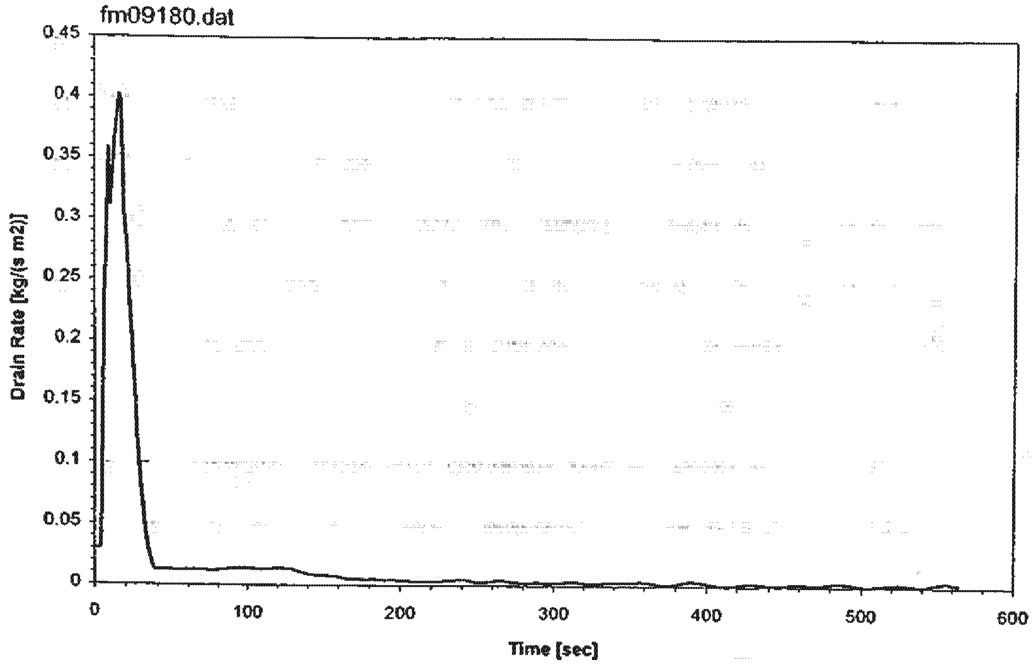

Fig. B3- Drain rate in tests with foam only. Test conditions: expansion ratio= 2.96, irradiance= 0kW/m2, initial foam height= 25mm.

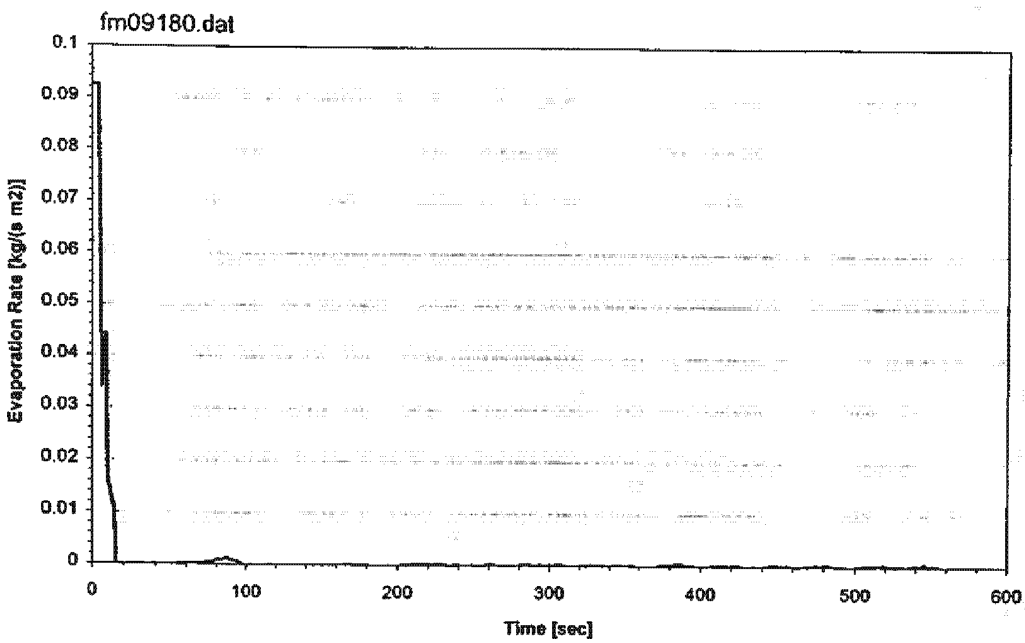

Fig. B4- Evaporation rate in tests with foam only. Test conditions: expansion ratio= 2.96, irradiance= 0kW/m2, initial foam height= 25mm.

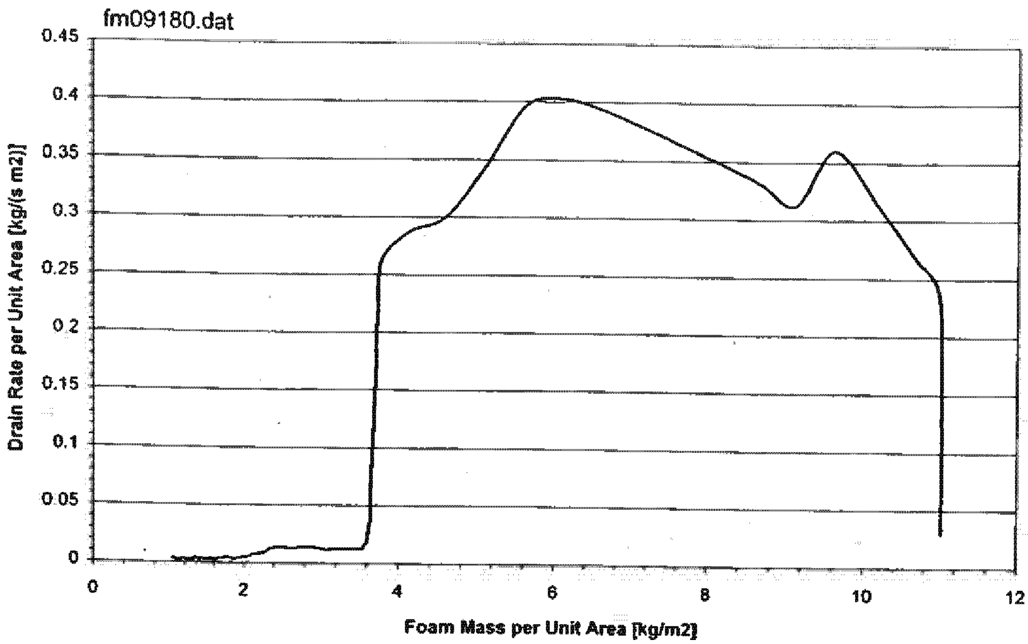

Fig. B5- Drain rate versus foam mass in tests with foam only. Test conditions: expansion ratio= 2.96, irradiance= 0kW/m2, initial foam height= 25mm.

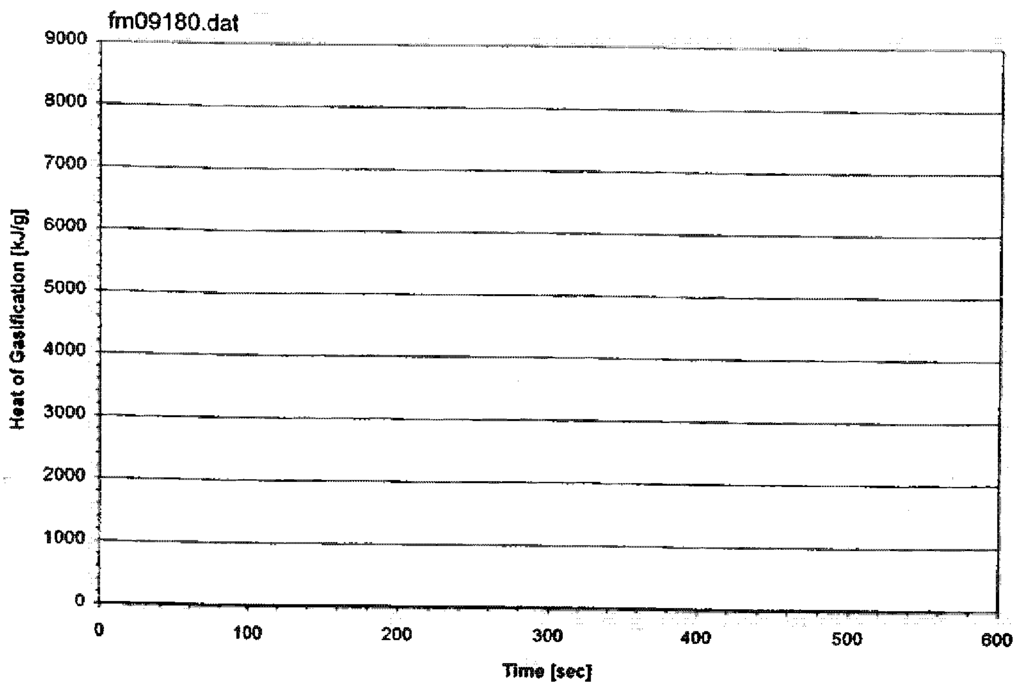

Fig. B6- Effective heat of vaporization in tests with foam only. Test conditions: expansion ratio= 2.96, irradiance= 0kW/m2, initial foam height= 25mm.

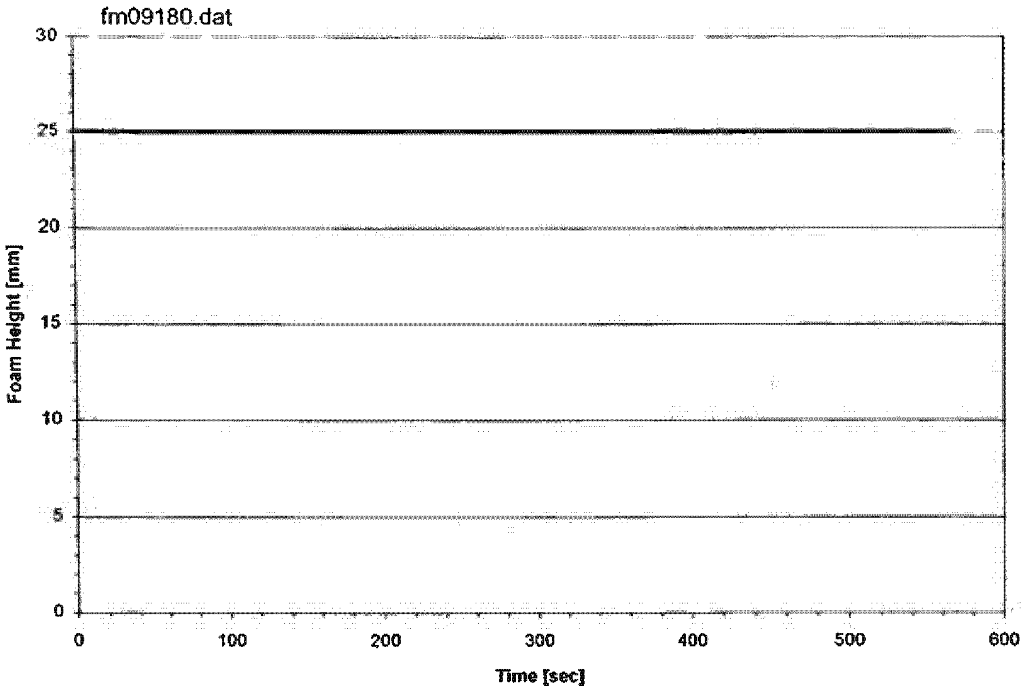

Fig. B7- Foam height in tests with foam only. Test conditions: expansion ratio= 2.96, irradiance= 0kW/m2, initial foam height= 25mm.

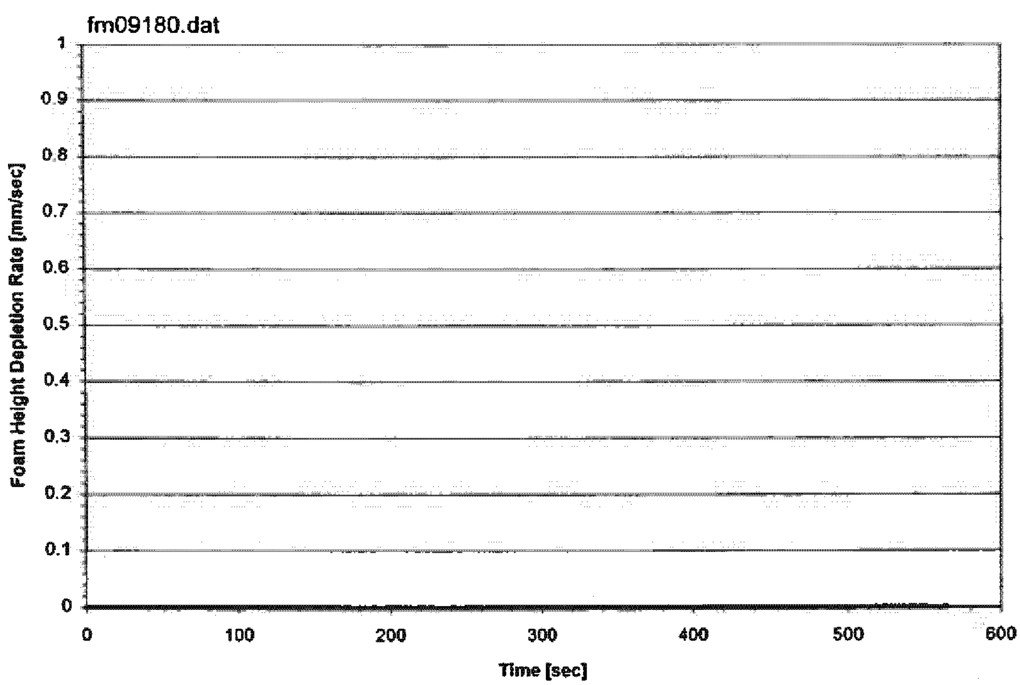

Fig. B8- Foam height depletion rate in tests with foam only. Test conditions: expansion ratio= 2.96, irradiance= 0kW/m2, initial foam height= 25mm.

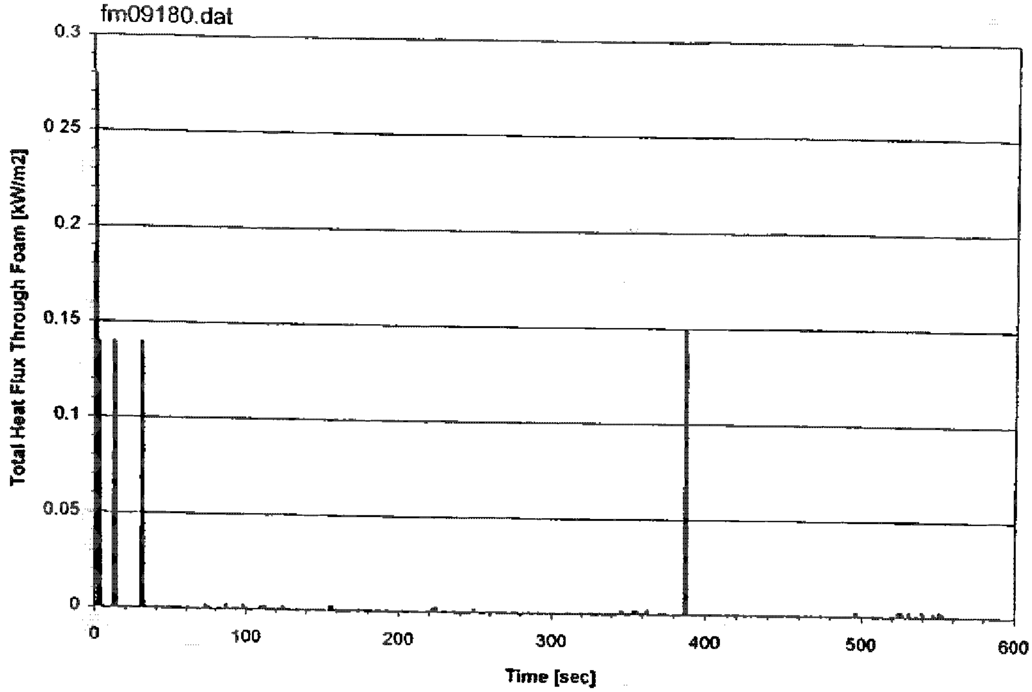

Fig. B9- Heat penetration through foam in tests with foam only. Test conditions: expansion ratio= 2.96, irradiance= 0kW/m2, initial foam height= 25mm.

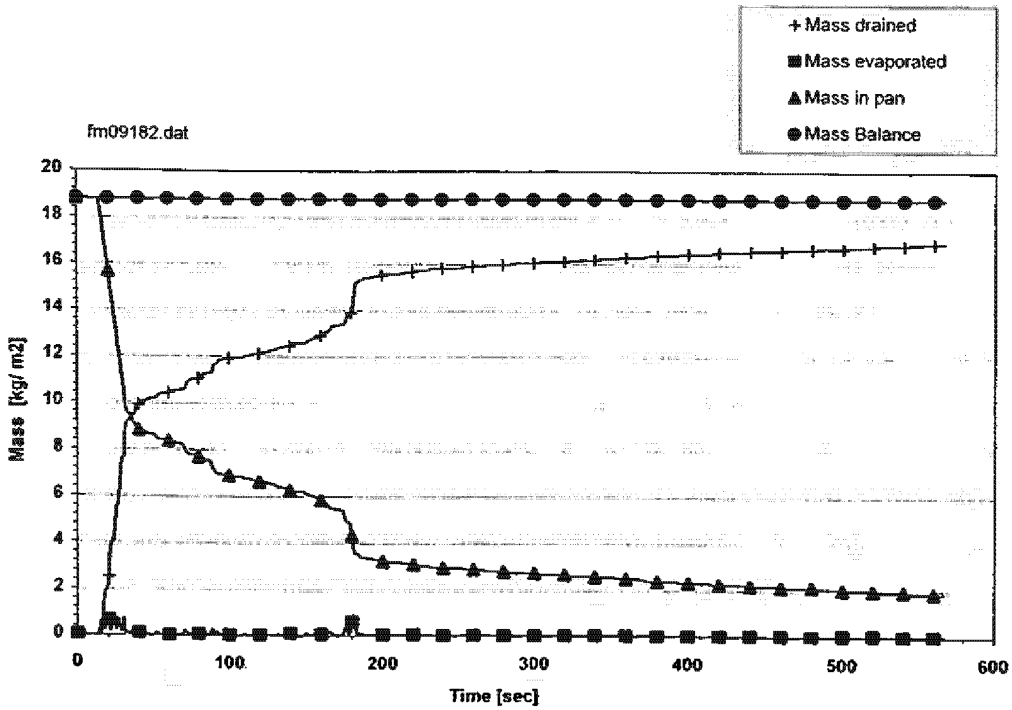

Fig. B10- Mass data in tests with foam only. Test conditions: expansion ratio= 3.14, irradiance= 0kW/m2, initial foam height= 50mm.

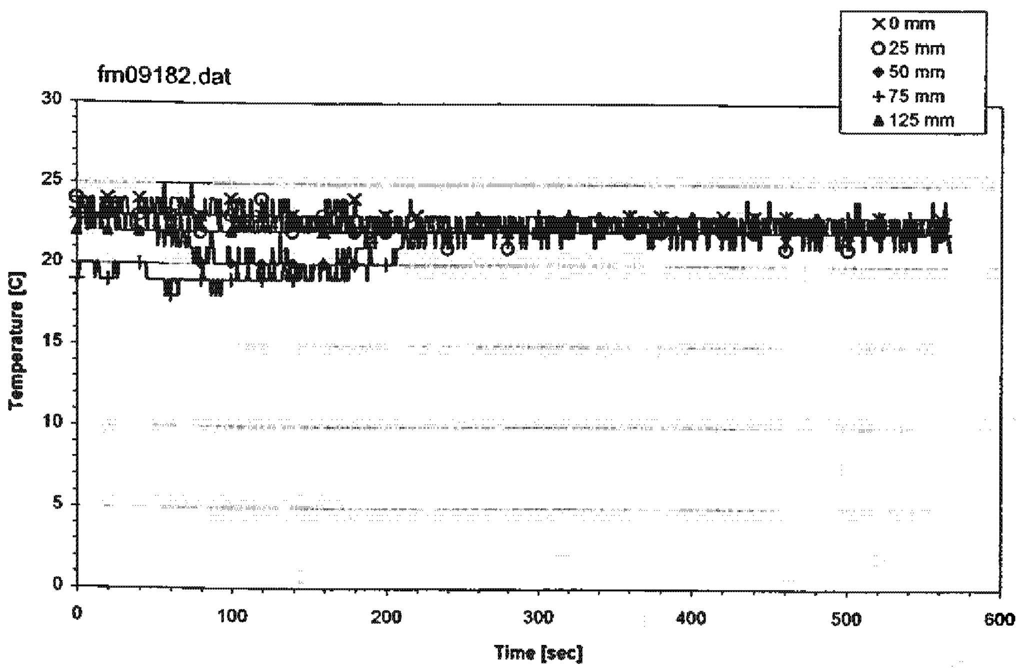

Fig. B11- Foam temperature in tests with foam only. Test conditions: expansion ratio= 3.14, irradiance= 0kW/m2, initial foam height= 50mm.

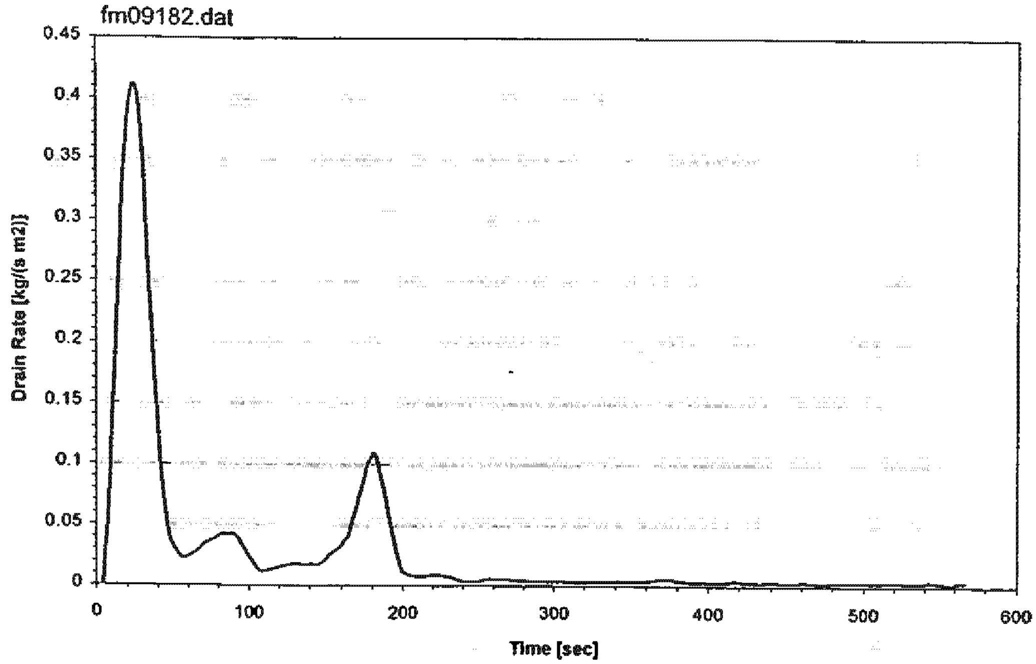

Fig. B12- Drain rate in tests with foam only. Test conditions: expansion ratio= 3.14, irradiance= 0kW/m2, initial foam height= 50mm.

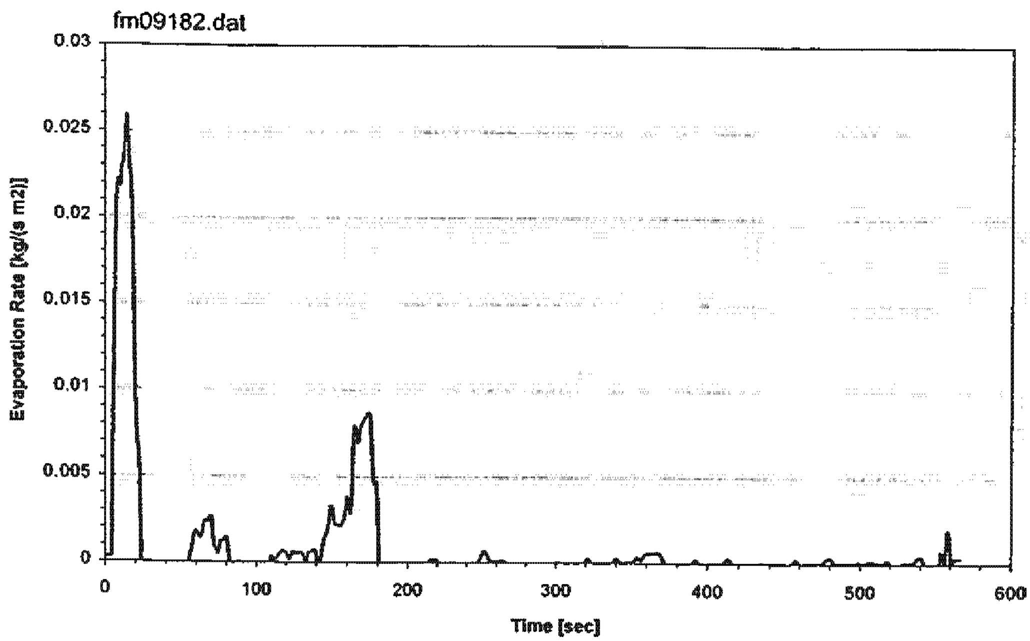

Fig. B13- Evaporation rate in tests with foam only. Test conditions: expansion ratio= 3.14, irradiance= 0kW/m2, initial foam height= 50mm.

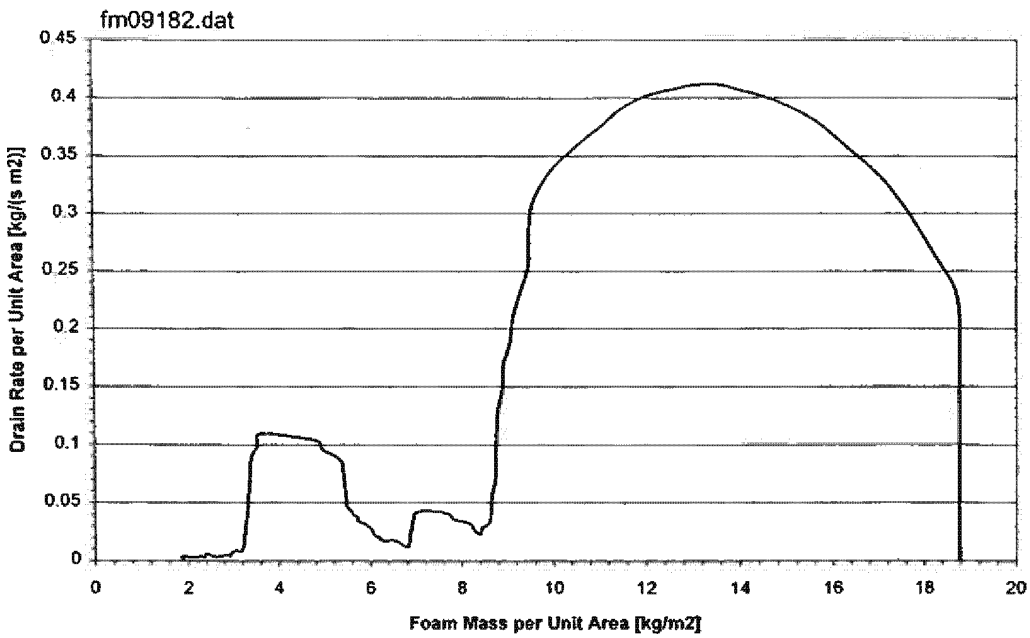

Fig. B14- Drain rate versus foam mass in tests with foam only. Test conditions: expansion ratio= 3.14, irradiance= 0kW/m2, initial foam height= 50mm.

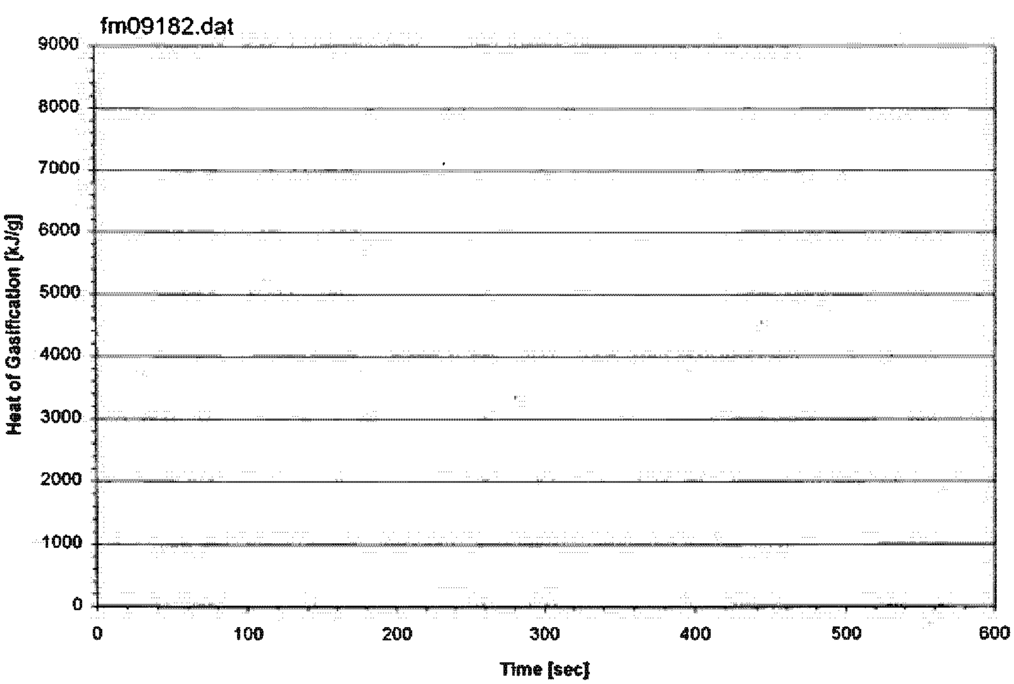

Fig. B15- Effective heat of vaporization in tests with foam only. Test conditions: expansion ratio= 3.14, irradiance= 0kW/m2, initial foam height= 50mm.

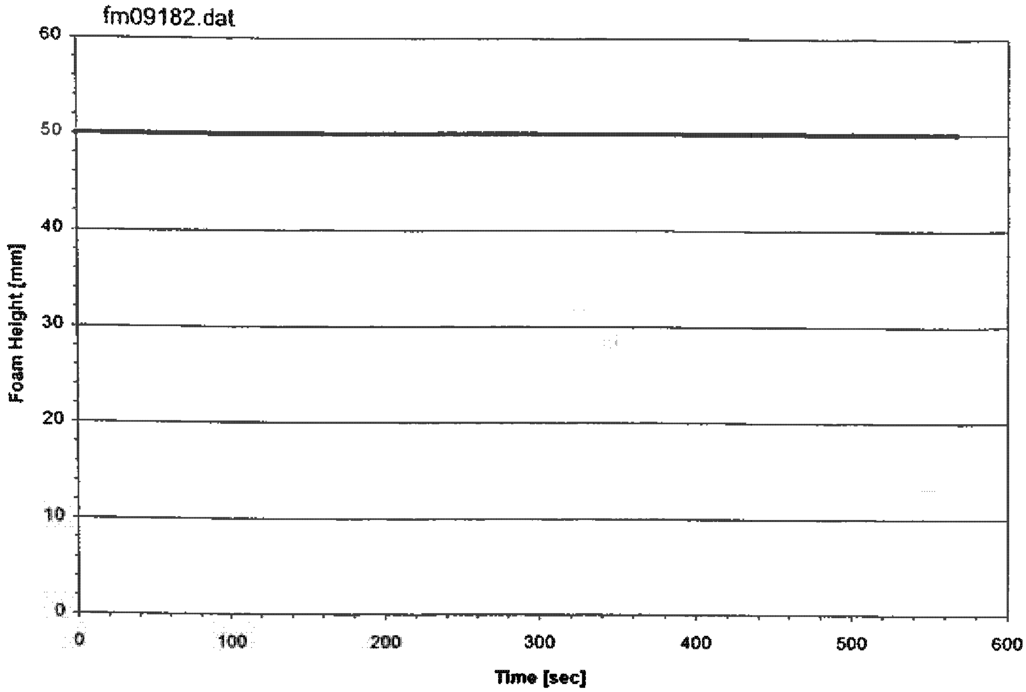

Fig. B16- Foam height in tests with foam only. Test conditions: expansion ratio= 3.14, irradiance= 0kW/m2, initial foam height= 50mm.

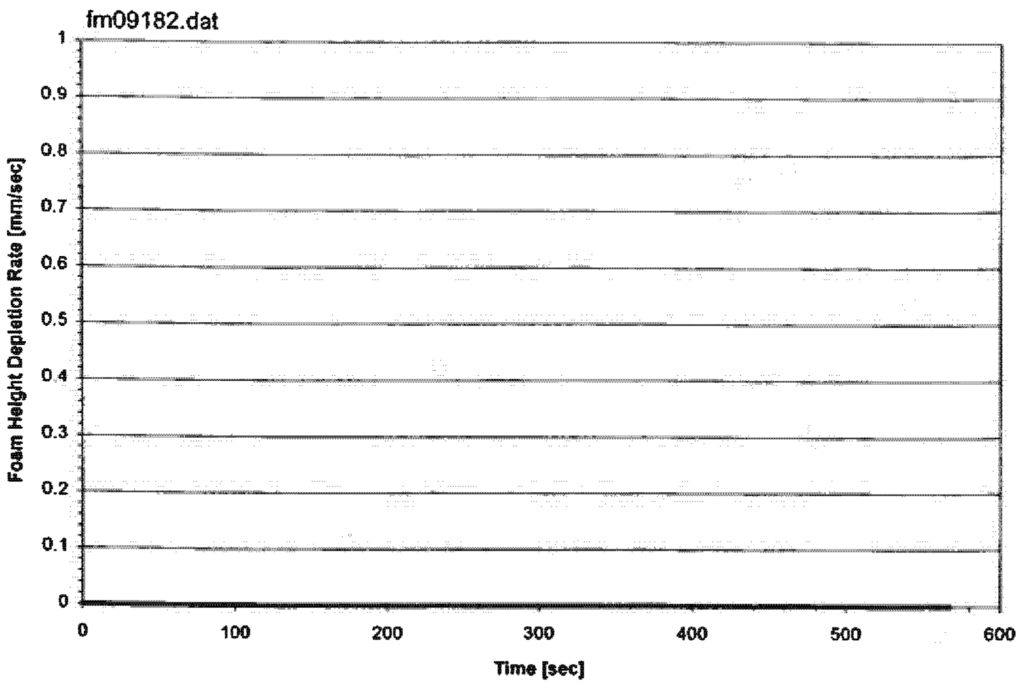

Fig. B17- Foam height depletion rate in tests with foam only. Test conditions: expansion ratio= 3.14, irradiance= 0kW/m2, initial foam height= 50mm.

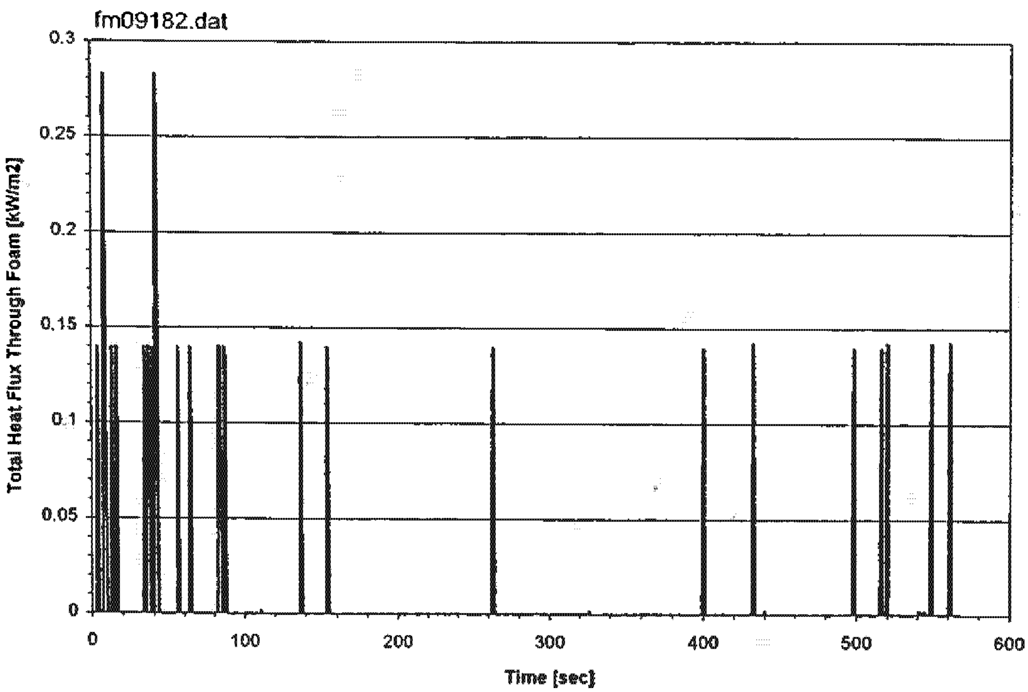

Fig. B18- Heat penetration through foam in tests with foam only. Test conditions: expansion ratio= 3.14, irradiance= 0kW/m2, initial foam height= 50mm.

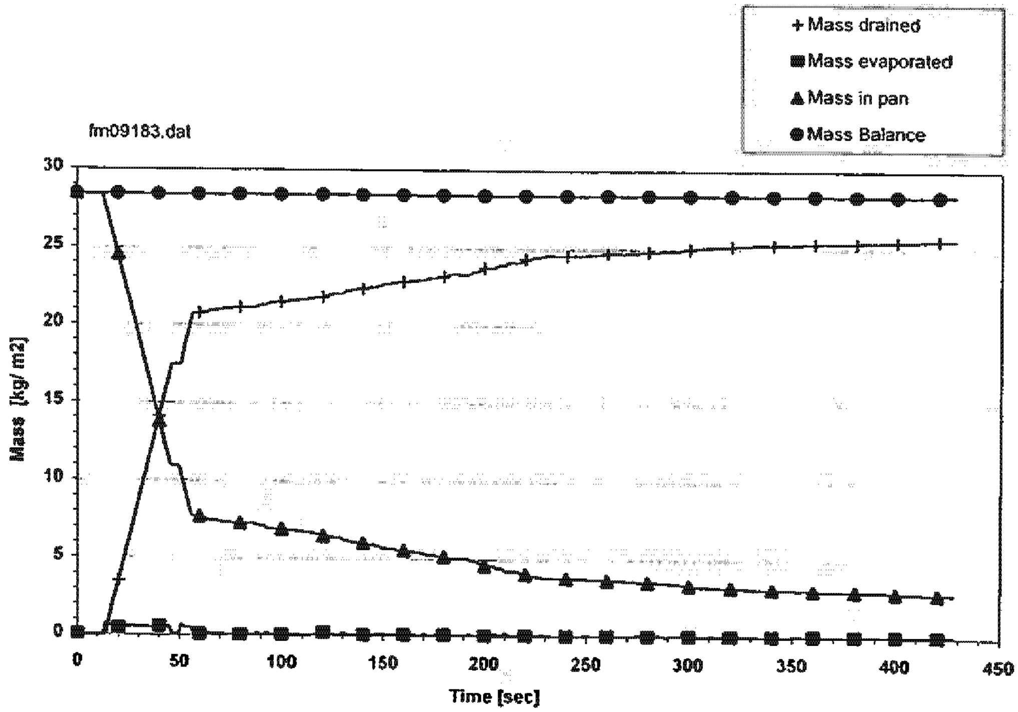

Fig. B19- Mass data in tests with foam only. Test conditions: expansion ratio= 3.02, irradiance= 0kW/m2, initial foam height= 75mm.

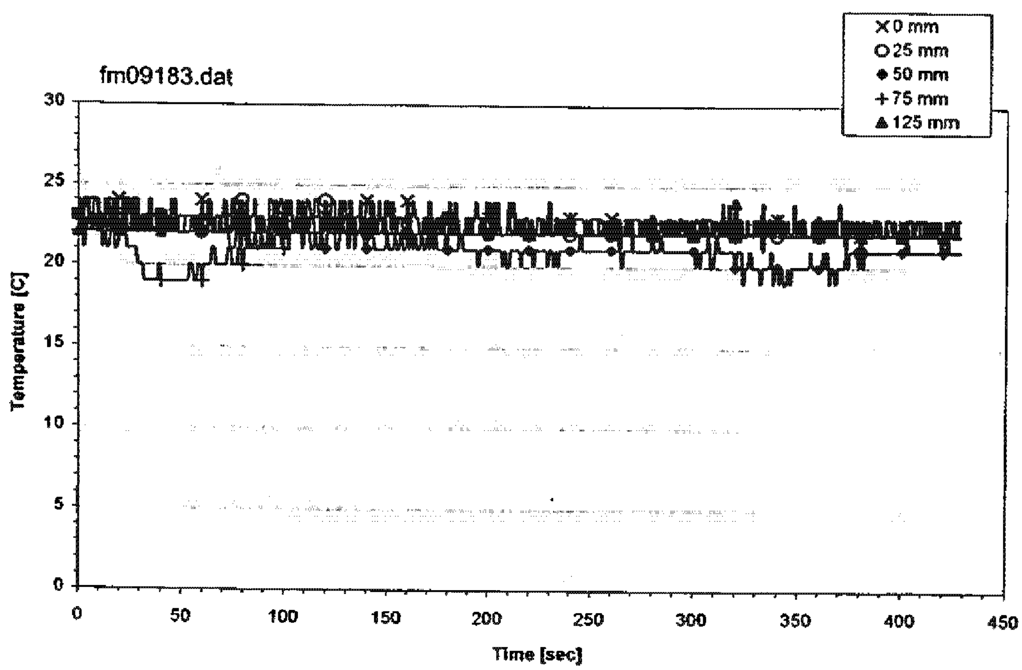

Fig. B20- Foam temperature in tests with foam only. Test conditions: expansion ratio= 3.02, irradiance= 0kW/m2, initial foam height= 75mm.

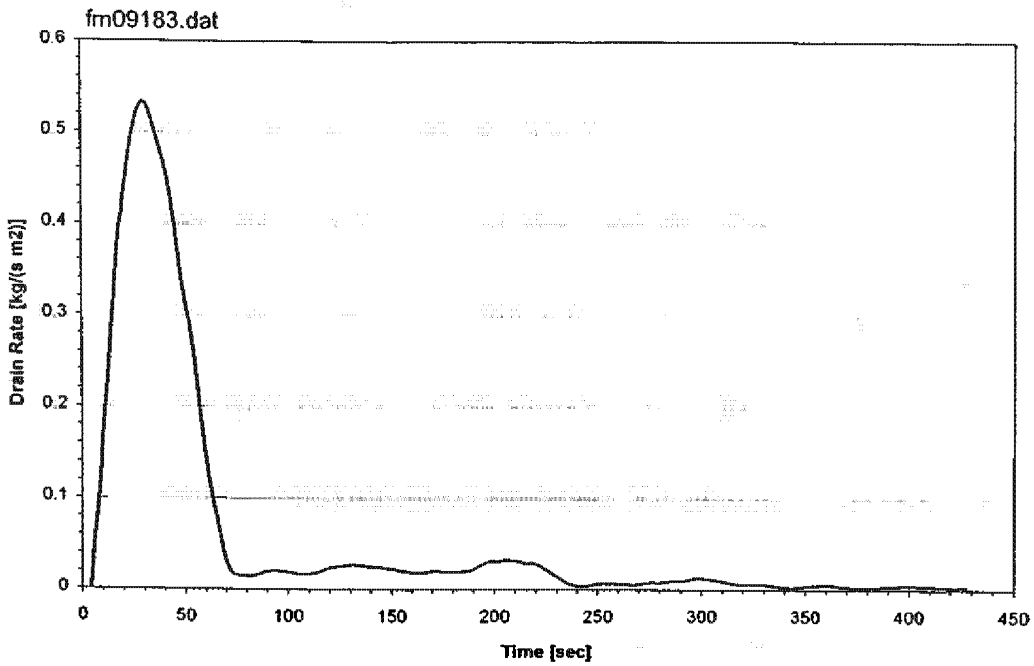

Fig. B21- Drain rate in tests with foam only. Test conditions: expansion ratio= 3.02, irradiance= 0kW/m2, initial foam height= 75mm.

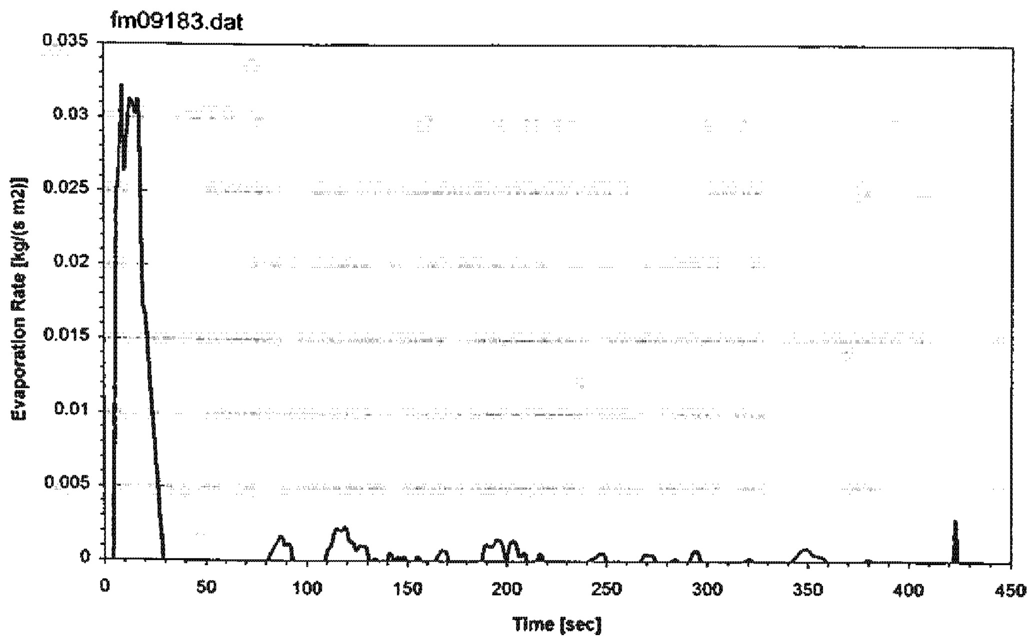

Fig. B22- Evaporation rate in tests with foam only. Test conditions: expansion ratio= 3.02, irradiance= 0kW/m2, initial foam height= 75mm.

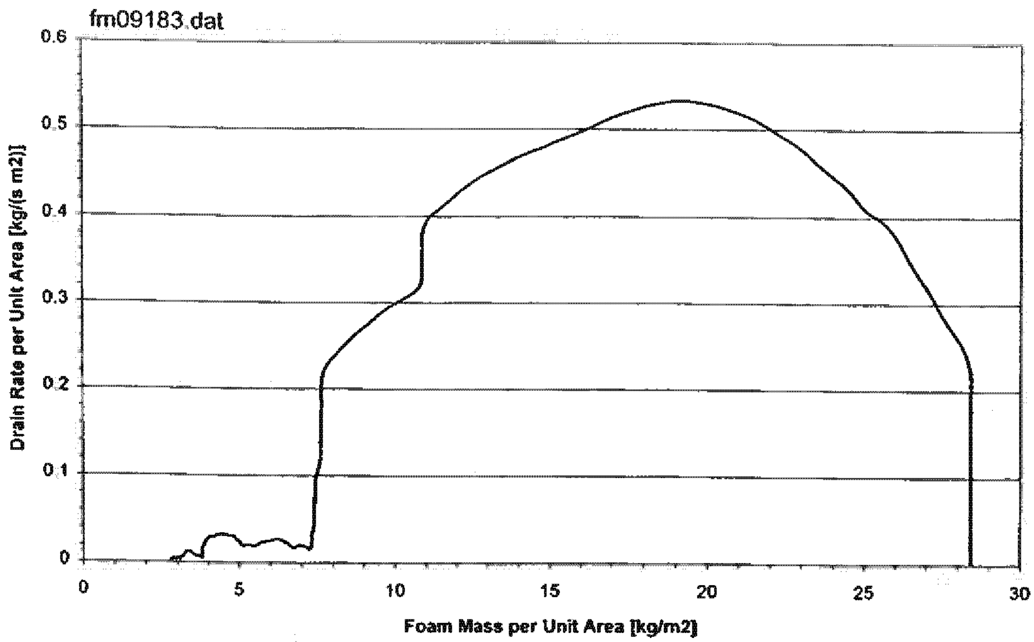

Fig. B23- Drain rate versus foam mass in tests with foam only. Test conditions: expansion ratio= 3.02, irradiance= 0kW/m2, initial foam height= 75mm.

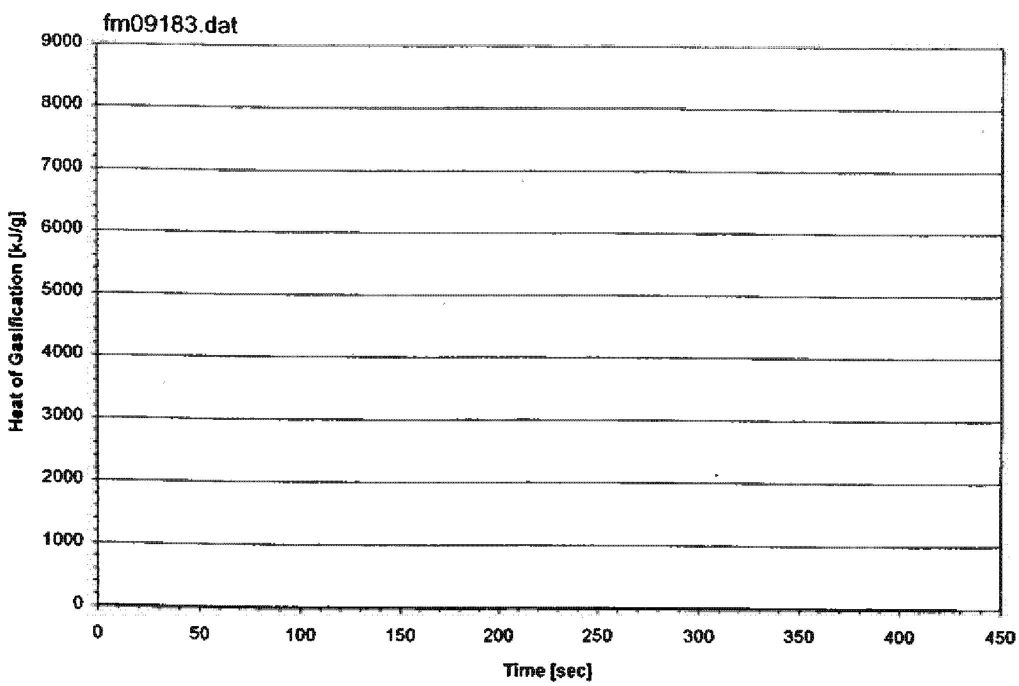

Fig. B24- Effective heat of vaporization in tests with foam only. Test conditions: expansion ratio= 3.02, irradiance= 0kW/m2, initial foam height= 75mm.

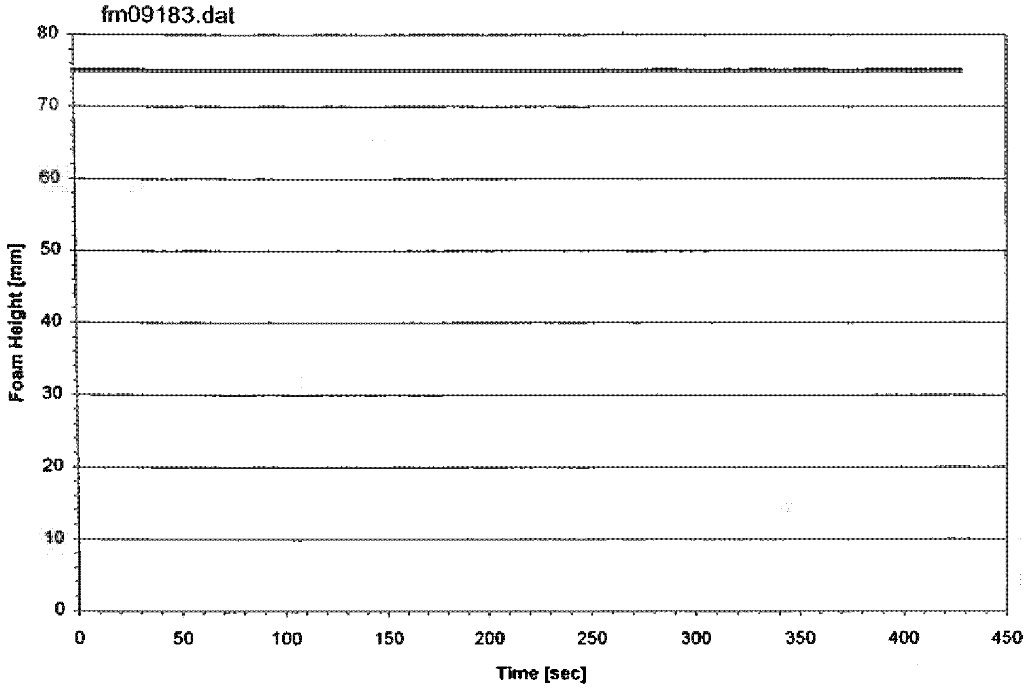

Fig. B25- Foam height in tests with foam only. Test conditions: expansion ratio= 3.02, irradiance= 0kW/m2, initial foam height= 75mm.

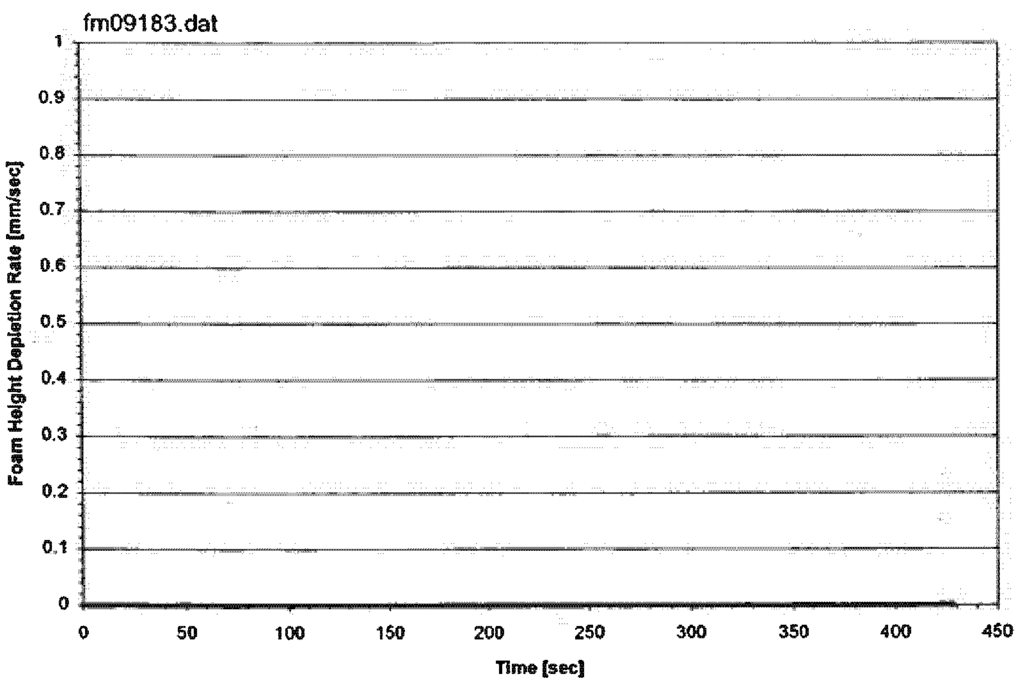

Fig. B26- Foam height depletion rate in tests with foam only. Test conditions: expansion ratio= 3.02, irradiance= 0kW/m2, initial foam height= 75mm.

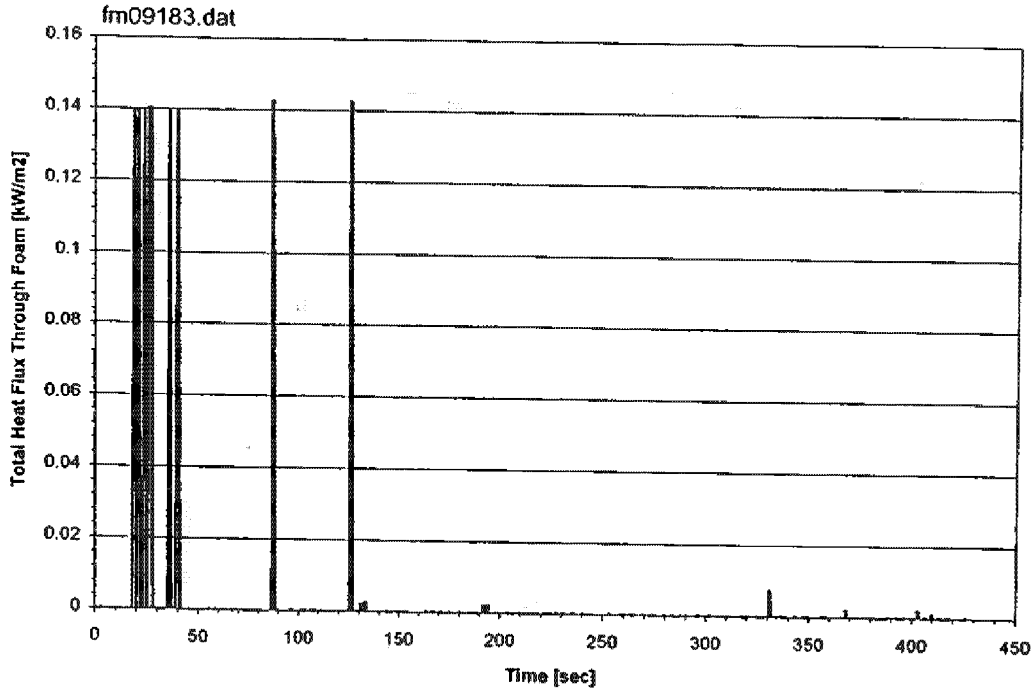

Fig. B27- Heat penetration through foam in tests with foam only. Test conditions: expansion ratio= 3.02, irradiance= 0kW/m2, initial foam height= 75mm.

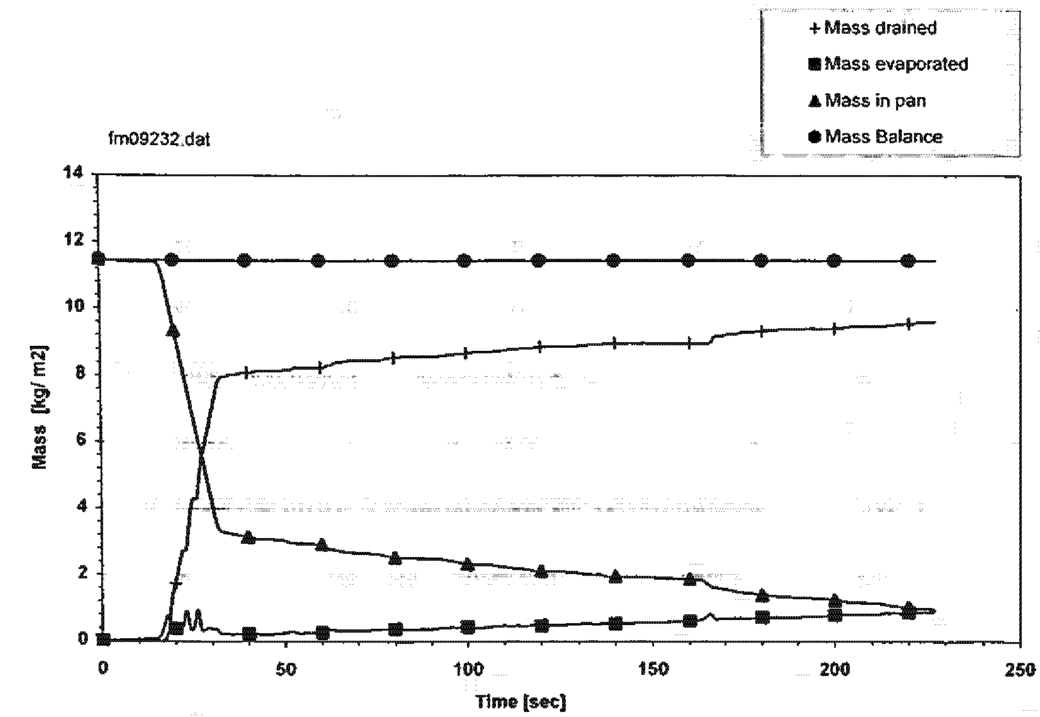

Fig. B28- Mass data in tests with foam only. Test conditions: expansion ratio= 2.85, irradiance= 20kW/m2, initial foam height= 25mm.

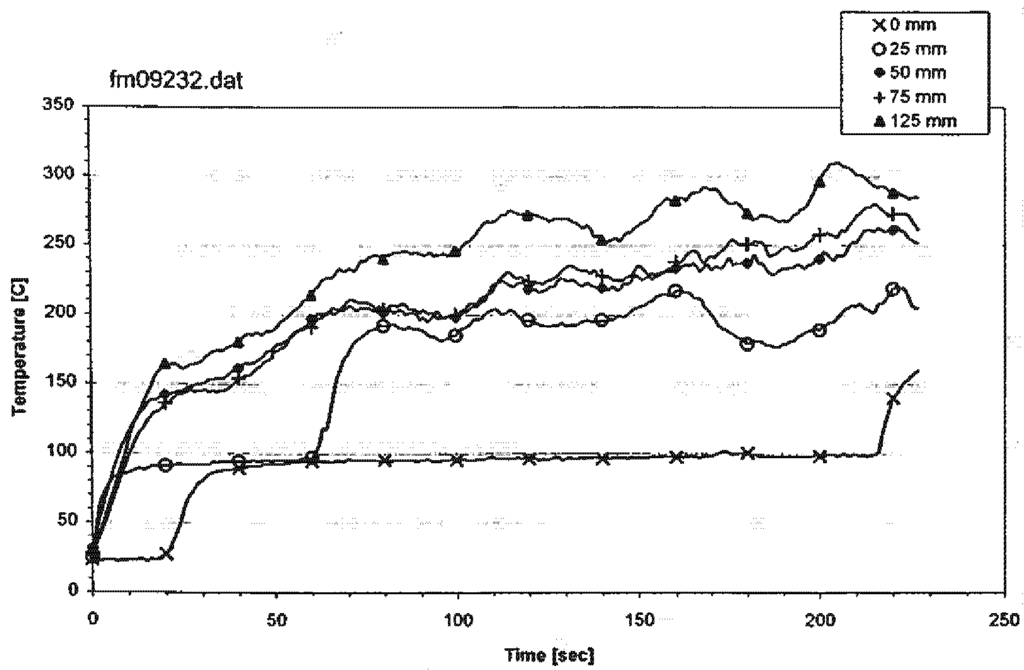

Fig. B29- Foam temperature in tests with foam only. Test conditions: expansion ratio= 2.85, irradiance= 20kW/m2, initial foam height= 25mm.

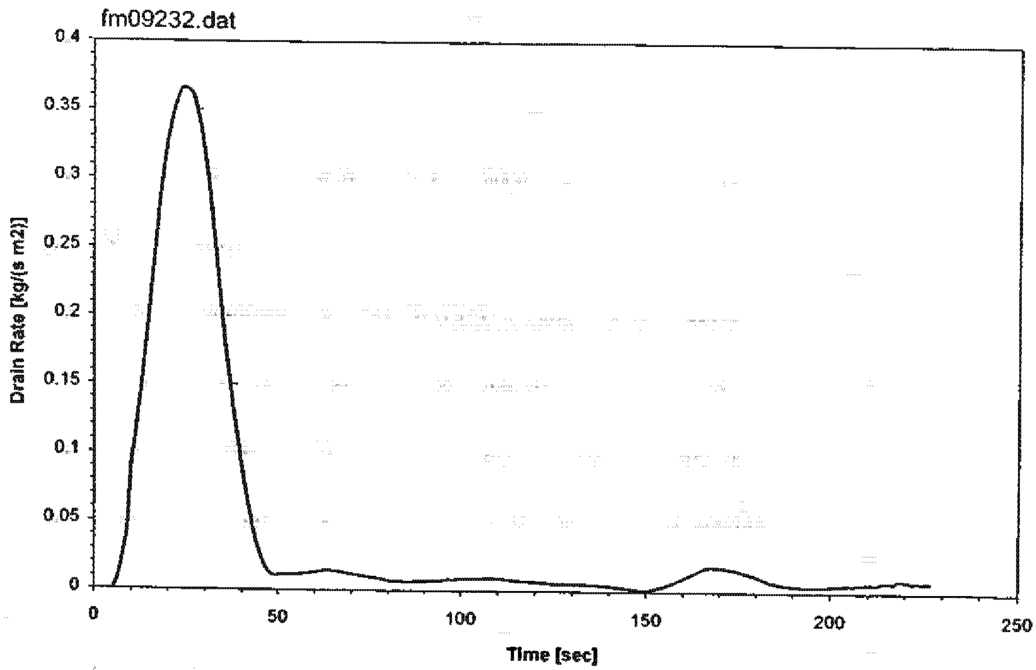

Fig. B30- Drain rate in tests with foam only. Test conditions: expansion ratio= 2.85, irradiance= 20kW/m2, initial foam height= 25mm.

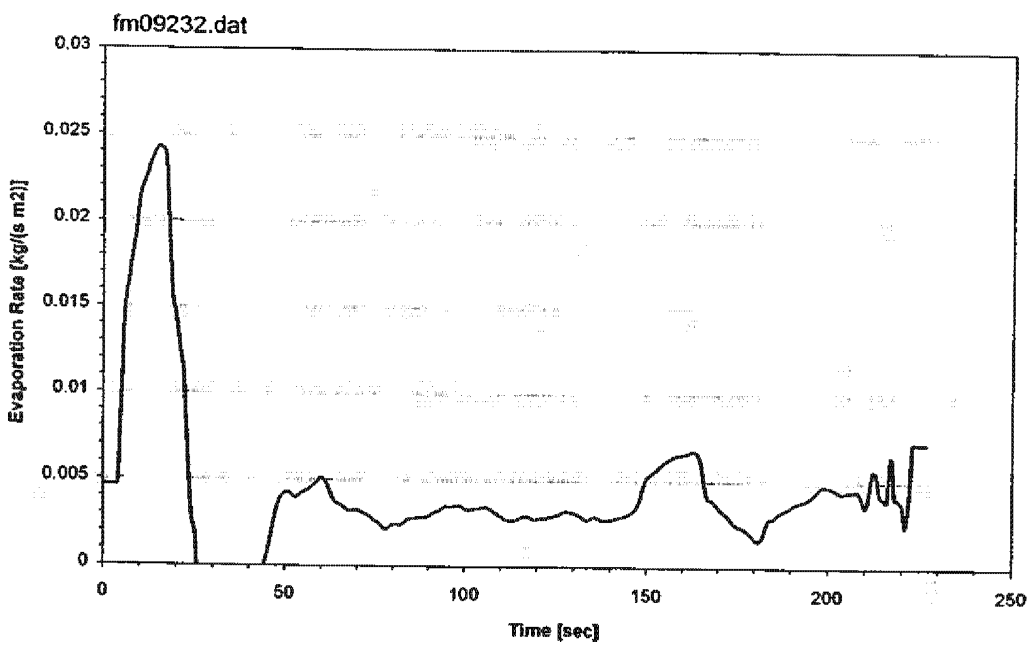

Fig. B31- Evaporation rate in tests with foam only. Test conditions: expansion ratio= 2.85, irradiance= 20kW/m2, initial foam height= 25mm.

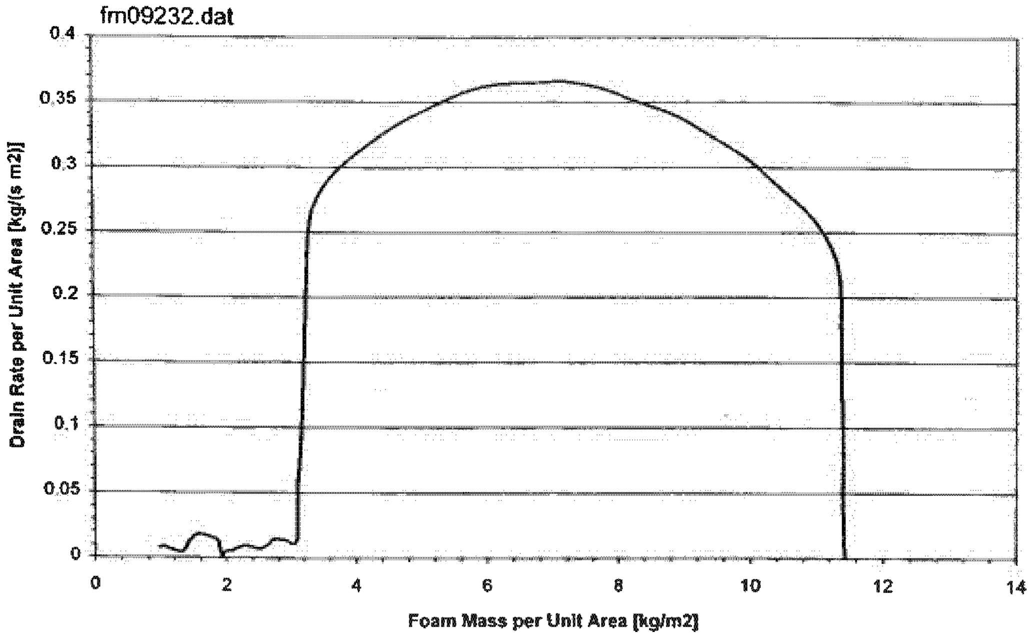

Fig. B32- Drain rate versus foam mass in tests with foam only. Test conditions: expansion ratio= 2.85, irradiance= 20kW/m2, initial foam height= 25mm.

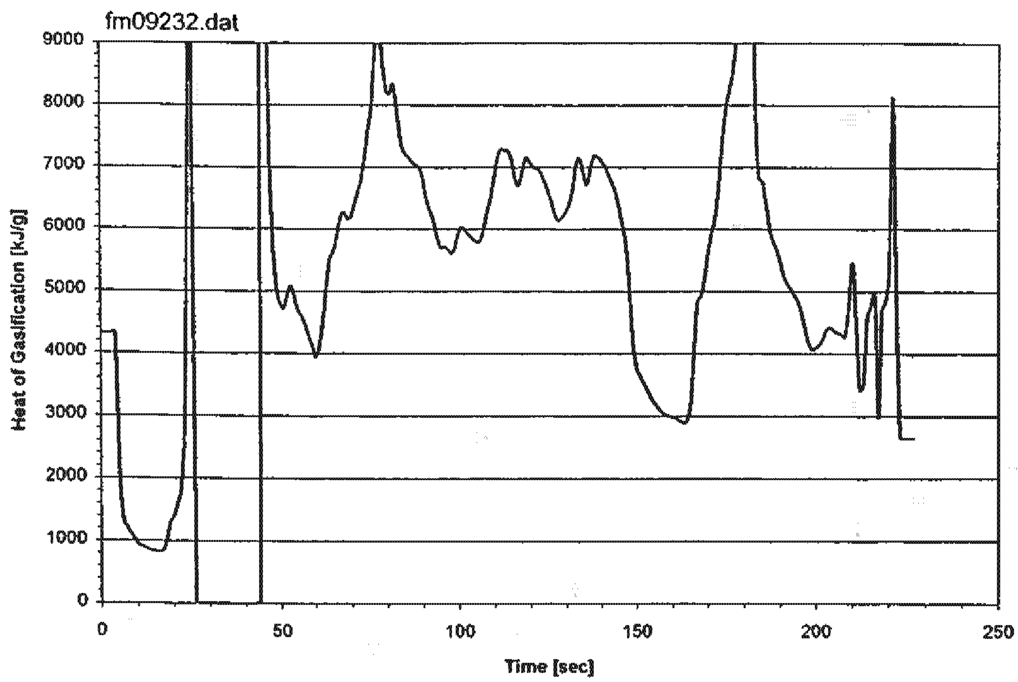

Fig. B33- Effective heat of vaporization in tests with foam only. Test conditions: expansion ratio= 2.85, irradiance= 20kW/m2, initial foam height= 25mm.

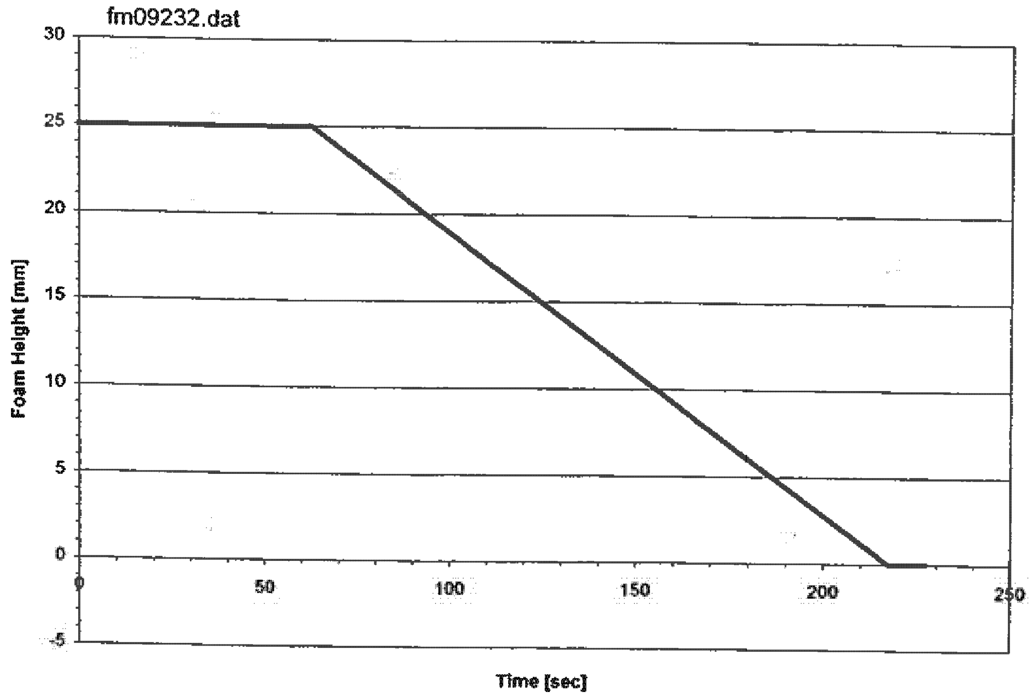

Fig. B34- Foam height in tests with foam only. Test conditions: expansion ratio= 2.85, irradiance= 20kW/m2, initial foam height= 25mm.

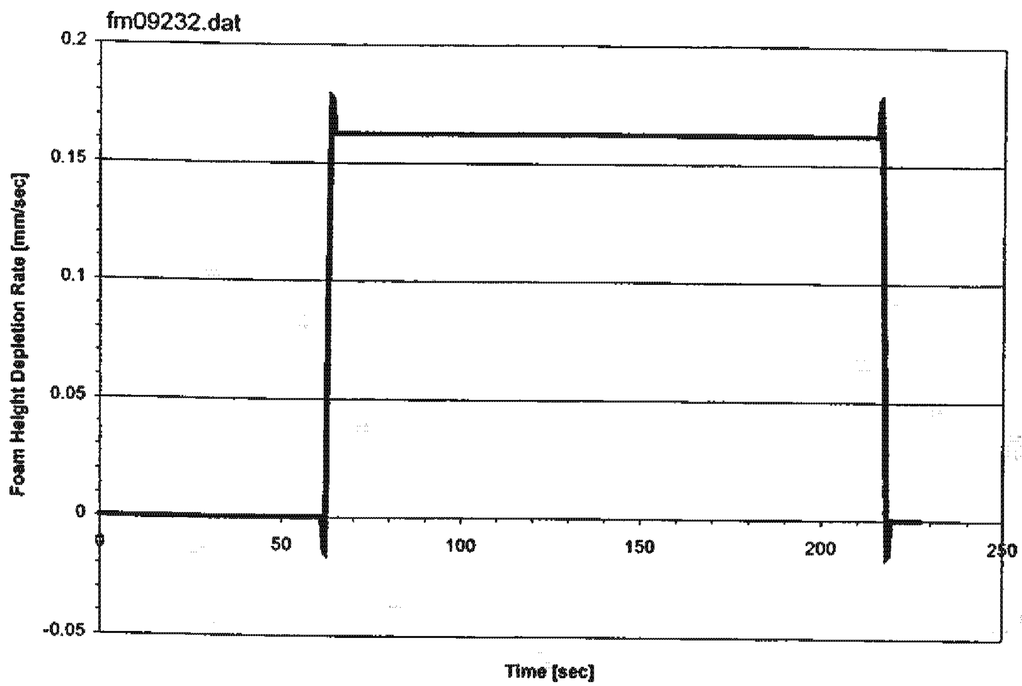

Fig. B35- Foam height depletion rate in tests with foam only. Test conditions: expansion ratio= 2.85, irradiance= 20kW/m2, initial foam height= 25mm.

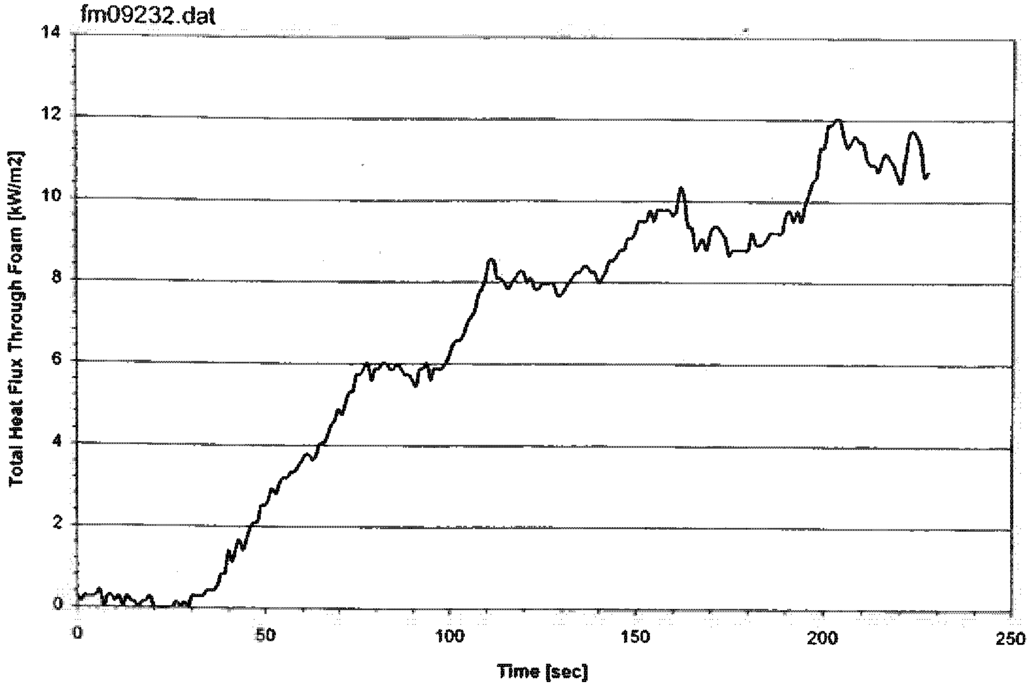

Fig. B36- Heat penetration through foam in tests with foam only. Test conditions: expansion ratio= 2.85, irradiance= 20kW/m2, initial foam height= 25mm.

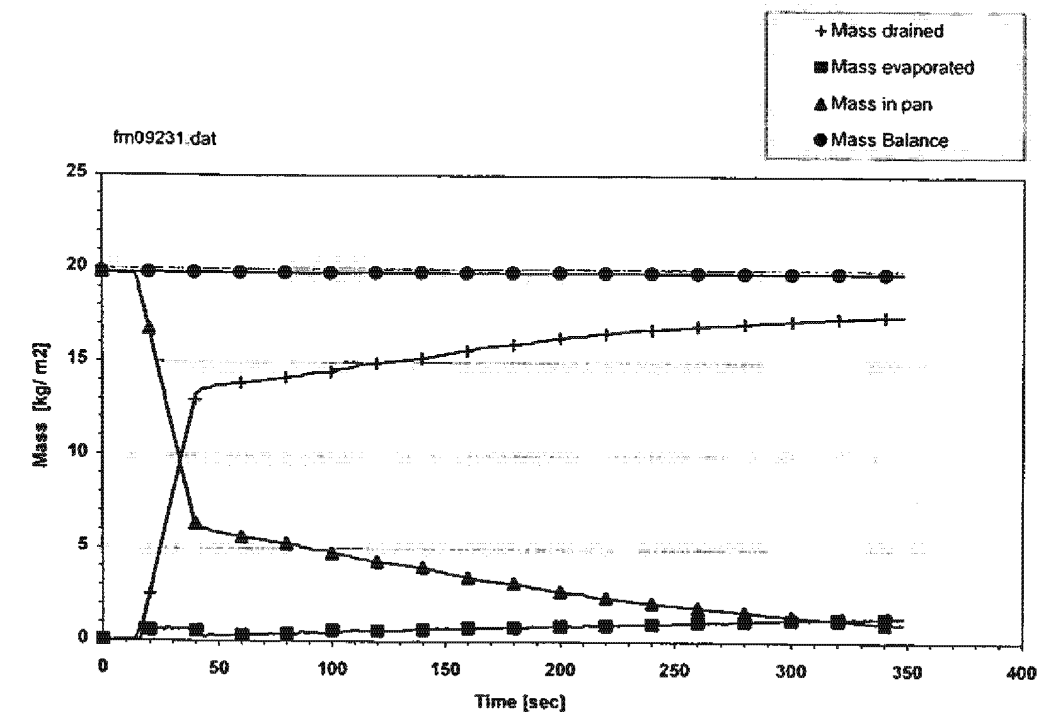

Fig. B37- Mass data in tests with foam only. Test conditions: expansion ratio= 2.98, irradiance= 20kW/m2, initial foam height= 50mm.

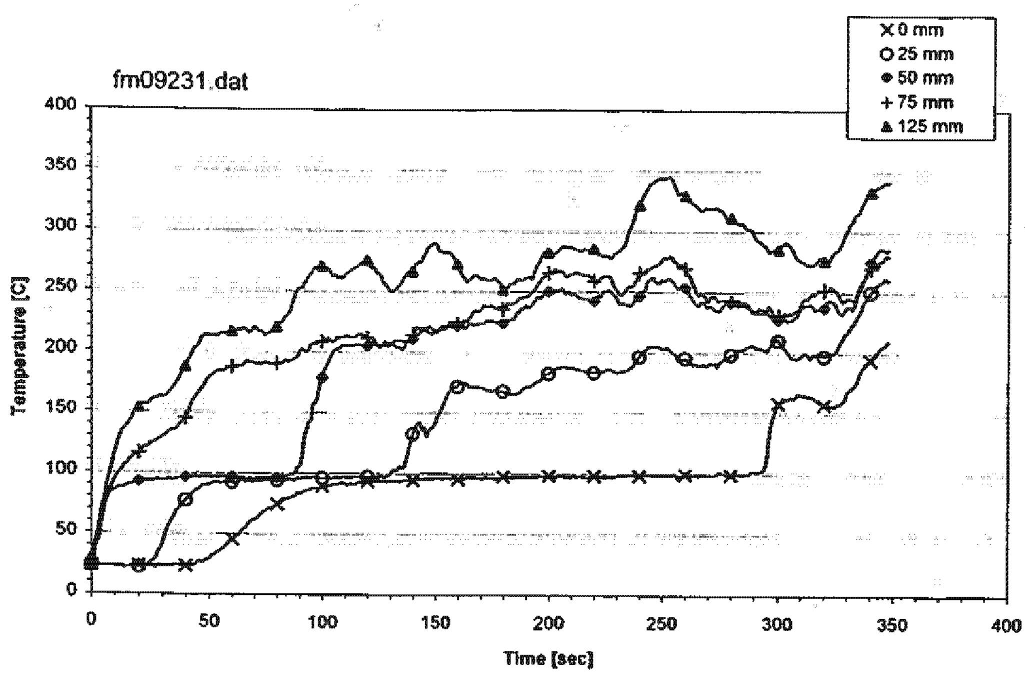

Fig. B38- Foam temperature in tests with foam only. Test conditions: expansion ratio= 2.98, irradiance= 20kW/m2, initial foam height= 50mm.

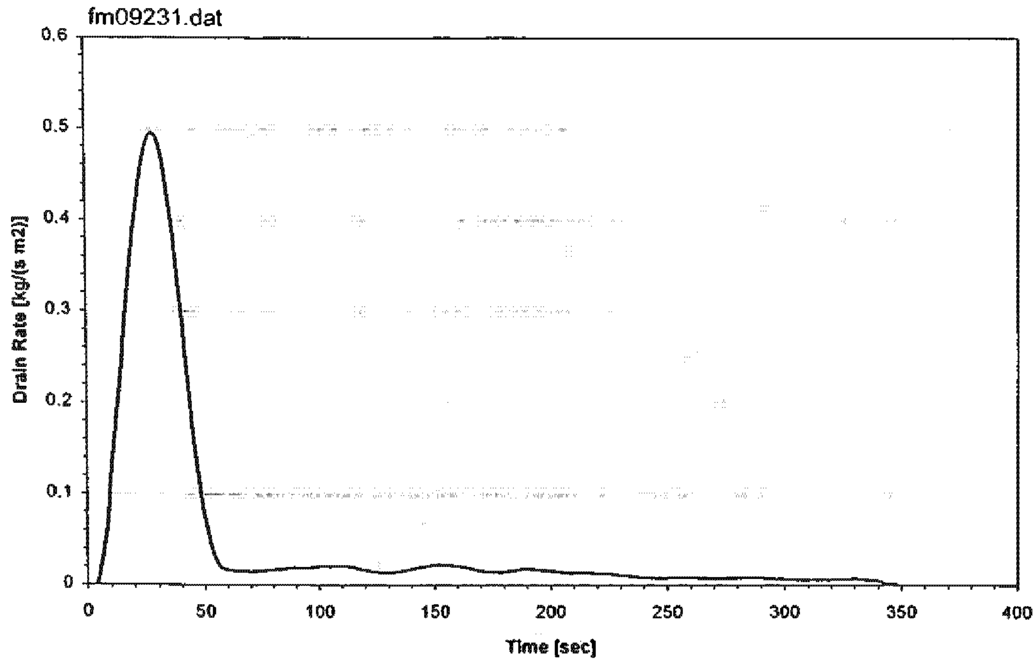

Fig. B39- Drain rate in tests with foam only. Test conditions: expansion ratio= 2.98, irradiance= 20kW/m2, initial foam height= 50mm.

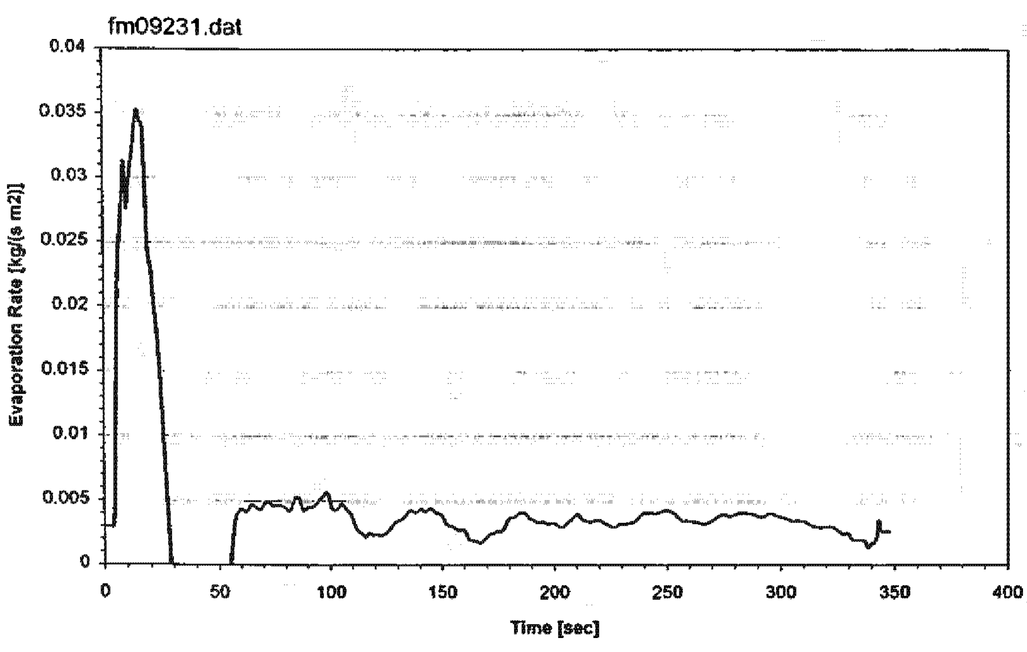

Fig. B40- Evaporation rate in tests with foam only. Test conditions: expansion ratio= 2.98, irradiance= 20kW/m2, initial foam height= 50mm.

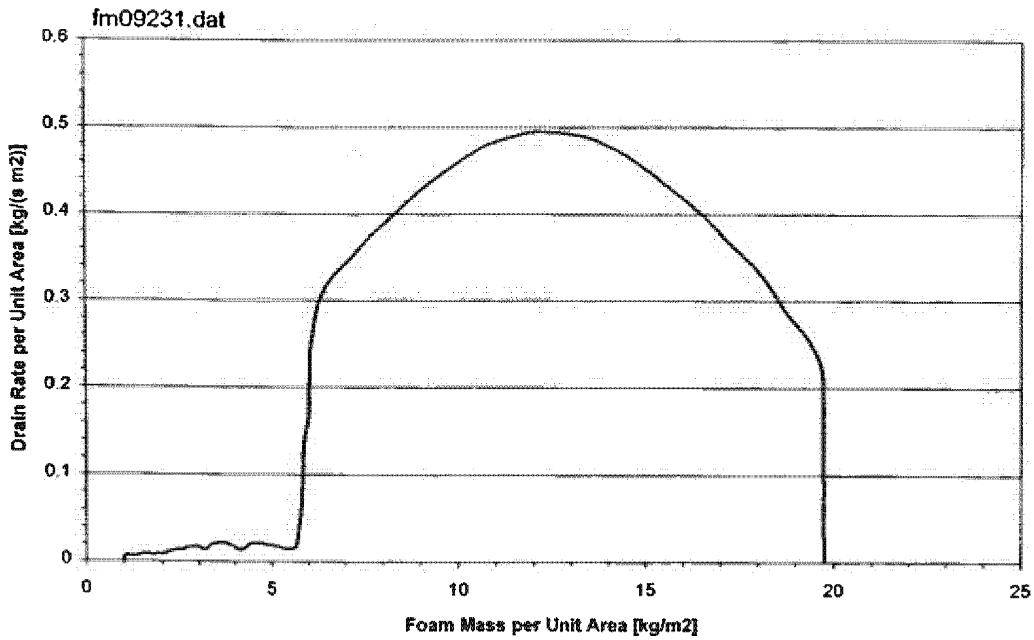

Fig. B41- Drain rate versus foam mass in tests with foam only. Test conditions: expansion ratio= 2.98, irradiance= 20kW/m2, initial foam height= 50mm.

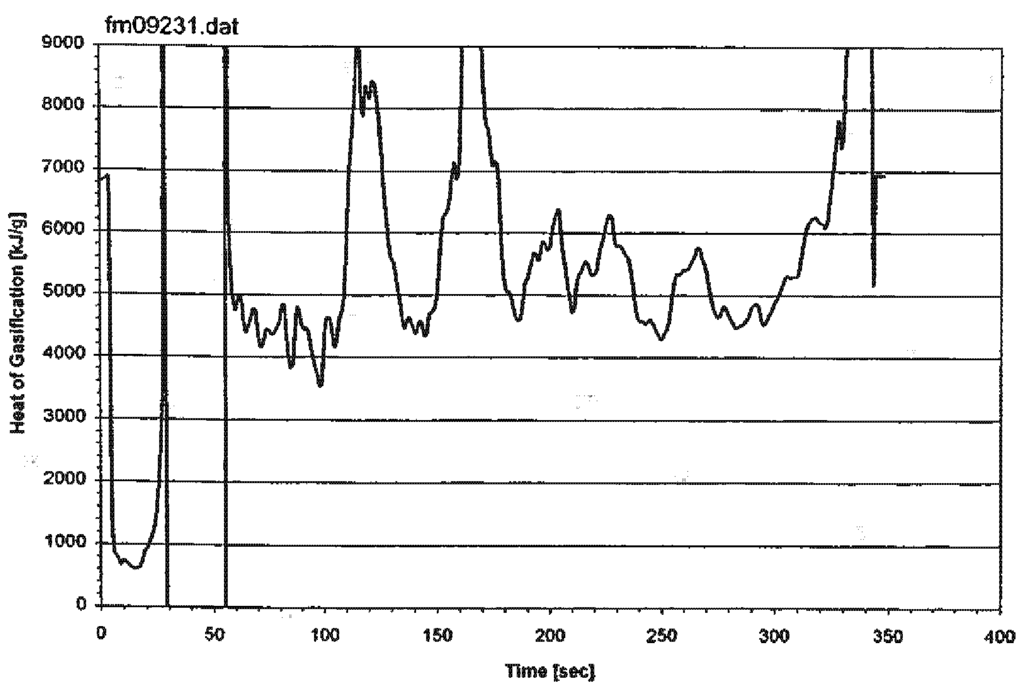

Fig. B42- Effective heat of vaporization in tests with foam only. Test conditions: expansion ratio= 2.98, irradiance= 20kW/m2, initial foam height= 50mm.

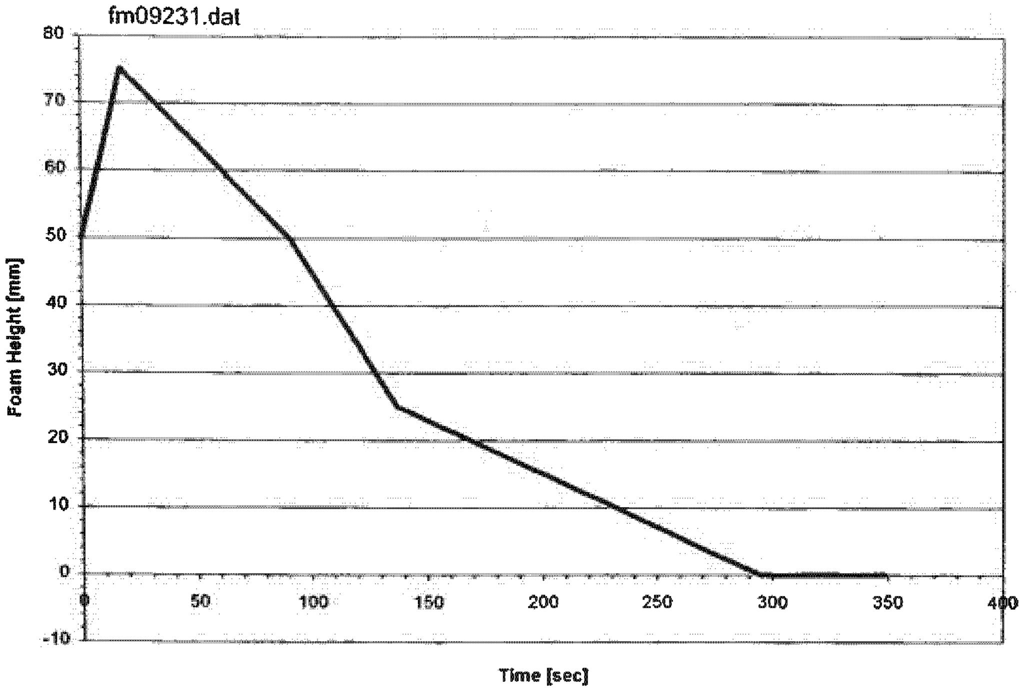

Fig. B43- Foam height in tests with foam only. Test conditions: expansion ratio= 2.98, irradiance= 20kW/m2, initial foam height= 50mm.

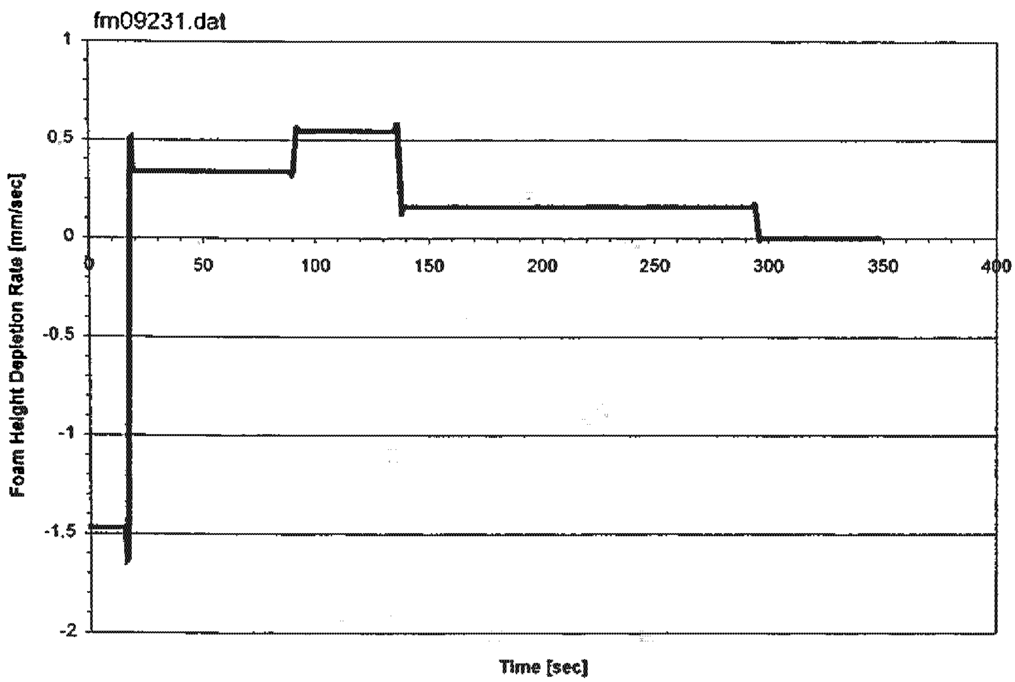

Fig. B44- Foam height depletion rate in tests with foam only. Test conditions: expansion ratio= 2.98, irradiance= 20kW/m2, initial foam height= 50mm.

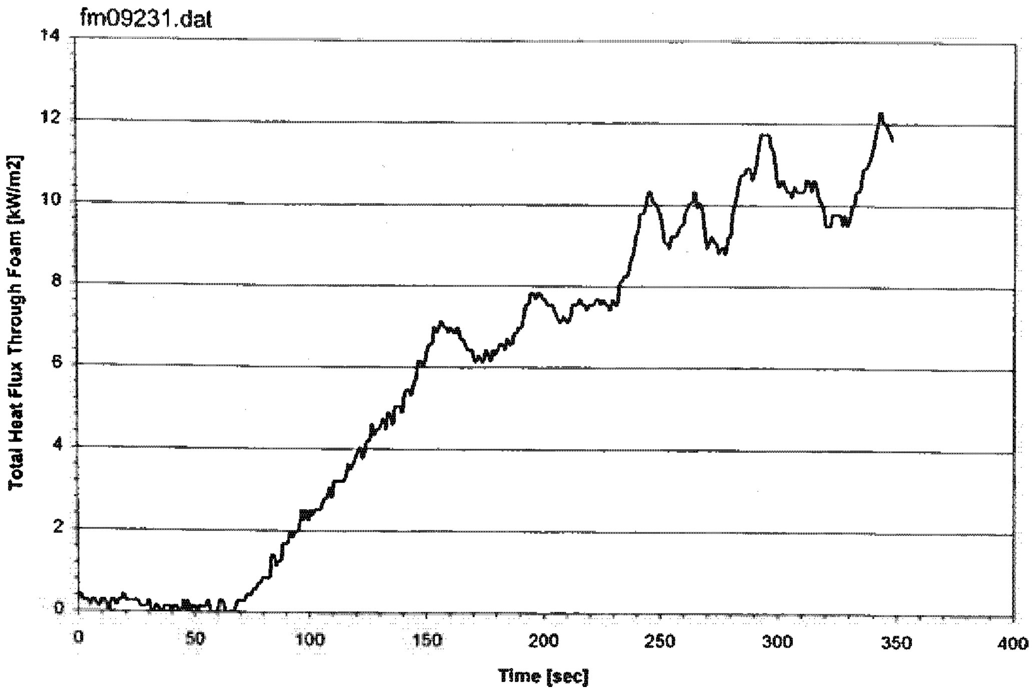

Fig. B45- Heat penetration through foam in tests with foam only. Test conditions: expansion ratio= 2.98, irradiance= 20kW/m2, initial foam height= 50mm.

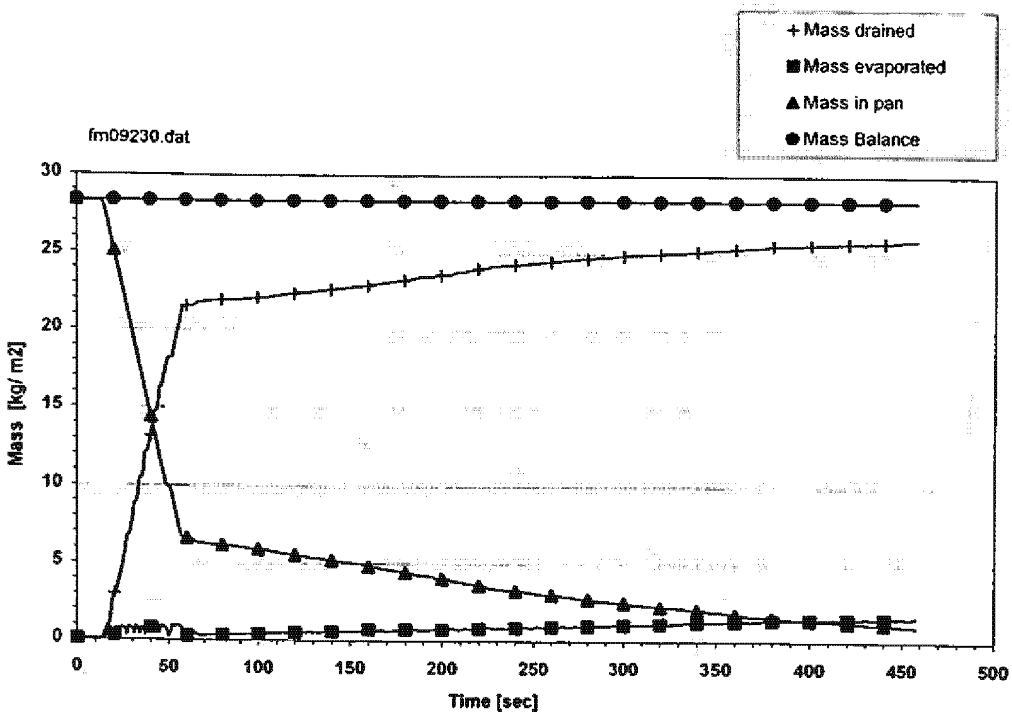

Fig. B46- Mass data in tests with foam only. Test conditions: expansion ratio= 3.03, irradiance= 20kW/m2, initial foam height= 75mm.

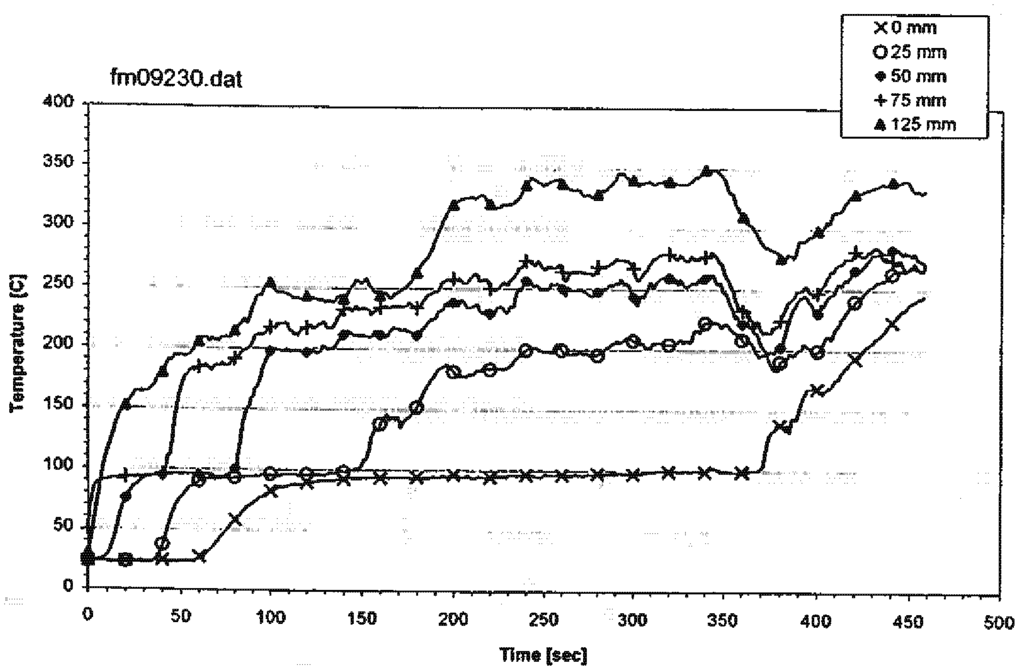

Fig. B47- Foam temperature in tests with foam only. Test conditions: expansion ratio= 3.03, irradiance= 20kW/m2, initial foam height= 75mm.

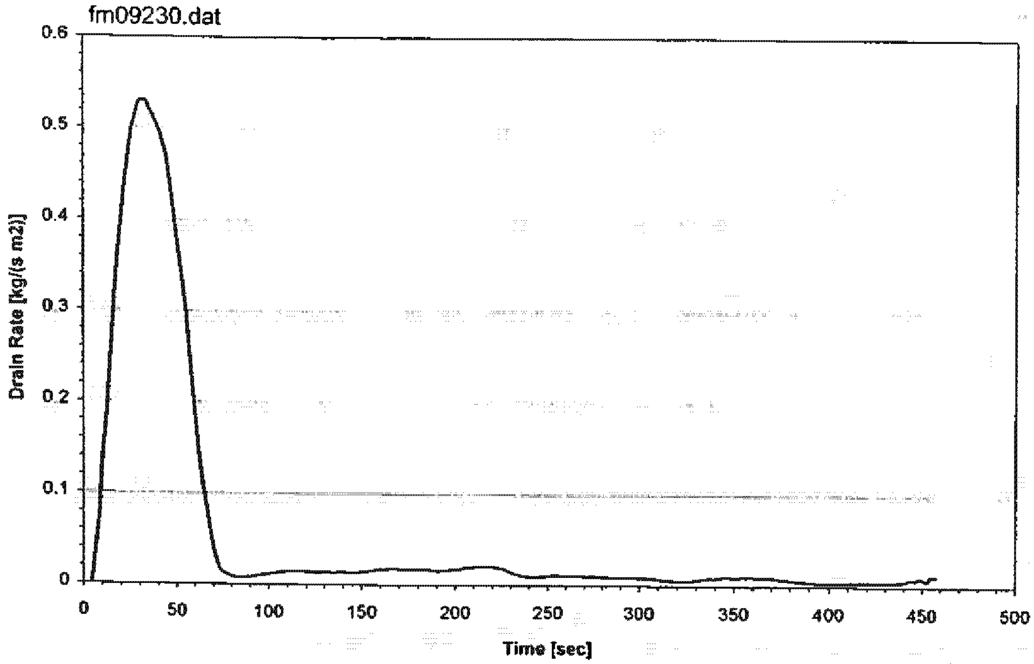

Fig. B48- Drain rate in tests with foam only. Test conditions: expansion ratio= 3.03, irradiance= 20kW/m2, initial foam height= 75mm.

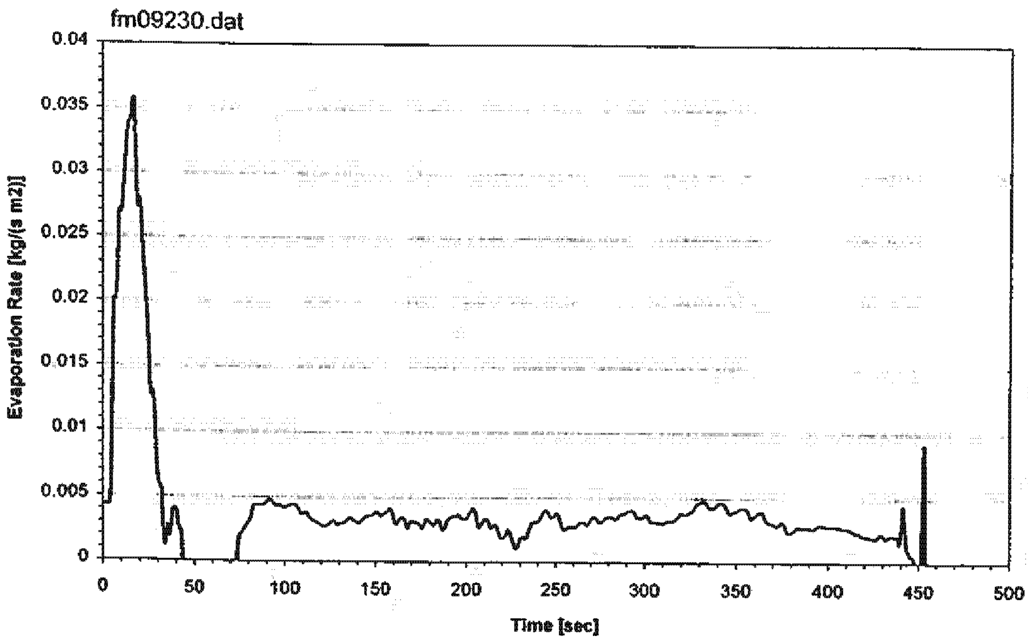

Fig. B49- Evaporation rate in tests with foam only. Test conditions: expansion ratio= 3.03, irradiance= 20kW/m2, initial foam height= 75mm.

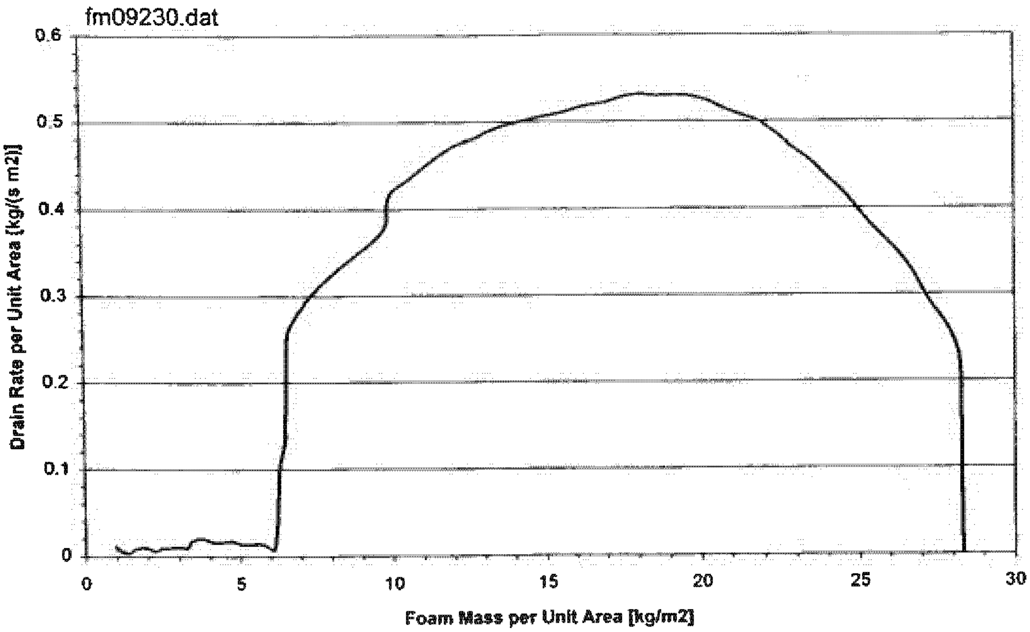

Fig. B50- Drain rate versus foam mass in tests with foam only. Test conditions: expansion ratio= 3.03, irradiance= 20kW/m2, initial foam height= 75mm.

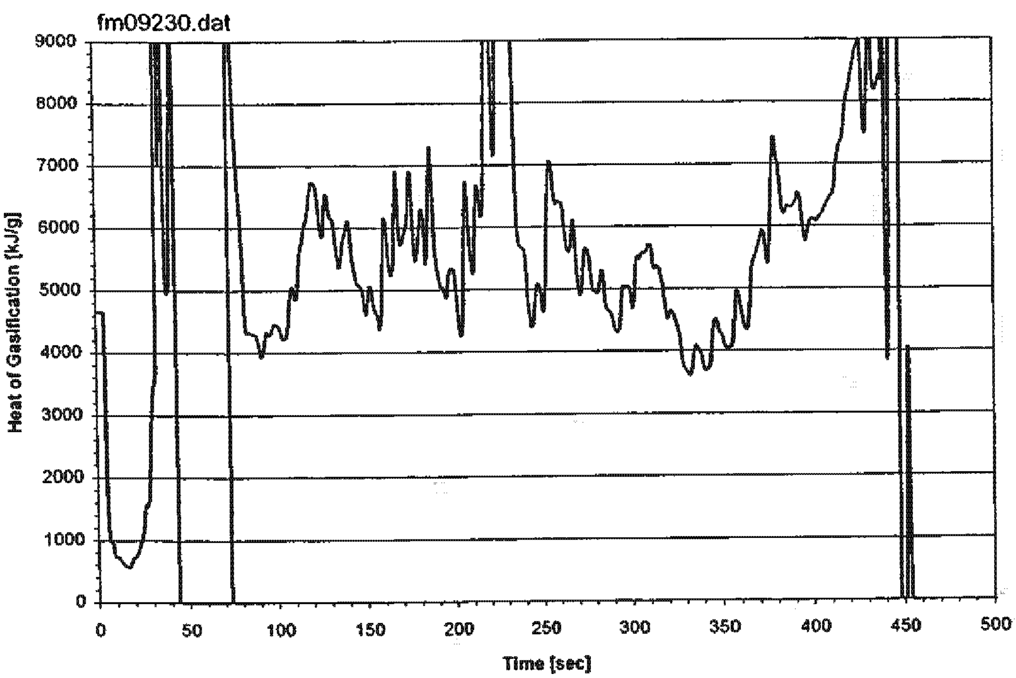

Fig. B51- Effective heat of vaporization in tests with foam only. Test conditions: expansion ratio= 3.03, irradiance= 20kW/m2, initial foam height= 75mm.

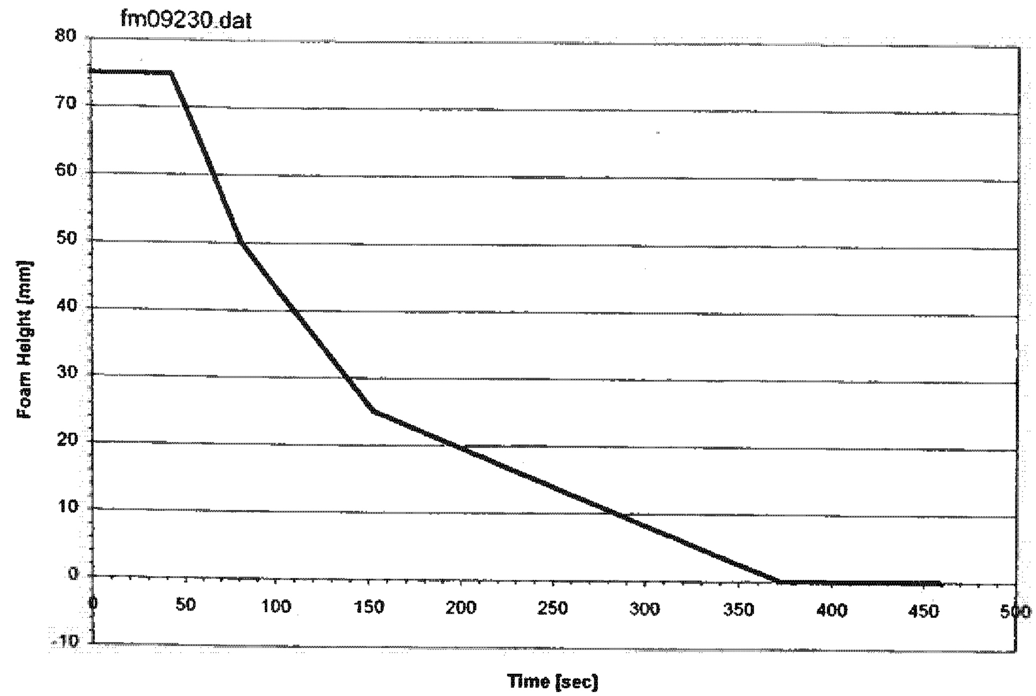

Fig. B52- Foam height in tests with foam only. Test conditions: expansion ratio= 3.03, irradiance= 20kW/m2, initial foam height= 75mm.

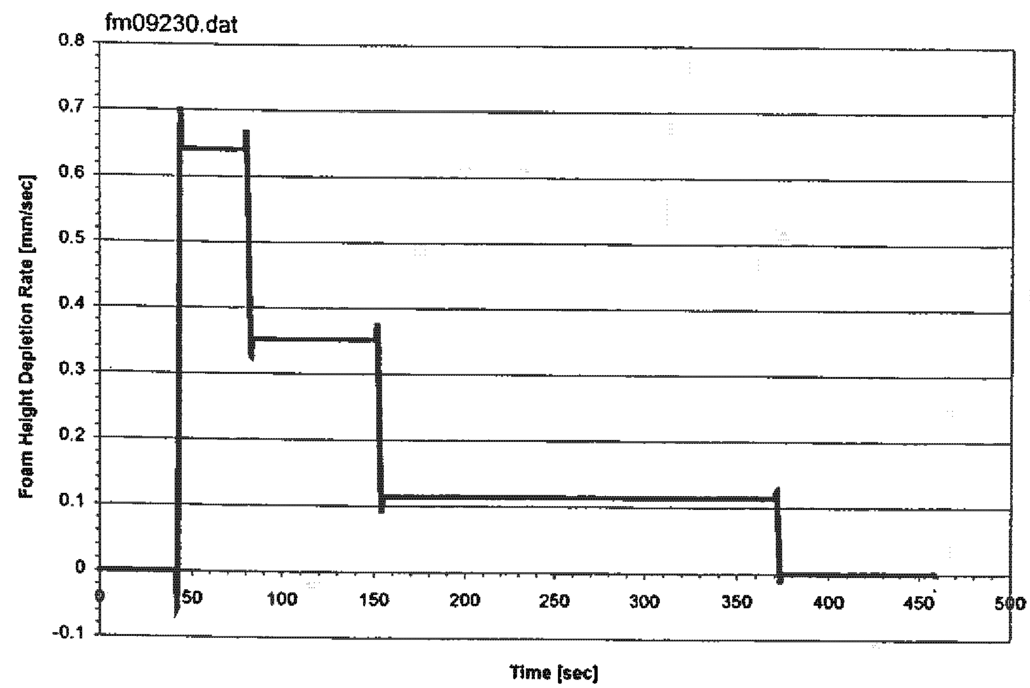

Fig. B53- Foam height depletion rate in tests with foam only. Test conditions: expansion ratio= 3.03, irradiance= 20kW/m2, initial foam height= 75mm.

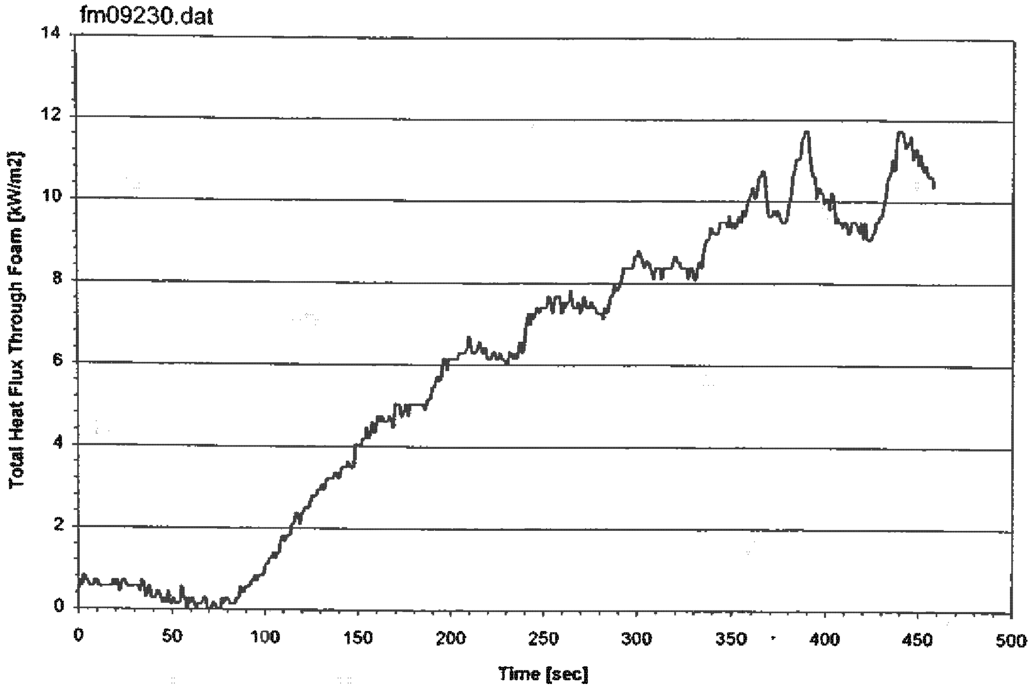

Fig. B54- Heat penetration through foam in tests with foam only. Test conditions: expansion ratio= 3.03, irradiance= 20kW/m2, initial foam height= 75mm.

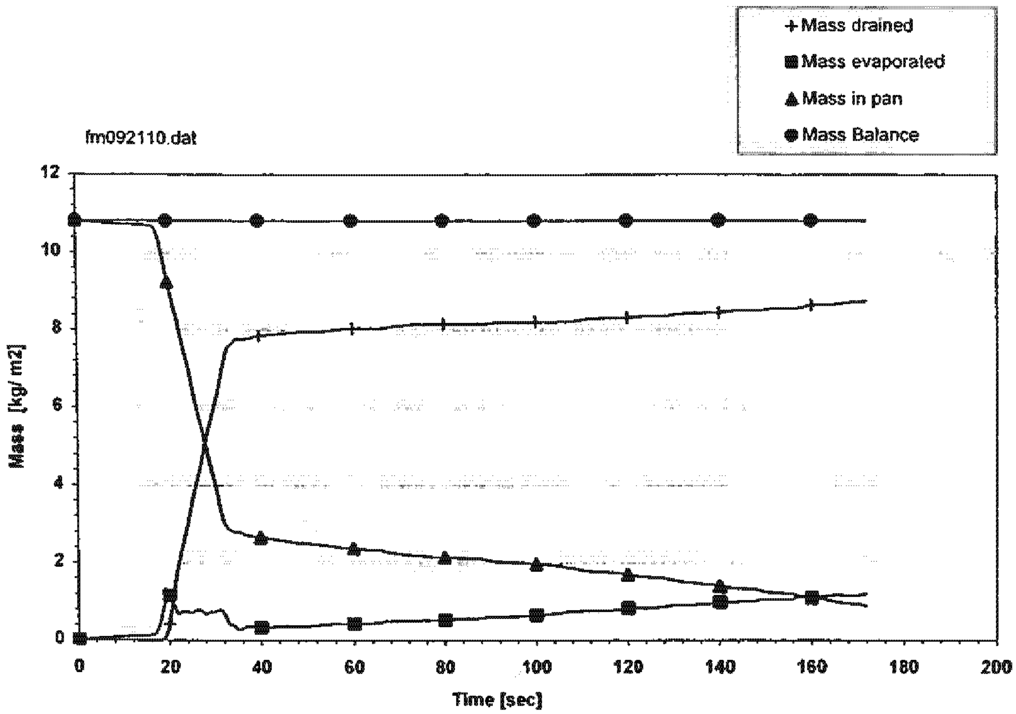

Fig. B55- Mass data in tests with foam only. Test conditions: expansion ratio= 3.02, irradiance= 35kW/m2, initial foam height= 25mm.

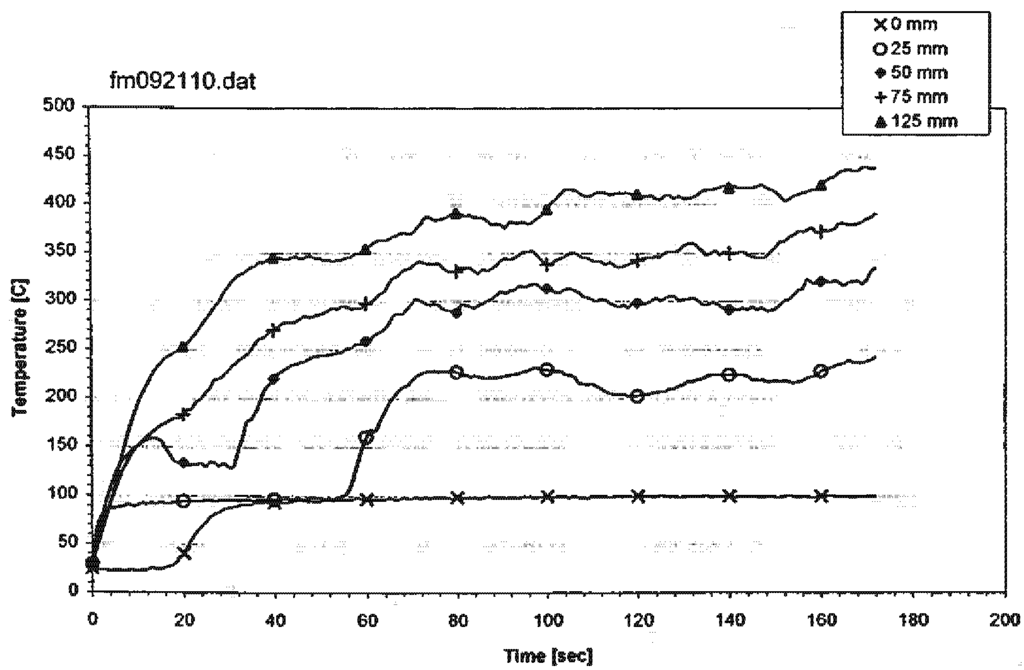

Fig. B56- Foam temperature in tests with foam only. Test conditions: expansion ratio= 3.02, irradiance= 35kW/m2, initial foam height= 25mm.

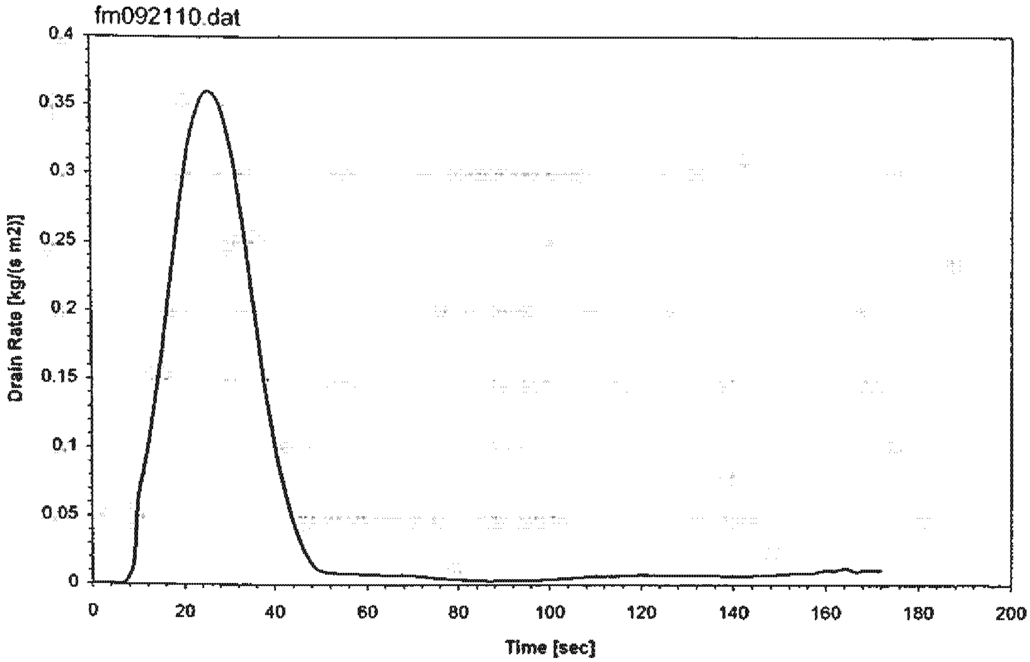

Fig. B57- Drain rate in tests with foam only. Test conditions: expansion ratio= 3.02, irradiance= 35kW/m2, initial foam height= 25mm.

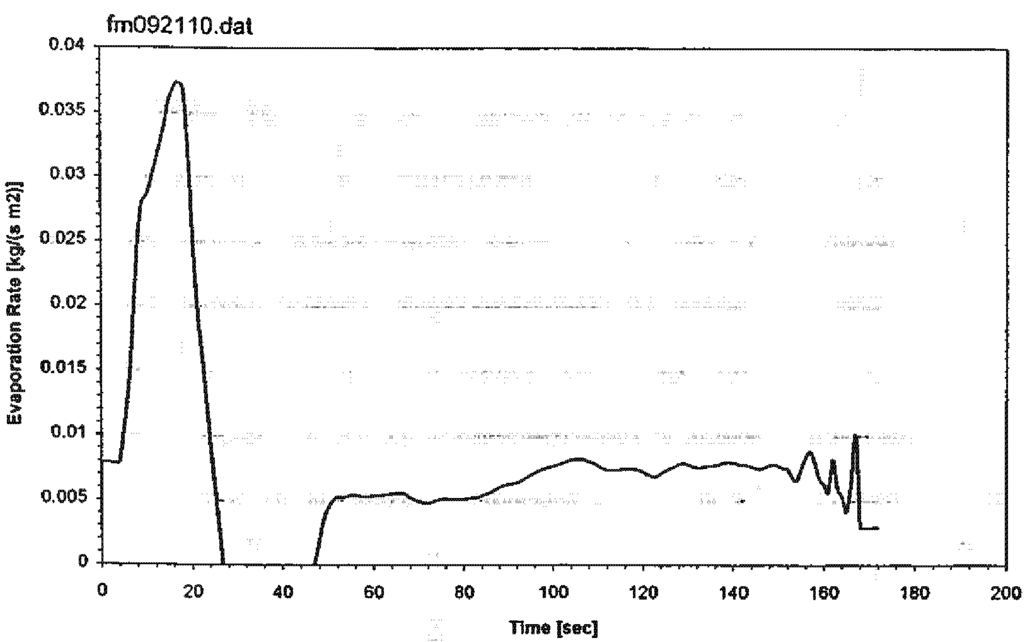

Fig. B58- Evaporation rate in tests with foam only. Test conditions: expansion ratio= 3.02, irradiance= 35kW/m2, initial foam height= 25mm.

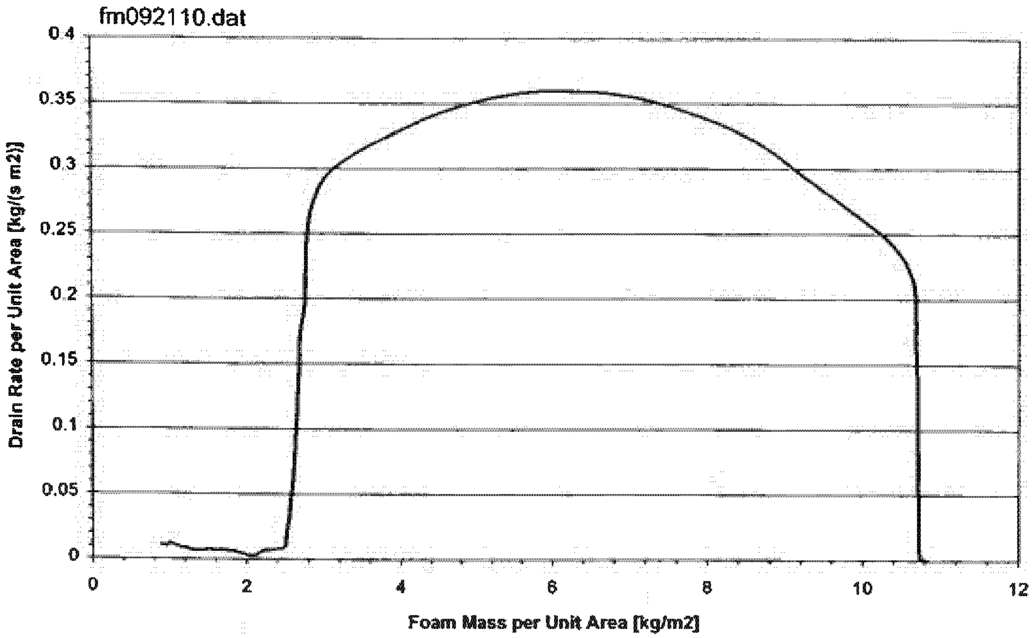

Fig. B59- Drain rate versus foam mass in tests with foam only. Test conditions: expansion ratio= 3.02, irradiance= 35kW/m2, initial foam height= 25mm.

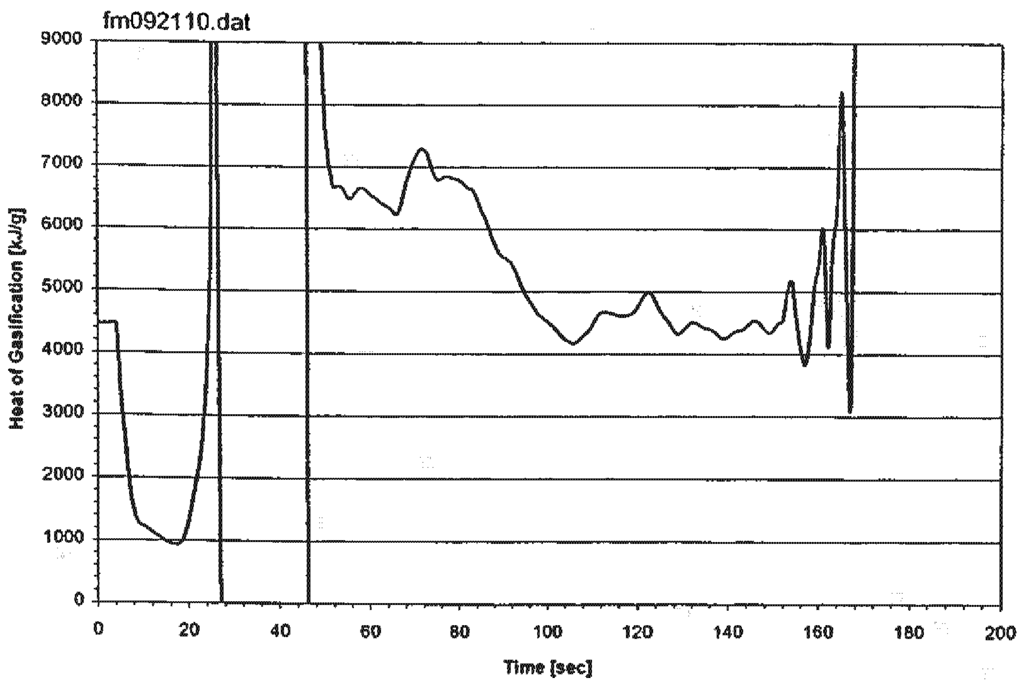

Fig. B60- Effective heat of vaporization in tests with foam only. Test conditions: expansion ratio= 3.02, irradiance= 35kW/m2, initial foam height= 25mm.

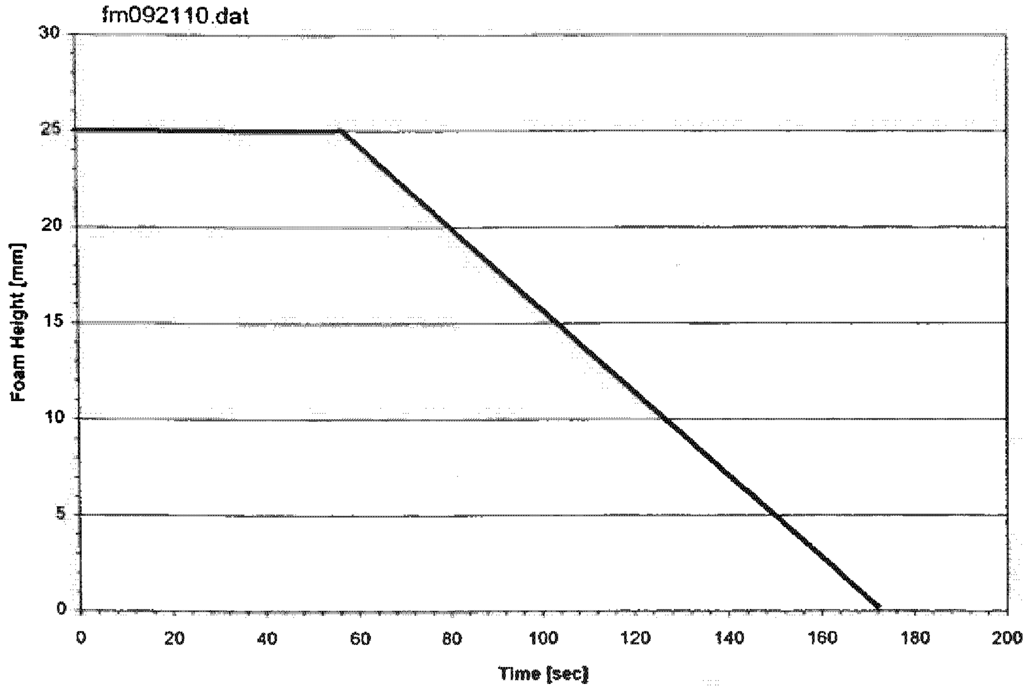

Fig. B61- Foam height in tests with foam only. Test conditions: expansion ratio= 3.02, irradiance= 35kW/m2, initial foam height= 25mm.

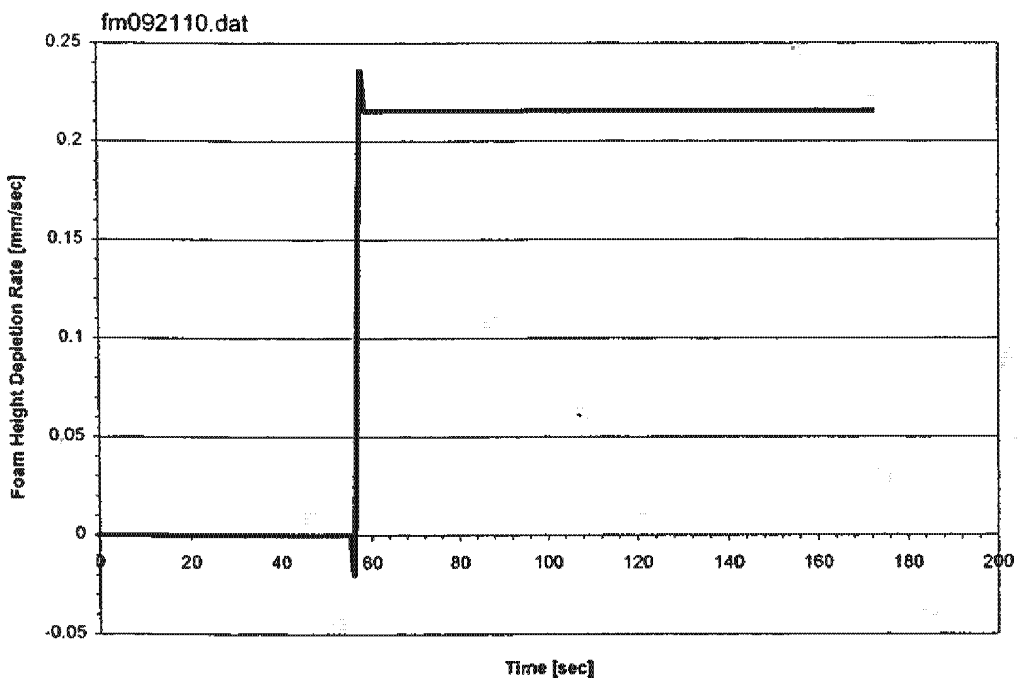

Fig. B62- Foam height depletion rate in tests with foam only. Test conditions: expansion ratio= 3.02, irradiance= 35kW/m2, initial foam height= 25mm.

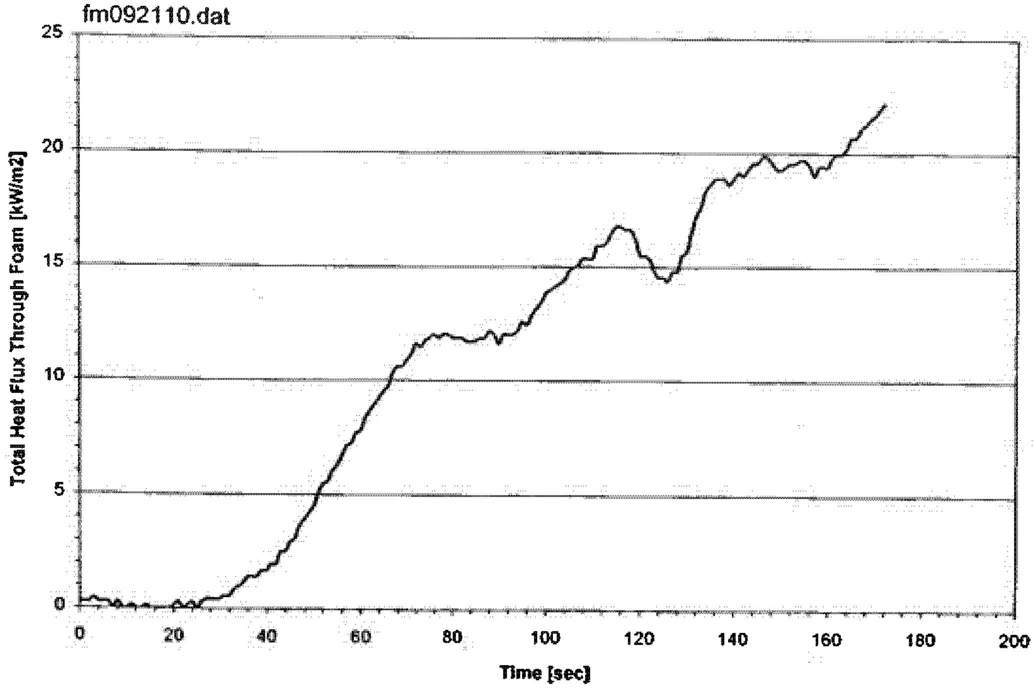

Fig. B63- Heat penetration through foam in tests with foam only. Test conditions: expansion ratio= 3.02, irradiance= 35kW/m2, initial foam height= 25mm.

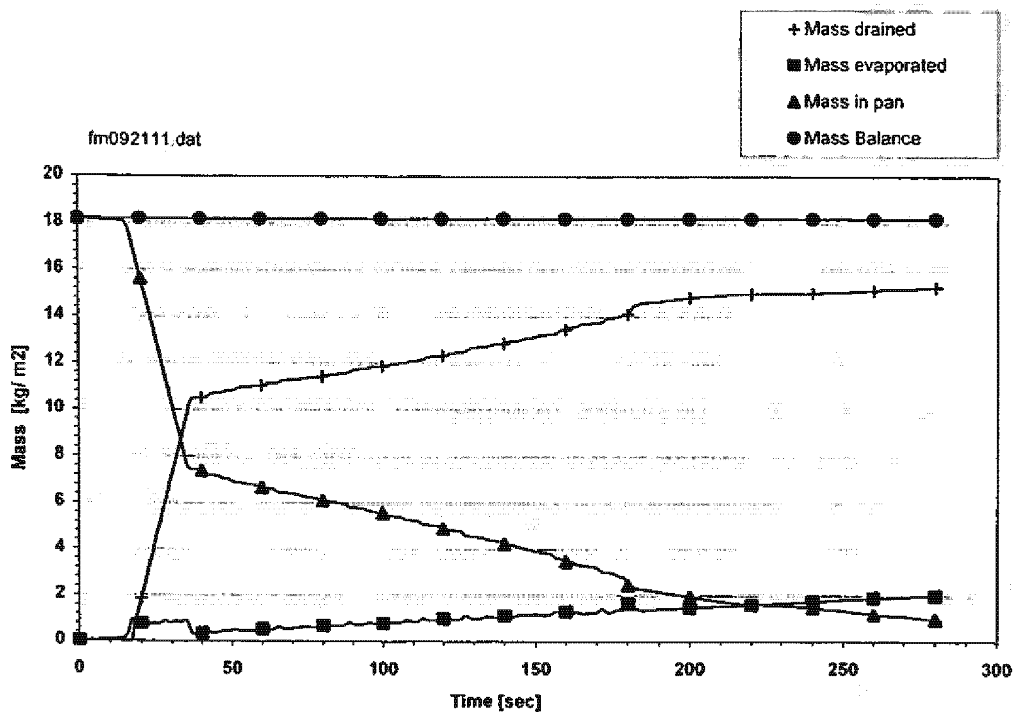

Fig. B64- Mass data in tests with foam only. Test conditions: expansion ratio= 3.24, irradiance= 35kW/m2, initial foam height= 50mm.

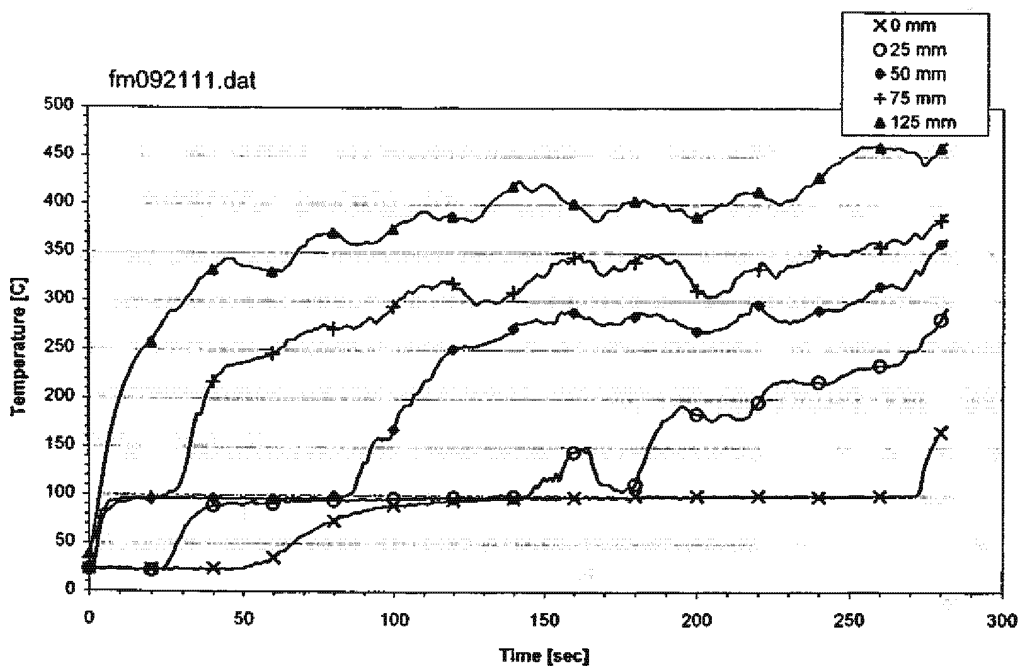

Fig. B65- Foam temperature in tests with foam only. Test conditions: expansion ratio= 3.24, irradiance= 35kW/m2, initial foam height= 50mm.

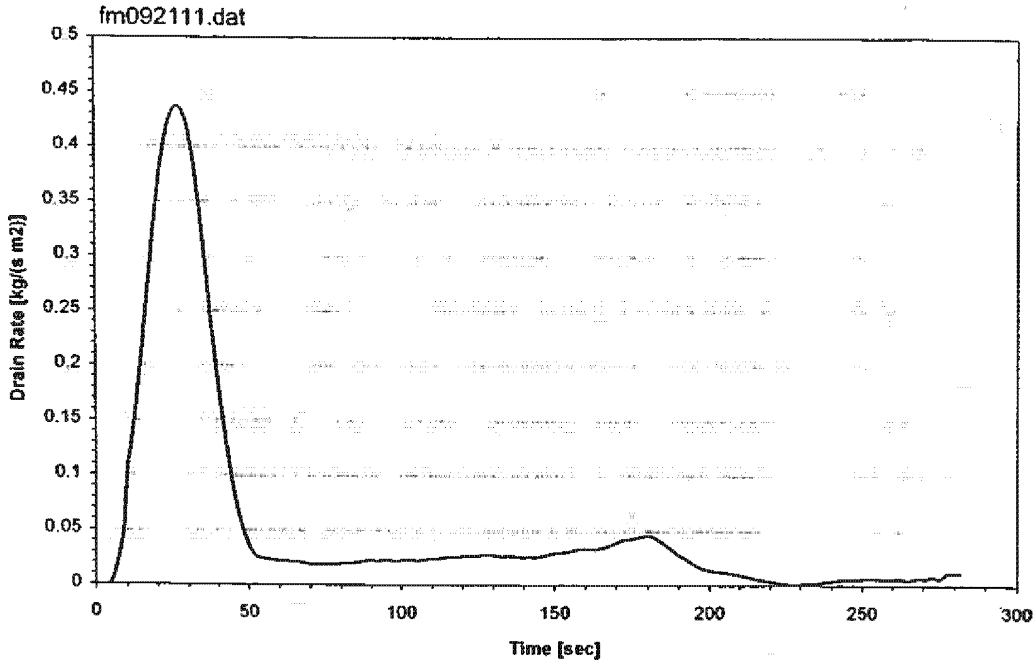

Fig. B66- Drain rate in tests with foam only. Test conditions: expansion ratio= 3.24, irradiance= 35kW/m2, initial foam height= 50mm.

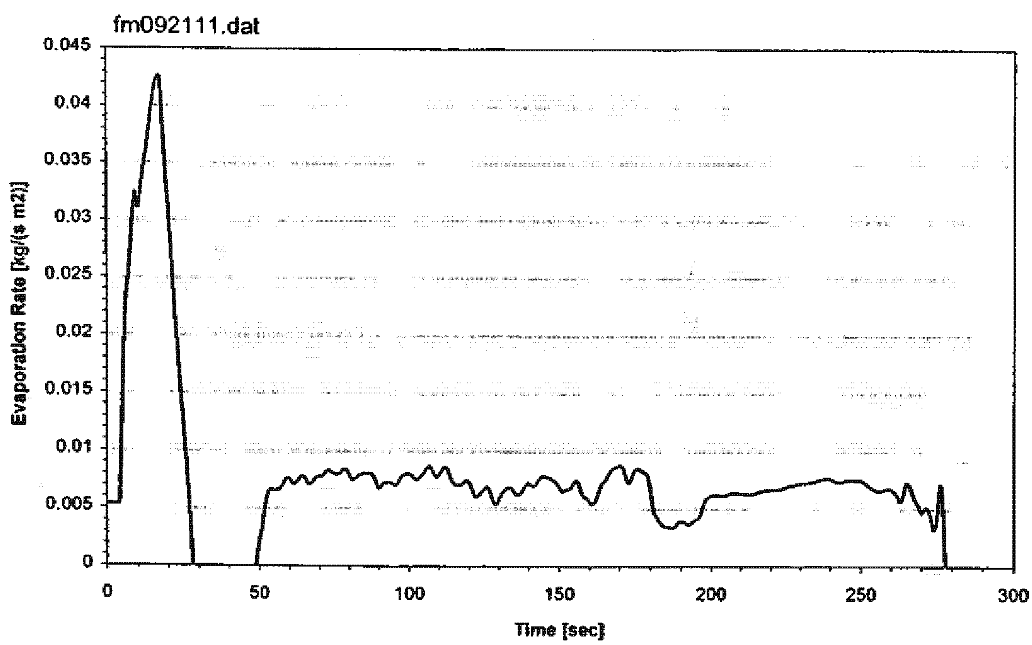

Fig. B67- Evaporation rate in tests with foam only. Test conditions: expansion ratio= 3.24, irradiance= 35kW/m2, initial foam height= 50mm.

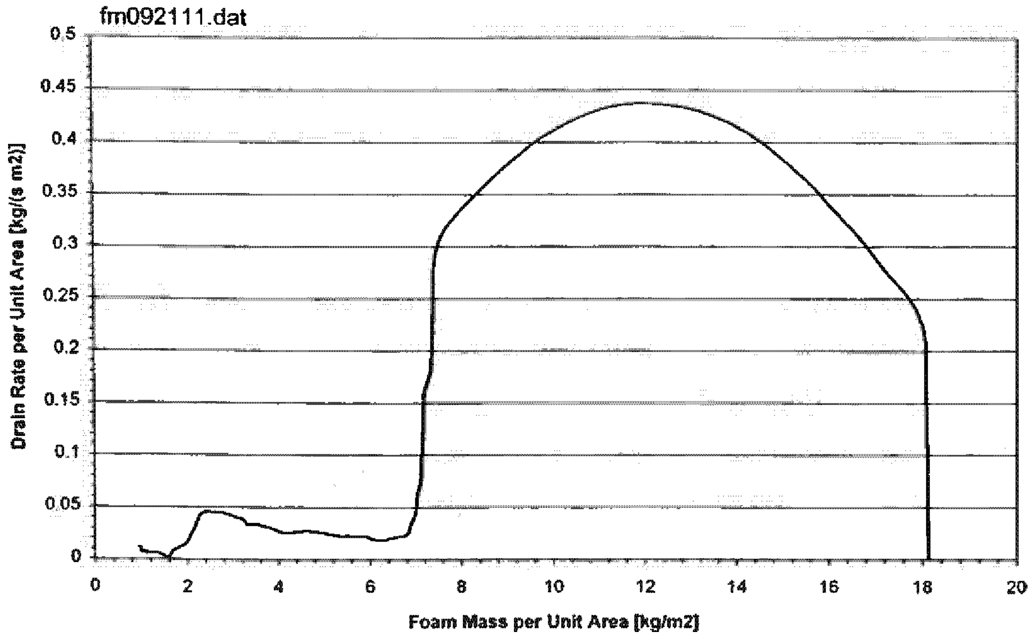

Fig. B68- Drain rate versus foam mass in tests with foam only. Test conditions: expansion ratio= 3.24, irradiance= 35kW/m2, initial foam height= 50mm.

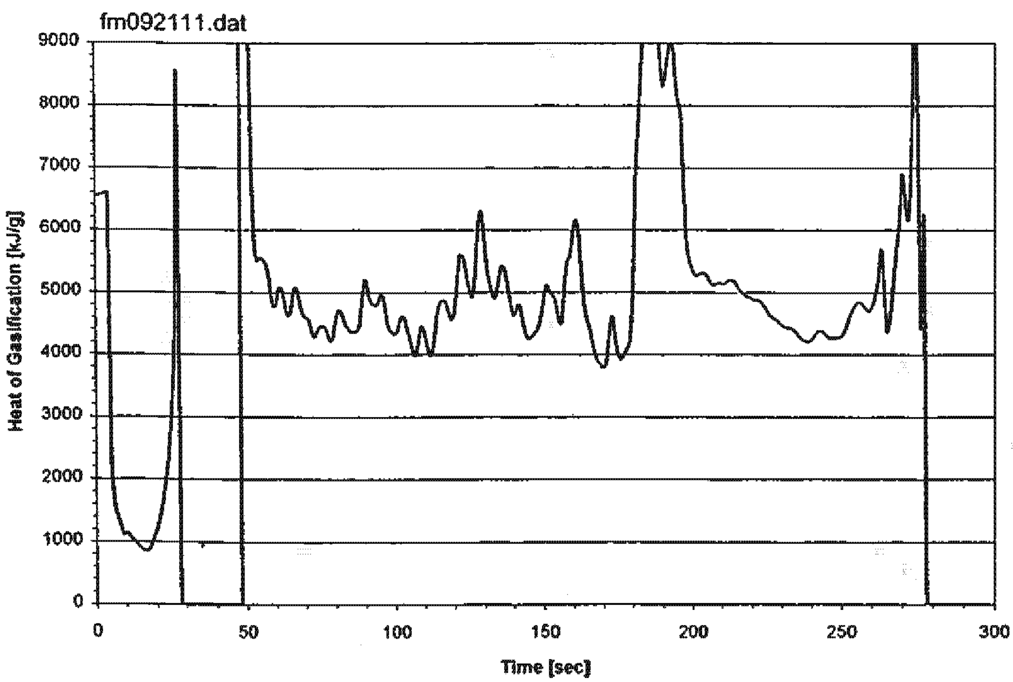

Fig. B69- Effective heat of vaporization in tests with foam only. Test conditions: expansion ratio= 3.24, irradiance= 35kW/m2, initial foam height= 50mm.

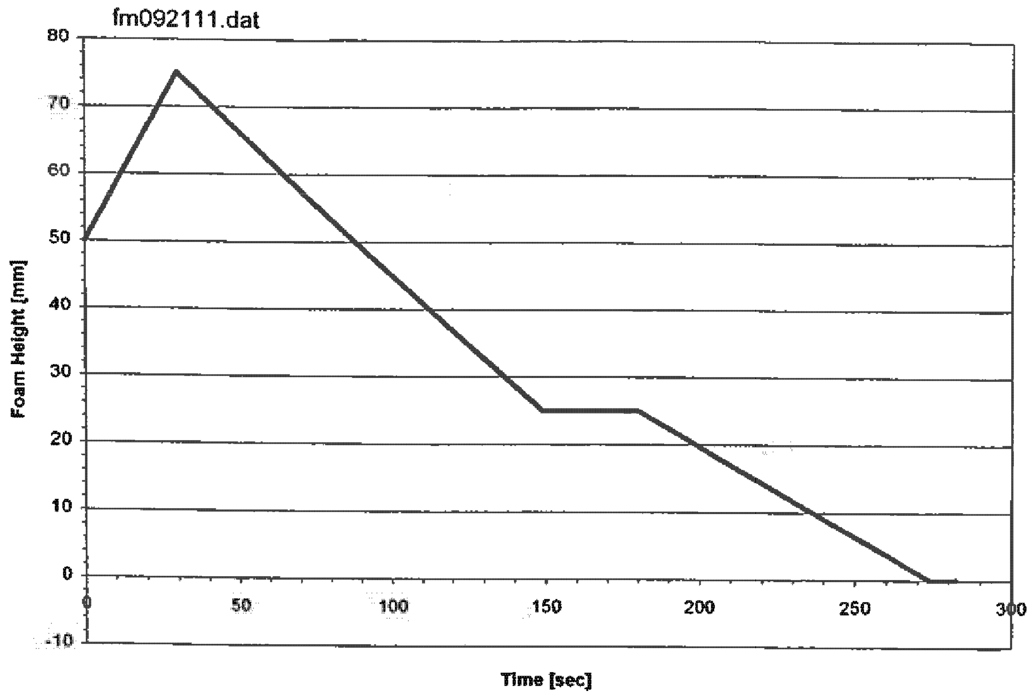

Fig. B70- Foam height in tests with foam only. Test conditions: expansion ratio= 3.24, irradiance= 35kW/m2, initial foam height= 50mm.

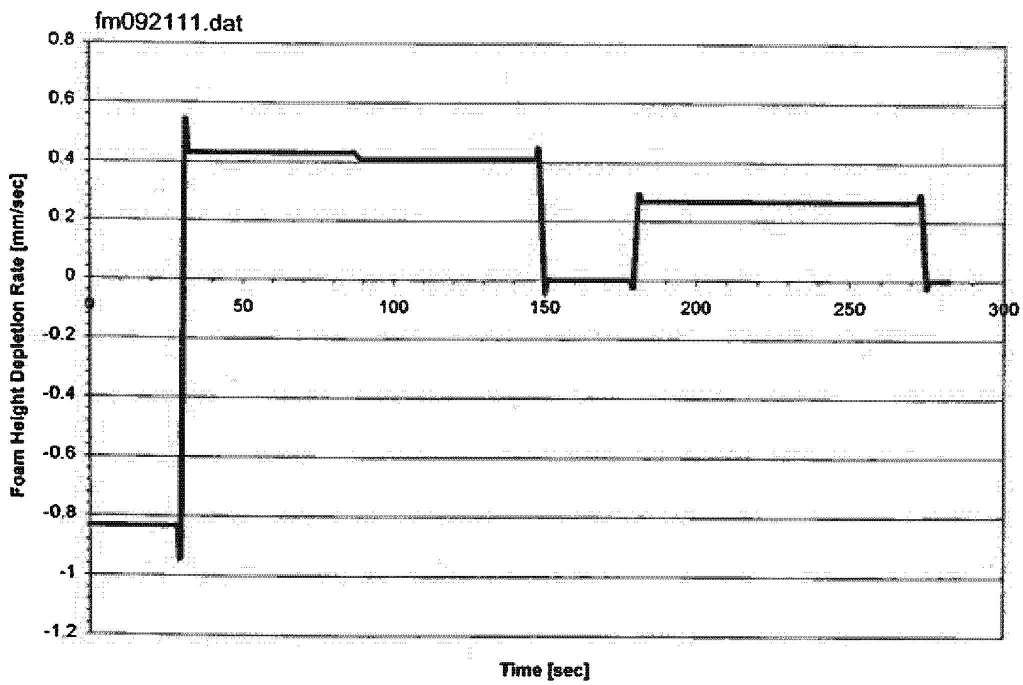

Fig. B71- Foam height depletion rate in tests with foam only. Test conditions: expansion ratio= 3.24, irradiance= 35kW/m2, initial foam height= 50mm.

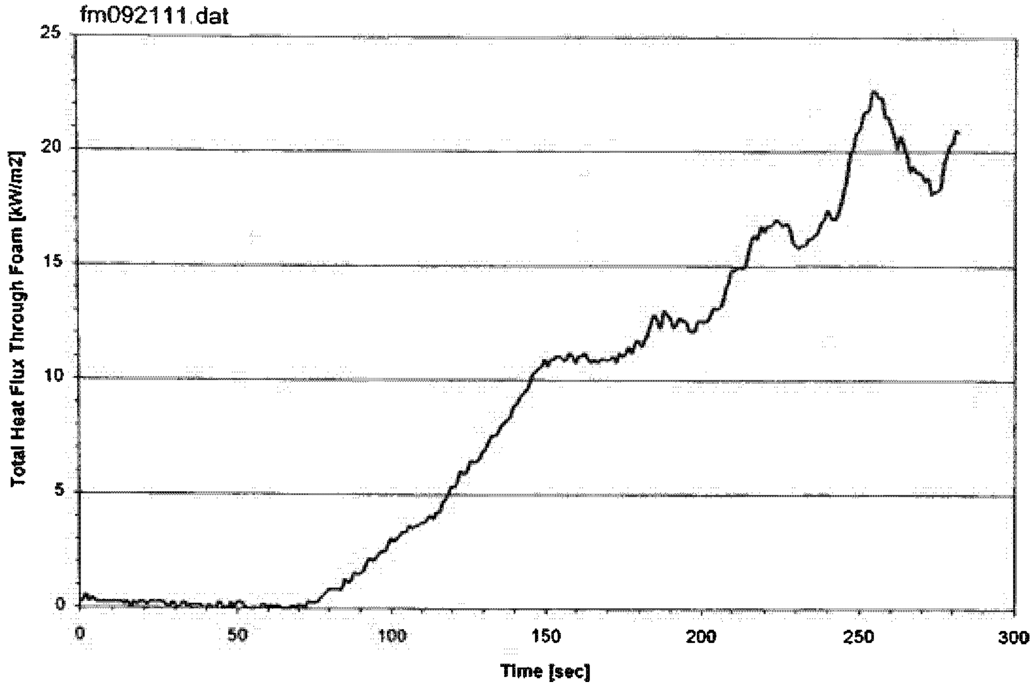

Fig. B72- Heat penetration through foam in tests with foam only. Test conditions: expansion ratio= 3.24, irradiance= 35kW/m2, initial foam height= 50mm.

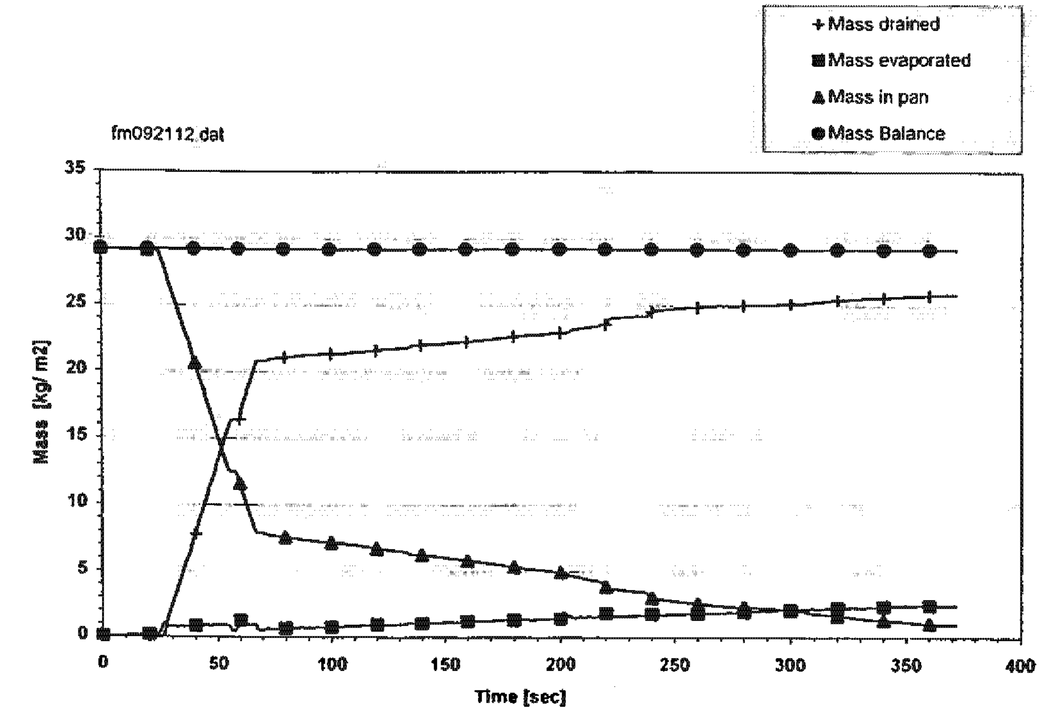

Fig. B73- Mass data in tests with foam only. Test conditions: expansion ratio= 2.94, irradiance= 35kW/m2, initial foam height= 75mm.

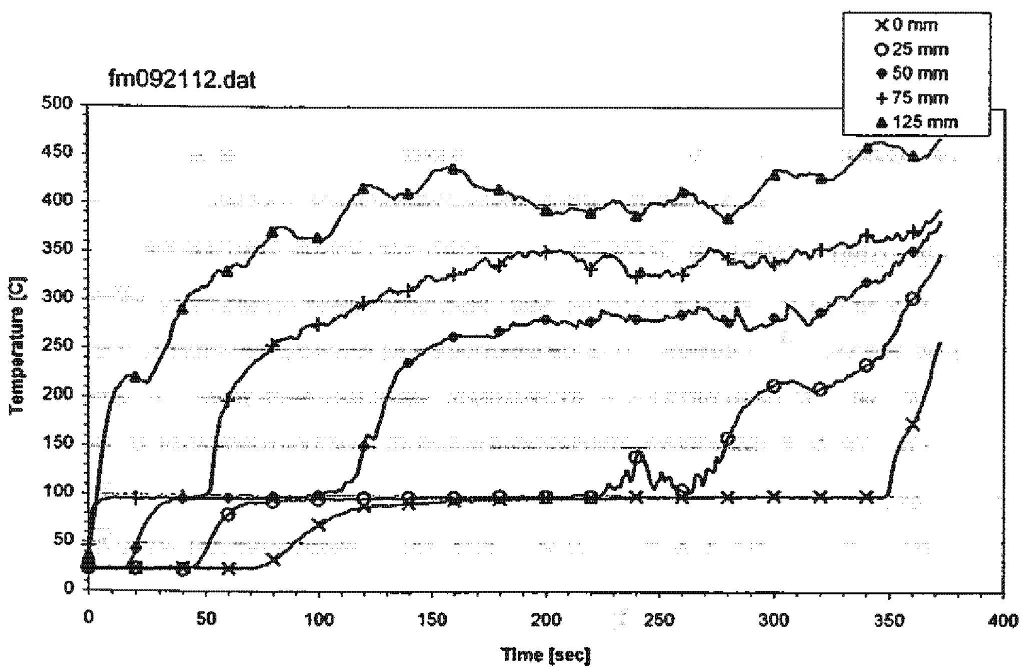

Fig. B74- Foam temperature in tests with foam only. Test conditions: expansion ratio= 2.94, irradiance= 35kW/m2, initial foam height= 75mm.